THE EFFECT OF DENERVATION ON THE MITOCHONDRIAL PROTEIN IMPORT SYSTEM IN SKELETAL MUSCLE

KAUSTABH SINGH

A THESIS SUBMITTED TO THE FACULTY OF GRADUATE STUDIES
IN PARTIAL FULFILMENT OF THE REQUIREMENTS FOR
THE DEGREE OF

MASTER OF SCIENCE

GRADUATE PROGRAM IN KINESIOLOGY & HEALTH SCIENCE
YORK UNIVERSITY
TORONTO, ONTARIO

MAY 2010

Library and Archives Canada

Published Heritage Branch

395 Wellington Street
Ottawa ON K1A 0N4
Canada

Bibliothèque et Archives Canada

Direction du Patrimoine de l'édition

395, rue Wellington
Ottawa ON K1A 0N4
Canada

Your file Votre référence
ISBN: 978-0-494-80616-6
Our file Notre référence
ISBN: 978-0-494-80616-6

NOTICE:

The author has granted a non-exclusive license allowing Library and Archives Canada to reproduce, publish, archive, preserve, conserve, communicate to the public by telecommunication or on the Internet, loan, distribute and sell theses worldwide, for commercial or non-commercial purposes, in microform, paper, electronic and/or any other formats.

The author retains copyright ownership and moral rights in this thesis. Neither the thesis nor substantial extracts from it may be printed or otherwise reproduced without the author's permission.

AVIS:

L'auteur a accordé une licence non exclusive permettant à la Bibliothèque et Archives Canada de reproduire, publier, archiver, sauvegarder, conserver, transmettre au public par télécommunication ou par l'Internet, prêter, distribuer et vendre des thèses partout dans le monde, à des fins commerciales ou autres, sur support microforme, papier, électronique et/ou autres formats.

L'auteur conserve la propriété du droit d'auteur et des droits moraux qui protège cette thèse. Ni la thèse ni des extraits substantiels de celle-ci ne doivent être imprimés ou autrement reproduits sans son autorisation.

In compliance with the Canadian Privacy Act some supporting forms may have been removed from this thesis.

While these forms may be included in the document page count, their removal does not represent any loss of content from the thesis.

Conformément à la loi canadienne sur la protection de la vie privée, quelques formulaires secondaires ont été enlevés de cette thèse.

Bien que ces formulaires aient inclus dans la pagination, il n'y aura aucun contenu manquant.

Canada

ABSTRACT

Many features of mitochondrial biogenesis are deregulated during chronic muscle disuse. The mitochondrial reticulum is normally maintained by the incorporation of newly synthesized proteins into existing organelles via the protein import system. We examined whether this pathway was impaired in denervated muscles of rats within the subsarcolemmal (SS) and intermyofibrillar (IMF) mitochondrial subpopulations. Our results indicate that the import of proteins into the mitochondrial matrix was reduced with denervation, and this effect was more pronounced in the SS subfraction. Additionally, the protein content of various components of the import machinery was also reduced. Interestingly, increased oxidative stress inhibited protein import and processing *in vitro*. Finally, we observed a close correlation between protein import and state 3 respiration, as well as import and mitochondrial content within whole muscle. Thus, the reduction of mitochondrial content and function observed with muscle disuse may be partially attributed to reduced activity of the import pathway.

ACKNOWLEDGEMENTS

The past few years have been a marvellous experience for me as a Master's student in this lab. Moving forward, I have a tremendous amount of respect for the people that I have worked with, and for their dedication to each other in the lab. None of this work would be possible without the help and guidance of the following people.

It is difficult to overstate my gratitude to my supervisor, Dr. David Hood. I fondly remember the day when you had accepted me into your lab as a naïve and confused graduate student. I was thrilled to be a part of your lab then, and have since never looked back. You are a brilliant researcher and an inspiring mentor, who has the ability to bring out the best in people who don't realize their own potential. I feel that you have helped me mature into a better researcher, student and person. The amount of work and dedication you show towards your lab students is unheralded, while your values and demeanour in our school make you an excellent role model for many of us. You have had a meaningful and positive influence in my life, and for that I will be forever grateful to you. I can only hope that I am able to reciprocate your contribution in a purposeful way.

To the past and present members of the Hood lab, along with other important people outside the lab, I want to thank you for making my life rewarding during this tenure. Being part of such remarkable company has left me with everlasting memories and life experiences that I will cherish for the rest of my life. Your role in this thesis has been instrumental, and I would like to acknowledge you. Vlad, for showing me how to act like a researcher who is both hard-working and cool. Mike, who has always looked out for me, provided me with invaluable advice and help throughout this time. Keir, who I have had a blast working with and rooming at conferences, as well as talking about other interesting aspects of life outside the lab. Ayesha (Bhaji), for being a caring and genuine person who has always been there to listen, and made me feel better at seemingly tough times. Sobia (Bubby), who is always been there to offer me a comforting hug, regardless of whether I felt like I needed one, as well as for keeping an eye out for me and sharing our experiences. Lawrence, for always being upbeat about progress in the lab, and amazing me with your knowledge and enthusiasm for research. Anna, J for being a wise and knowledgeable source of information when I started in the lab. Julie, who pretty much taught me most of the work I know in the lab, and mentoring me during those critical first few months.

I remember feeling intimidated and even fearing exclusion when I first found out that I was going to be a part of a cohort which included four other girls in my first year. However, one of the main reasons why I enjoyed my time here in this lab greatly influenced by my experiences with Giulia, Melania, Linda and Ruanne. I want to thank Giulia, for being awesome at everything, and being the most fantastic company one could ever ask for. Ruanne, for being a close friend, and introducing me to several unusual perspectives of the world. Linda, for being surprisingly effective at anything she put her mind to, and for all those fun times during the times we spent together. Melania, for her enthusiasm and the ability to party hard anywhere and anytime.

Finally to the rest of the lab members that arrived after my first year, you never ceased to amaze me and helped me stay me grounded in the latter years. To Dr. Michael Shuen and Dr. Deepthi Kumar, who have opened my eyes to the research industry with their vast experiences. It was extremely gratifying to listen to their wisdom, and gain insight into the countless number of issues that were bought up. To Anna, who was always motivated to work and provided a fun and quirky personality to our lab, I will miss having her around. To Luke, who I have had the pleasure of first mentoring, working along and then being good friends with, it has been a wild ride. I have managed to finish this with a lot of help and encouragement from him, and I hope his dedication and ability to grind through tough times will help him finish his thesis successfully very soon. To Donna, who has always been a lot of fun to be around, has a personality that is reflective of someone who always strives to make others feel comfortable before herself. Watching her develop as a better researcher with improved critical thinking skills over the years has been worthwhile. To dear Heather, who can seem very quiet and pedestrian at first glance, but is really chock full of vivid thoughts, insightful opinions and compassion, has been a welcome addition to the lab. She had a tremendous influence on my productivity during the writing process, and I want to thank her for being a friend. I hope you can achieve all that you want to be. I am proud of our accomplishments in the lab, and watching Olga, Steve and Yuan leads me to believe that the foundation and direction of this lab is stronger today, than when I became a Master's student in 2007. It was great to spend a limited amount of time with you, I know it would have been great to work with you. Good luck with all your work, and I hope you will thoroughly enjoy your tenure in the lab.

There are also a number of people outside the lab that I would like to who also helped me accomplish this thesis. Aki and Deep, for being true to research and sticking through till the bitter end. Roberto, for listening to my rants in the evenings and providing pleasantly surprising feedback. Marco for being a good friend throughout this thesis and for providing several funny moments. Countless staff and faculty members who have provided me the opportunity to get through this program, as well many of our lab volunteers and NSERC summer students who have helped run the lab seamlessly. I thank all of you.

Lastly, and importantly, I wish to thank my family. To Mom, who relentlessly loves and cares for all of us without asking for anything in return, I want to thank you for sacrificing so many of your dreams, just so that I could have an opportunity to pursue some of mine. I do not always show the amount of appreciation that you deserve, but I want you to know that I am grateful for all that you do for us. To Dad, whose patience and understanding has helped me navigate through life, I want to thank you for teaching me how to think critically and to let me learn about many of life's lessons. I am a better man because of you, and I am proud of you. To Juhi, I am lucky to have a little sister like you. You make life enjoyable, curious and even a little bit more interesting. I want to thank you for causing me to be more responsible and for showing me alternative points of views, something that I could not have necessarily done on my own. I hope I can work on being a better big brother to you, and that you continue to be my most favourite person in the whole world ☺. Finally I wanted to thank Bianca, the best cat anybody could ever ask for. She made writing this thesis a lot more manageable by being my regular sparring partner when I got bored, and for staying up with me on many nights, as I worked on the computer. I love all of you very much!

TABLE OF CONTENTS

LIST OF FIGURES

REVIEW OF LITERATURE

MANUSCRIPT

ADDITIONAL DATA

LIST OF ABBREVIATIONS

ΔP	proton motive force
Ψ_m	mitochondrial membrane potential
ADP	adenosine diphosphate
AMP	adenosine monophosphate
ATP	adenosine triphosphate
AMPK	AMP-activated protein kinase
ANT	adenine nucleotide translocase
BW	body weight
CL	cardiolipin
COX	cytochrome c oxidase
DNA	deoxyribonucleic acid
EDL	extensor digitorum longus
ETC	electron transport chain
FTR	fast twitch red
FTW	fast twitch white
GIP	general insertion pore
GRP	glucose response protein
H_2O_2	hydrogen peroxide
HSP	heat shock protein
IMF	intermyofibrillar
IMS	intermembrane space
kDa	kilodalton
KO	knock out
mRNA	messenger ribonucleic acid
MHC	myosin heavy chain
MPP	matrix processing peptidase
MSF	mitochondrial import stimulating factor
mtDNA	mitochondrial DNA
mtHSP	mitochondrial heat shock protein
mtPTP	mitochondrial permeability transition pore
NAD^+	nicotinamide adenine dinucleotide
NADH	reduced nicotinamide adenine dinucleotide
O_2^-	superoxide anion
OCT	ornithine carbamyltransferase
PAM	presequence translocase-associated motor complex
PGC-1α	PPAR γ coactivator-1α
Pi	inorganic phosphate
RCR	respiratory control ratio
RNA	ribonucleic acid
ROS	reactive oxygen species
SAM	sorting and assembly machinery
SDS-PAGE	sodium dodecyl sulfate polyacrylamide gel electrophoresis

SR	sarcoplasmic reticulum
SS	subsarcolemmal
STR	slow twitch red
TA	tibialis anterior
TFAM	mitochondrial transcription factor A
TIM	translocase of the inner mitochondrial membrane
TL	translation lane
TOM	translocase of the outer mitochondrial membrane
VO_2	oxygen consumption

INTRODUCTION

Chronic muscle disuse results in decreased muscle size, function and endurance capacity. Furthermore, several adaptive changes in mitochondrial content and function occur during conditions of prolonged disuse such as denervation. Mitochondrial biogenesis involves a complex series of events involving the activation, expression and coordination of both the nuclear and mitochondrial genomes, along with the incorporation of newly synthesized proteins into existing organelles. While several aspects of this process are altered during denervation, this thesis was undertaken to evaluate potential adaptations in one particular facet of mitochondrial biogenesis during denervation: the precursor protein import pathway.

The majority of mitochondrial proteins are encoded by genes found in the nucleus, and require the protein import pathway to be incorporated into growing organelles. Skeletal muscle experiencing mitochondrial biogenesis exhibits elevated rates of protein import. These increases in protein import kinetics are conducive for increasing mitochondrial content and improving functioning. However, the import system has never been characterized during muscle inactivity, and its role in mediating any adaptations in content and function are unknown. Thus, developing a better understanding of the role of the protein import system during muscle disuse would help elucidate some of the underlying mechanisms regulating alterations in skeletal muscle mitochondria. This requires measuring protein import kinetics, along with any changes in organelle structure or function which regulate this process. This includes the protein import machinery and respiratory chain behaviour in subsarcolemmal (SS) and intermyofibrillar (IMF) mitochondria. Specifically, the purposes of this thesis were to:

1. Investigate the effect of denervation on mitochondrial protein import in both SS and IMF mitochondrial subfractions;
2. Measure the protein content of various components of the import machinery which are involved in mediating protein import in SS and IMF mitochondria;
3. Evaluate the effect of reactive oxygen species (ROS) on mitochondrial protein import;
4. Assess the relationship between mitochondrial respiration and protein import, as well as precursor import and mitochondrial content.

REVIEW OF LITERATURE

1.0 SKELETAL MUSCLE

As the name implies, skeletal muscle is a type of muscle responsible for skeletal movements such as locomotion. Skeletal muscles are anchored by tendons to bone and are under the voluntary control of the central nervous system. A whole skeletal muscle consists of muscle, connective, nerve and vascular tissue. Each muscle is made up of large numbers of muscle fibers, which are formed from the fusion of many myoblasts during development. As a result, muscle fibers have multiple nuclei. In addition, these fibers are striated in appearance, which is due to the arrangement of the myofibrillar proteins actin and myosin. The interaction of actin with projections on the myosin results in cross-bridge cycling and the production of muscle contractions. Skeletal muscle constitutes 40% of body mass, and adaptations in response to genetic cues or environmental stimuli can result in dramatic phenotypic and functional changes. However in order to appreciate these alterations, it is important to understand the structural basis of skeletal muscle.

1.1 Fiber types

Skeletal muscle is classified into three classes of fibers, slow-twitch red (STR), fast-twitch red (FTR) and fast-twitch white (FTW) fibers. They are categorized according to their metabolic properties, which reflect the fuel choice used to generate energy for muscle contractions, and the contractile apparatus, which is denoted by the myosin heavy chain (MHC) expression. The majority of muscles are composed of a mixture of slow and fast fiber types, but it is possible to have some muscle groups that primarily comprise of

either fast or slow fibers. For instance the soleus muscle in rodents is considered to be primarily a slow-twitch muscle whereas the extensor digitorum longus (EDL) muscle would be an example of a fast-twitch muscle (12). Fast-twitch muscles have bigger motor units that innervate their fibers and they contract powerfully with more force in a shorter period of time when compared to slow-twitch muscles. Slow-twitch muscle fibers are primarily used as postural and weight bearing muscles, which requires them to be active over long periods of time without being fatigued. In contrast, fast-twitch fibers are recruited according to the size principle, when slow-twitch fibers cannot produce sufficient muscle contractions, or when the force requirement is high (100). There is a difference in the mitochondrial content among fast- and slow-twitch fibers, and this determines the oxidative capacity of each fiber type (130). Fast-twitch fibers have lower amounts of mitochondria, and rely on glycolytic metabolism to generate energy for contractions. This makes them more susceptible to fatigue. In contrast, slow-twitch fibers are more fatigue-resistant and this serves them well for their function of sustaining muscle activity for long durations. The heterogeneity of fiber types observed in skeletal muscle suggest that different fiber types adapt differentially when exposed to different forms of external stimuli.

1.2 Multinucleation of skeletal muscle

Mature skeletal muscle cells are the only organelles in the body that are multinucleated. This gives them a distinctive appearance as well as an unusual regulation system. Since most cells have their transcriptional processes controlled by one nuclei,

multiple nuclei in muscle cells have to work together in regulating gene expression in the whole muscle cell. The myonuclear domain theory is a theoretical concept used to explain how a fixed amount of cytoplasm is controlled by the action of a single myonucleus located at the periphery of the muscle cell (6). Increases in the number of myonuclei are governed by the activation of quiescent satellite cells which donates a nucleus to the muscle fiber (64). Having multiple nuclei is beneficial to the survival and functioning of muscle cells, as the loss of a few myonuclei does not necessarily lead to the death of the cell. Other myonuclei can take over the functions of the lost nuclei and the muscle cell can adapt by reducing its size. This property plays an important role during alterations in muscle contractile activity.

1.3 Alterations in muscle contractile activity – Muscle disuse

Skeletal muscles demonstrate enormous plasticity when subjected to differential states of contractile activity. The extent of these adaptations depends on the nature and duration of contractile activity that is administered. As mentioned in the previous section, there is a relationship between the cross-section area of muscle fibers and number of myonuclei. In response to increases in contractile activity, satellite cell activation leads to an increase in myonuclear number and contractile apparatus proteins (6; 64). However the opposite is expected with chronic muscle disuse. This section will explore some common models of muscle disuse, as well as the morphological and functional adaptations observed with reduced contractile activity.

1.3.1 Experimental models of chronic muscle disuse

A variety of invasive and non-invasive techniques have been developed to induce skeletal muscle atrophy in animal models. Invasive techniques such as denervation, tenotomy and joint pinning have been historically used to understand the underlying causes and mechanisms of muscle atrophy (120). Non invasive techniques such as limb casting and body suspension has been used mainly because of the interest of the National Aeronautics and Space Administration in exploring the causes of and appropriate countermeasures for the disuse atrophy associated with exposure to space flight (113). This section briefly looks at some of the common techniques used to study muscle disuse and atrophy.

Denervation occurs when the nerve supply to a muscle is interrupted and the muscle no longer receives electrical impulses from the central nervous system (107). This can be achieved through mechanical means (i.e. surgical sectioning or crushing) or chemical blocking (e.g. tetrodotoxin). Denervation is an excellent model to study both muscle disuse as well as neurotrophic effects (120). However the loss of innervation to non-muscle tissue may be a confounding variable when interpreting results for muscle atrophy. One common criticism is the possible contribution of altered blood flow to the atrophic muscle, due to interrupted neural input to vascular tissue in the local area.

Tenotomy is the surgical procedure of cutting a tendon. In contrast to denervation, this process leaves neurons intact, but since the tendinous connection of muscle to bone is severed, the muscle length is below its optimal resting length (120; 162). All muscle contractions become isotonic, and the tenotomised muscle undergoes atrophy. In

addition, the synergetic muscles undergo hypertrophy and as a result this model is more commonly used as a model to study compensatory hypertrophy, in lieu of atrophy.

Limb casting and joint pinning represent models of disuse where the muscles are held at a fixed length. In joint pinning, metal rods are implanted at the junction of two long bones so that the limb is immobilized and the researcher can control the degree of passive stretch by changing the angle at which the joint is immobilized (154). In contrast, limb cast immobilization can be used to achieve a similar effect without the implanting metal rods. Instead, the limb is fixed with a layer of orthopaedic or casting material to fix the joint (120). Both methods result in the atrophy of various hindlimb muscles depending on the angle of immobilization. However, one must factor in the role of isometric contractions while being immobilized in the interpretation of muscle atrophy.

The hindlimb suspension (HLS) or unloading (HLU) model was developed to mimic spaceflight. In the 1970s, space exploration researchers wanted to design a ground-based model to study the effect of weightlessness on astronauts while in space (113). Although there have been several modifications to the technique since the model was first initiated in 1975, the basic concept has not changed. In this model, rodents are elevated to produce a head-down tilt, eliminates weight-bearing activity by the hindquarters (115). Animals are free to move, eat and groom with the forelimb muscles and the hindlimb muscles unload without paralysis. This model is intended to study the effects of weightlessness on different physiological systems and apply it directly to space flight studies (114). While unloaded muscles experience differential atrophy (168), some

researchers question whether hindlimb unloading is an appropriate model of muscle disuse, as electrical activity continues in muscles (106).

The aforementioned models of disuse are all valid techniques that can be used to induce muscle atrophy. Each method has its strengths and weaknesses, and choosing the appropriate model is dependent on the desired outcome of the study.

1.3.2 Muscle disuse-induced alterations in skeletal muscle

With chronic disuse, there are morphological, functional and biochemical changes in skeletal muscles which are dependent on the type and duration of disuse. The most obvious morphological characteristic of muscle disuse atrophy is a reduction in fiber size and perhaps fiber number (4; 148). It would appear logical to suggest that slow-twitch fibers should be most affected by disuse, as these fibers receive continual neural input to maintain their weight-bearing and postural functions. However, experimental evidence suggests that when atrophy is present, it is more prevalent in fast-twitch fibers (7; 152). One possible explanation is the apoptotic susceptibility of fast-twitch fibers is higher (3; 152), and they are more readily sacrificed to adjust to lower metabolic levels. It must be noted that the fiber type expression patterns vary with extended periods of disuse, as one study reported that seventy months following spinal cord injury, upper motor neuron paralysed muscles lose the normal slow and fast fibre mosaic pattern and become predominantly composed of type II fibers (32). In addition several investigators have reported contrasting reports on the trends of fiber switching as well as the degree of restructuring. These differences may be attributed to comparing

different types of disuse atrophy as well as the location of cross sections taken within the muscle for examination. Nonetheless, regardless of the model or the period of disuse used, an overall reduction in fiber area is a hallmark feature of muscle disuse-induced atrophy.

A different morphological characteristic in skeletal muscle is the consideration of the distribution of capillaries in relation to muscle fibers. Fiber size is reduced with muscle atrophy, and capillaries appear to become more concentrated (49). However in denervation and other forms of muscle disuse there is also a reduction in the vasculature around disused muscle (172). Still it must be noted that blood flow and distribution increases initially due to rapid decreases in muscle size, but after extended periods of time blood flow to disused muscles becomes attenuated (54). All in all, the overall capillary/fiber ratio density does not seem to be different in denervated muscles, even though there is elevated blood flow.

A common functional adaptation of skeletal muscle disuse is an overall loss in muscle strength (26; 53; 107). There is a direct relationship between reduced cross-section area of muscle and loss in force production. In the case of muscle disuse, diminished electrical activity leads to myofibrillar restructuring (131), which in turn affects the availability and turnover of ATP, calcium regulation and metabolite factors affecting muscle contractions (53). ATP and calcium ions are necessary for the contractile apparatus to contract and generate force. Muscles produce metabolites upon contracting which are then recycled. During muscle disuse, these systems are altered which then lead to functional impairments in force production.

ATP is the fuel which drives muscle contractions. During muscle disuse, the availability of ATP is compromised because of a reduction in the enzymes of Krebs' Cycle and oxidative phosphorylation (27; 183). Since the majority of ATP is aerobically generated using these pathways, ATP becomes less freely available for muscle contractions. In addition, the ATP that is present during disused condition comes from anaerobic sources such as glycolysis, which generates lactic acid as a by-product in order to replenish the factors necessary for ATP generation. The production and consequent build up of hydrogen ions during anaerobic metabolism interferes with the normal contractile apparatus and selectively competes with calcium binding sites and inhibits troponin and tropomyosin interactions (93). As a result muscles are unable to contract, and are fatigued. An overall remodelling of ATP generation within disused muscles contributes to muscle weakness during repeated contractions.

As indicated above, calcium also plays a crucial role in facilitating muscle contractions. Calcium (Ca^{2+}) ions are stored in sarcoplasmic reticulum (SR) freely, or bound to calsequestrin, and are normally released when evoked by an action potential (171). The rise of Ca^{2+} in the muscle cytoplasm leads to increased calcium binding with troponin which permits muscle contractions. Upon the completion of a cross-bridge cycle, Ca^{2+} is taken up again into the SR which is facilitated by parvalbumin (171). Reductions in muscle electrical activity lead to decreased SR Ca^{2+} uptake as well as Ca^{2+}-ATPase activity. In addition levels of parvalubmin are under neural regulation, and decrease markedly during disuse. Increased cytosolic Ca^{2+} levels have been observed in a

number of different studies, and this can contribute to muscle proteolysis and programmed cell death (150).

Finally, metabolites produced as a result of muscular contractions may also contribute to muscle weakness during conditions of muscle disuse. ADP, reactive oxygen species (ROS) and inorganic phosphate are produced during normal muscle contractions, and the accumulation of these factors can produce metabolic fatigue by interfering with the release of SR calcium, or by reducing the sensitivity of contractile molecules to calcium (9). Due to reduced electrical activity, ATP turnover is diminished during muscle disuse. This increases the availability of ADP and inorganic phosphate. In addition, muscle disuse is accompanied by an elevation in ROS which also contributes to muscle fatigue (135). More importantly, ROS plays a greater role in facilitating other catabolic processes during denervation and other models of reduced contractile activity.

1.3.3 Mechanisms of denervation-induced atrophy

Muscle atrophy occurs largely due to a reduction in protein synthesis and an increase in protein degradation (18; 53; 58; 60). The signals that regulate these two processes during muscle disuse are related (143), and the molecular mechanisms controlling this process are similar to other conditions where muscle atrophy is observed, such as muscle wasting diseases and sarcopenia (18; 44; 140). In addition, oxidative stress plays a key role in regulating these processes (78; 133; 138).

As mentioned earlier, the myonuclear domain theory dictates that the number of myonuclei is related to the size of muscle fiber. Therefore it is expected that denervation-

induced atrophy is accompanied with decreases in myonuclei (96). Myonuclei house the DNA which is needed for synthesizing proteins in the muscle. The lack of muscle contractions require less protein synthesis in the muscle, and this holds true for each domain of cytoplasm overseen by individual myonuclei. As a result the muscle undergoes a program to eliminate some of the myonuclei along with a reduction in the cytosolic components. This is achieved through myonuclear apoptosis, where the end product is DNA fragmentation and muscle cell shrinkage (3; 153). However apoptosis only accounts for a small portion of muscle atrophy (4), and other processes help contribute in remodelling the muscle.

Protein synthesis is reduced during denervation because signalling cascades which initiate the translation of protein synthesis are downregulated (10; 55; 101). At the same time, protein degradation is increased as several components of the muscle fiber are targeted to be degraded (14; 15; 55). An important pathway in determining these two processes is the IGF-1/PI3K/Akt pathway (101). Under normal or increased conditions of muscle activity, IGF-1 produced through muscle contractions activates the PI3K-Akt pathway which enhances protein synthesis by activating S6K-mTOR pathway, while inhibiting protein degradation by preventing the translocation of an important transcription factor known as Foxo into the nucleus. The S6K-mTOR pathway activates a number of translation initiating factors whereas Foxo promotes the transcription of genes such as Atrogin, which enhances protein degradation (141; 143). The ubiquitin proteasome system plays a key role in mediating protein degradation, particularly the ubiquitin ligases MAFbx/atrogin-1 and MuRF1 have been identified as crucial regulators

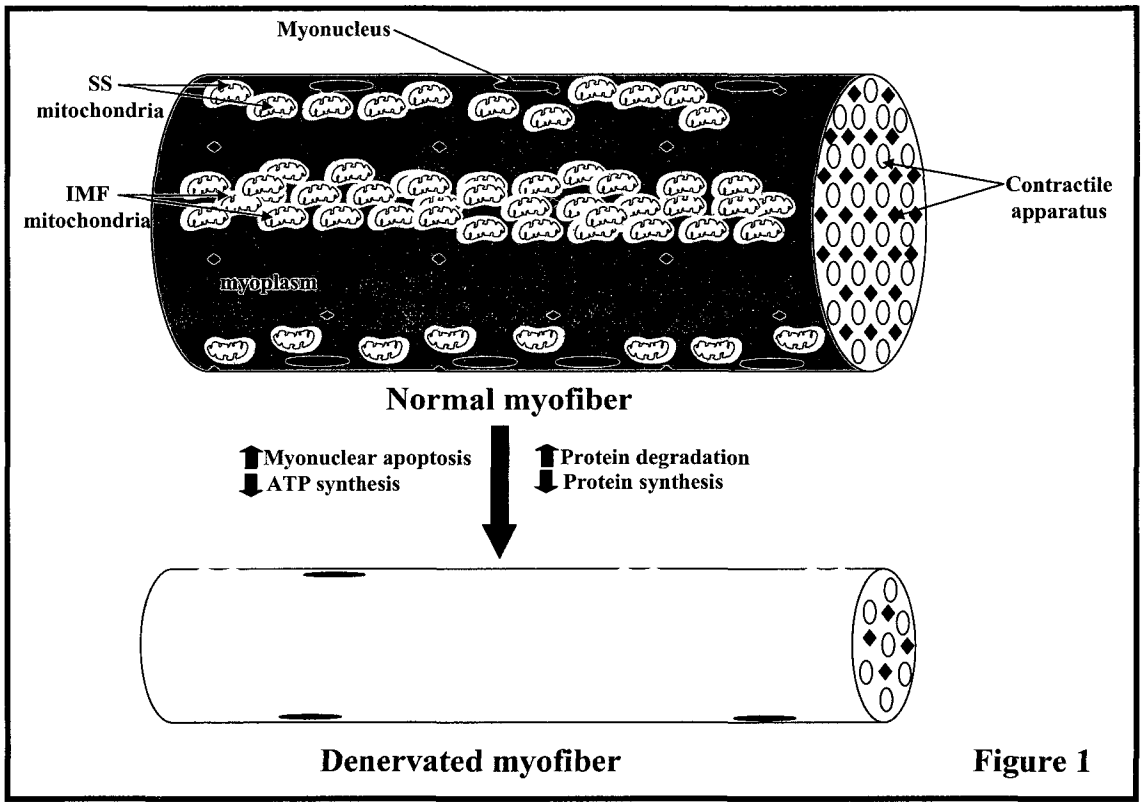

Figure 1: Effect of denervation on skeletal muscle fiber structure and function. Skeletal muscle fibers are multinucleated and contain two distinct subfractions of mitochondria which generate ATP needed by the contractile apparatus. Subsarcolemmal (SS) mitochondria are located peripherally near myonuclei, whereas intermyofibrillar (IMF) mitochondria are intermingled with myofibrils. Denervation leads to myofiber atrophy and an overall reduction in mitochondrial content. This is mediated by parallel increases in protein degradation and decreases in protein synthesis, which leads to a net decrease in muscle protein. Furthermore, diminished contractile activity lowers mitochondrial content, which reduces ATP synthesis in skeletal muscle. There is also an upregulation of mitochondrially-mediated pro-apoptotic events which culminates in myonuclear apoptosis. The combination of the aforementioned processes produce muscle atrophy, reduced force production and increased fatigability.

of muscle mass during disuse (60; 78). During muscle disuse, the absence of contractions does not activate the IGF-1 signalling cascade, and these result in a reduction in protein synthesis and increased degradation. All together, an overall reduction in protein synthesis concomitant with accelerated protein degradation during extended muscle disuse accelerates negative protein balance, and contributes to muscle atrophy.

ROS are produced naturally during muscle contractions and participate in redox reactions necessary for maintaining homeostasis (135). In addition, they also act as important signalling molecules that help regulate normal functioning. Muscle atrophy induced by denervation and other disuse models produce high levels of ROS. When ROS molecules are systematically produced by muscles beyond basal levels, they are capable of causing significant damage to cell structures. Oxidative stress occurs when the muscle is unable to neutralize this rise in ROS with antioxidants (4; 133). The increase in ROS generation comes mainly from the mitochondrial electron transport chain (ETC), but there are also other non-mitochondrial sources such as NADPH oxidase, xanthine oxidase and nitric oxide synthase-induced free radicals (133). In addition to oxidizing cellular contents (inactivating enzymes, oxidizing amino acids) and damaging their structure (lipid peroxidation), ROS are involved in initiating oxidative signalling pathways that promote muscle atrophy. These include the onset of mitochondrially-mediated apoptosis, activation of apoptotic-stimulating kinase 1 (ASK1), lysosomal- (20), calpain- (150) and proteosome-mediated proteolysis (14; 16; 43; 119), and via NF-kB signalling (58; 133; 175). While it is beyond the scope of this review to examine all of the aforementioned

processes, their activation by ROS are related to many of the molecular mechanisms which govern muscle atrophy.

One important yet unresolved question is whether ROS are required for disuse muscle atrophy, or if they only act as secondary messengers in controlling the extent of atrophy. Several laboratories are actively investigating oxidative stress related systems, and although this area of research is still not well understood, it is clear that ROS play a crucial role in mediating denervation-induced muscle atrophy.

2.0 MITOCHONDRIA

Mitochondria are unique organelles as demonstrated by their structure, organization, and arrangement within cells (50). Furthermore, their involvement in a number of cellular functions, which include energy metabolism (180), thermogenesis (52), programmed cell death (4), steroid biosynthesis (136) and intracellular signaling (47; 139; 181), add to their complexity. Mitochondrial biogenesis refers to an increase in mitochondrial volume as well as possible changes in mitochondrial composition (68). Increased mitochondrial synthesis, particularly in skeletal muscle, promotes an increase in oxidative capacity, which can lead to higher muscle endurance (70).

2.1 Ultrastructure and morphology

Mitochondria were originally derived from endosymbiotic prokaryotes (61), and are phospholipid-dense organelles containing hundreds of proteins distributed within four distinct compartments (22). The sub-compartmentalization of mitochondria is an

evolutionary reflection of its endosymbiotic incorporation into eukaryotic cells (94). The mitochondrion contains two membranes which enclose the organelle from outside and within. The outer membrane (OM) contains different channels which allow the transit of both small molecules and large proteins into the organelle (122). Additionally, the OM is involved in the association of mitochondria with the endoplasmic reticulum, which is important for calcium signaling and lipid transport (62; 82). The inner membrane (IM) has different functional properties than the OM, but also possesses proteins for transporting substrates and participating in organelle morphology (36; 38). Furthermore, the IM houses the electron transport chain (ETC) and the ATP-synthase, which are the machinery used for generating ATP by oxidative phosphorylation. The spaces enclosed by the outer and inner membranes are called the intermembrane space and the matrix respectively.

The intermembrane space (IMS) is a highly acidic and oxidizing environment where hydrogen ions are transitorily amassed after being pumped across the ETC during oxidative phosphorylation (OXPHOS). The matrix contains the majority of mitochondrial proteins, several of which are enzymes used in the oxidation of substrates within the Krebs Cycle and in the production of ATP (145). Furthermore, the internal subdivisions of the matrix form a cristae structure, which increases the surface area for reactions. Mitochondria contain its own DNA (mtDNA), which is also found in the matrix. Compared to the nuclear genome, mtDNA is not highly conserved, is more susceptible to oxidative damage (19), and encodes only 37 genes (13 proteins, 2 rRNAs and 22 tRNAs). mtDNA can only be inherited maternally (145), and the lack of protective histones

increases its susceptibility to mutations (166). These factors, coupled with its relatively simple structure (16.5kb), make mtDNA very appealing in the study of evolutionary relationships (33) and mitochondrial diseases (46).

2.1.1 SS and IMF mitochondria

It is possible to study mitochondrial morphology in skeletal muscle using high-voltage electron microscopy (EM), if the muscle fibers are transversely sectioned (85). Mitochondria exist as a reticulum in striated muscle (heart and skeletal), intertwined with the cytoskeleton to form a network that is meshed underneath the sarcolemma and woven into the myofibrils. The main advantage of combining muscle subsarcolemmal (SS) and intermyofibrillar (IMF) mitochondria with the cytoskeletal organization is enhanced function (87), particularly in the permeability and diffusion of gases, as well as substrates such as lipids and ADP. The assembly of mitochondrial lattices with the cytoskeleton determines organelle morphology, structure and function (134). The formation and stability of the reticulum are particularly dependent on the combination of perpetual fusion and fission events which promote elongation and fragmentation, respectively (38).

SS mitochondria primarily function to provide ATP for transmembrane ATPases and other sarcolemma operations such as the active transport of substrates across the membrane. IMF mitochondria, on the other hand, represent the majority (~80%) of muscle mitochondria, and are responsible for synthesizing ATP during muscle contractions. In addition to being localized in divergent cellular compartments, SS and IMF mitochondria have contrasting morphological characteristics. High resolution EM

pictures of skeletal muscle reveal that IMF mitochondria have a denser cristae structure and exist in more extensive mitochondrial networks (86). These differences may be comparable to differential biochemical and functional parameters, which include rates of ATP synthesis, precursor protein import, protein turnover, ETC activity, apoptotic susceptibility and membrane composition (2; 42; 45; 164). However, when exposed to physiological perturbations such as alterations in muscle contractile activity, SS mitochondria are more sensitive in responding to a common intracellular stimulus (1; 3; 149; 163). The reasons for these discrepancies in intracellular arrangement and organelle function within the heterogeneous sub-populations are not clear, but may be related to their relative location to myonuclei as well as differences in protein turnover and import.

2.2 Mitochondrial biogenesis

Mitochondrial content increases through the net synthesis and assembly of proteins derived from both the nuclear and mitochondrial genomes. Mitochondrial biogenesis in skeletal muscle involves a series of complex cellular events, beginning with signalling pathways which bolster the activation of transcription factors, leading to increased mRNA expression of mitochondrial genes. Most proteins found within mitochondria are first translated in the cytosol, and all proteins rely on exclusive passage routes for the transport and assembly into various complexes in existing organelles (67).

2.2.1 Signaling pathways

There have been various investigations into the signal transduction pathways that coordinate mitochondrial proliferation in different tissues. In skeletal muscle, there are three contractile-dependent messengers involved in augmenting mitochondrial content. These identified factors are increased 1) ATP turnover, 2) cytoplasmic calcium (Ca^{2+}) and 3) reactive oxygen species (ROS) production during respiration (68). All of these agents accelerate the transcription of mitochondrial genes by either, directly interacting with transcription factors (TF) or through the activation of downstream kinases or phosphatases (156). In either case, the underlying mechanisms governing the eventual increase in TF-DNA binding are post-translational modifications such as phosphorylation, acetylation, sumoylation and methylation of transcription factors or downstream agents.

First, increased activity in the contractile apparatus of myofibers requires more ATP. This increase in muscle activity lead to the activation of mitogen activated protein kinases (MAPK) such as p38 and ERK 1/2 (95; 188), as well as the metabolic sensor, adenosine monophospate-activated protein kinase (AMPK) (65). This culminates in signalling cascades that promote the transcription of mitochondrial genes in the nucleus. AMPK in particular is a critical contributor to this progression. Depletions in intramuscular ATP can promote the association of two ADP molecules by myokinase to regenerate ATP and produce AMP as a by-product (125). AMP can bind to AMPK, and induce a conformational change in this enzyme which exposes the active site of it

catalytic unit. This exponentially increases AMPK activity, and plays a major role in increasing mitochondrial content in skeletal muscle (186).

Second, skeletal muscle Ca^{2+} is stored in the sarcoplasmic reticulum, and its ionized form acts as an important second messenger during gene induction (34). Muscle depolarization releases Ca^{2+} into the cytosol, and this increase contributes to enhanced mitochondrial gene expression by the activation of multiple calcium-dependent kinases such as the Ca^{2+}/calmodulin-dependent protein kinase (CaMK), calceneurin and protein kinase C (PKC) (40). These signalling agents promote the upregulation of transcriptional regulators and nuclear translocation of transcription factors such as NFAT which promote oxidative capacity (187). Additionally, increased Ca^{2+} can also stimulate AMPK activation and enhance its effects in skeletal muscle (76).

Third, ROS have been shown to mediate the activation of signalling cascades that are needed to promote mitochondrial synthesis. Mitochondria are the major producers of ROS, and the formation of ROS occur during cellular respiration when single electrons being transported in the ETC are inappropriately donated to oxygen (118). Large quantities of ROS are considered deleterious due to their role in promoting protein and lipid peroxidation, DNA mutations and initiating cell death (51). However, physiological concentrations of ROS are important for normal cell function, and modest increments in ROS during muscle contractions are conducive to altering the activity of downstream transcription factors during mitochondrial biogenesis. The mechanisms mediating these changes have not been effectively elucidated. However, in addition to directly interacting with regulators of transcription, ROS may also potentially moderate the activity of other

signalling molecules with their downstream targets in a synergistic fashion. One such example includes the intricate relationship between ROS, AMPK activation and the gene expression of the coactivator PGC-1α (75). Increased ROS production during muscle contractions increases PGC-1α promoter activity, both directly and via ROS-induced decreases in ATP levels, which activates AMPK. Increased AMPK function then acts on its downstream targets to supplement greater promoter activity.

2.2.2 Transcriptional activation

The signals discussed above lead to increased expression and activation of transcription factors, which then increase the transcription of nuclear genes encoding mitochondrial proteins (NUGEMPs) by binding to the DNA promoter elements in nuclear genes which encode these proteins. There is an increase in the mRNA expression of transcription activators, and these events precede any alterations in mitochondrial gene expression and content. Various genes are upregulated within a short time frame (minutes-hours) following the activation of kinases. Usually, the first increases are observed in the immediate early genes (c-fos, c-jun), early growth response gene-1 (Egr-1) and specificity protein 1 (Sp1) (68; 70). Egr-1 and Sp1 are involved in regulating the gene expression of cytochrome *c*, an important component of the ETC often used as an indicator of mitochondrial biogenesis (74).

Soon thereafter, there is an increase in the mRNA abundance of other important transcriptional regulators such as the peroxisome proliferator-activated reception-γ coactivator-1α (PGC-1α) (189), and the nuclear respiratory factors (NRF)-1, and -2 (24).

Although PGC-1α is not a transcription factor, it is arguably the most critical regulator of mitochondrial biogenesis. PGC-1α interacts with other transcription factors to coactivate the transcription of other regulators, including its own expression, as well as other NUGEMPs (176). PGC-1α also moderates the expression of NRF-1 and NRF-2, which regulate the expression of numerous NUGEMPs. The regulation of NRF-1 by PGC-1α is particularly important because, in addition to a variety of mitochondrial proteins, NRF-1 also induces the expression of mitochondrial transcription factor A (Tfam) (73). Tfam is important for mtDNA replication, transcription and repair, and its expression determines the fate of all the proteins encoded by the mitochondrial genome (144). It is also important to note that PGC-1α activity may be regulated by post-translational modifications. AMPK can phosphorylate PGC-1α to increase its interactions with transcription factors. Additionally, the histone deacytelase Sirt1, which is part of the Sirtuin family of longevity proteins, has been shown to control the nuclear-localization of PGC-1α by modifying its acetylation status (195).

2.2.3 Post-transcriptional regulation

Post-transcriptional events influencing mitochondrial biogenesis include the regulation of mRNA decay and synthesis of NUGEMPs in the cytosol, the import and assembly of proteins into multi-subunit complexes in mitochondria, along with the integration of mitochondrial genome expression.

Following the increase in transcription of NUGEMPs, the nuclear export of mRNA into the cytoplasm increases its abundance, where it can either be translated into

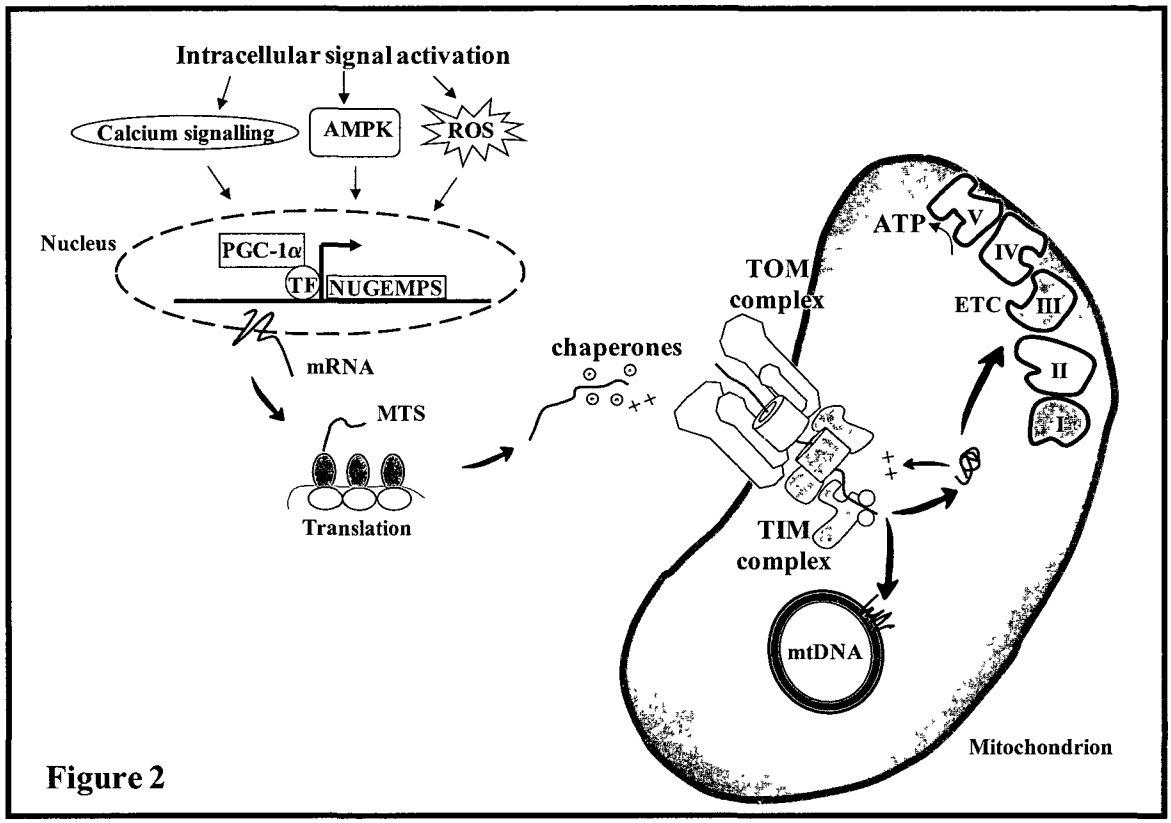

Figure 2: Mitochondrial biogenesis in skeletal muscle. There are multiple signaling pathways initiated via alterations in Ca^{2+} flux, reactive oxygen species (ROS) production and the activation of AMP kinase (AMPK). These signaling pathways provoke changes in the transcription of nuclear genes encoding regulatory proteins such as PGC-1α. Once synthesized, PGC-1α modulates the transcription of other regulatory genes (transcription factors) as well as nuclear genes encoding mitochondrial proteins (NUGEMPS) such as mitochondrial transcription factor A (Tfam) as well as proteins involved in the electron transport chain (ETC). Following mRNA translation, these nuclear-encoded mitochondrial proteins are targeted to mitochondria via chaperones and translocated into the organelle via the protein import machinery, which consists of the TOM and TIM complexes. Nuclear- and mtDNA-transcribed proteins are assembled to form the multi-subunit complexes (I to V) that are incorporated into the ETC where they are required for oxygen consumption and ATP synthesis.

proteins by ribosomes, or be degraded by cytosolic RNAses (66). Reducing the rate of mRNA decay is beneficial for facilitating mitochondrial content, as a lower rate of degradation increases the feasibility of generating a mitochondrial protein through translation. mRNA stability is regulated by the binding of stabilizing or destabilizing agents to non-coding regions of processed mRNA. These portions of mRNA that do not code for protein are present at the proximal and distal end, and are known as the 5'- and the 3'-untranslated regions (UTRs) (108). The 5'-UTR contains sequences important for initiating translation and may also contain binding sites for proteins that affect mRNA stability. However, it is the 3'-UTR which is believed to be more important in determining mRNA survival. It consists of several regulatory components that serve as putative binding sites for cytosolic factors. One important feature is the AU-rich element (ARE), whereby mRNAs possessing this sequence are far more susceptible to rapid degradation in the cytosol. ARE-mediated mRNA decay is initiated by deadenylation of the PolyA tail, and is subsequently followed by the cleavage of the entire transcript by a conglomerate of exonucleases termed the exosome (48). The kinetics of mRNA decay may be delayed if the initiation of deadenylation is offset by the transient association of the ARE with RNA-binding proteins (RBPs) such as the Human-antigen R (HuR). HuR has been known to stabilize the mRNA of a number of skeletal muscle and mitochondrial genes (30). On the other hand, the ARE-associated factor-1 (AUF1) is yet another RBP that binds to the ARE of mRNA, but in contrast to HuR, it destabilizes the mRNAs that it associates with. There is some evidence to suggest that both stabilizing and destabilizing RBPs may simultaneously compete for the same ARE binding site (92). Thus, the activity

and expression of antagonizing RBPs under altered physiological states represents yet another important determinant of mitochondrial content.

As mentioned above, Tfam is an important regulator of mitochondrial biogenesis because of its role in mitochondrial genome expression (144). Since all of the proteins encoded by mtDNA are subunits of the respiratory chain, the regulation of ATP synthesis in the whole cell is partially dependent on the mitochondrial genome. Thus, the stability and transcriptional activity of mtDNA is critical for maintaining normal function. Tfam primarily functions to upregulate the mRNA expression of mitochondrial genes by binding to the light- and heavy-strand promoter regions within mtDNA. Additionally, Tfam is essential for mtDNA copy number, as it can indirectly initiate replication during transcription (79). Thus, Tfam expression is closely correlated to mtDNA abundance, and may also play a crucial role in maintaining the integrity of mtDNA by serving as a nucleoid structure (80). Since Tfam is a nuclear-encoded protein, it must also be transcribed and processed like other NUGEMPs that need to be incorporated into existing mitochondria. Thus the regulation of the mitochondrial genome is dependent on the expression and activity of Tfam, which itself is induced through nuclear-related events.

2.3 Mitochondrial function

The main function of mitochondria is regulating cell metabolism by producing ATP. They play a key role in energy conversion by oxidizing pyruvate, fatty acids or amino acids, transporting these oxidized metabolites into the citric acid cycle, thereby generating intermediates for the electron transport chain. ETC activity is used to drive the

formation of a proton motive force (ΔP), for the generation of ATP through the coupling of oxidized intermediates in the ETC with the phosphorylation of ADP molecules. In addition to producing ATP by OXPHOS-linked reactions, this system also plays a role in thermogenesis by the uncoupling of the ATP synthase to the electron transport chain, which unleashes the energy stored in the proton motive gradient as heat (29).

2.3.1 Respiration

ATP may be generated from anaerobic glycolysis, but this reaction is generally inefficient in meeting the cellular demands during most physiological conditions. The energy yield from the end-products of glycolysis may be further increased by their oxidation in Krebs' Cycle. A complete series of enzymatic reactions produce three molecules of NADH and one molecule of $FADH_2$. The potential energy stored within these reduced intermediates can be released and coupled during OXPHOS to create ATP.

During OXPHOS, the reduced intermediates generated from Krebs' Cycle are oxidized by the ETC where they donate electrons to the appropriate respiratory complex. The energy generated from transferring the electron is used to pump hydrogen ions, which dissociate from NADH/$FADH_2$ and move across the IM. Respiratory enzymes of the electron transport chain comprise the following multisubunit holoenzymes: NADH dehydrogenase (complex I), succinate dehydrogenase (complex II, SDH), cytochrome bc_1 (complex III) and cytochrome *c* oxidase (complex IV, COX) (63). Protons are only pumped across complexes I, III and IV, and accumulate in the IMS. The brief accumilation of protons creates an electrochemical gradient across the IM, which is

referred to as the membrane potential (Ψ_m). Furthermore, since the protons being pumped into the IMS are going against the diffusion gradient, they have a strong drive to re-enter the matrix, so that they may achieve equilibrium again. This propelling energy is the (ΔP).

The proton motive force is transduced into chemical energy by the ATP-synthase complex, which harness this energy and converts it to a high energy phosphate bond between an ADP and an inorganic phosphate (P_i). Meanwhile, the coupling of the ΔP to ATP-generation dissipates Ψ_m. It is also feasible to decrease Ψ_m without having ATP-synthesis. The movement of protons in the absence of ADP-phosphorylation is refereed to as proton leaking (28). This process may be aided by a special family of uncoupling proteins, which serve as a channel for protons in the IM (29). In this case, the energy buildup of ΔP is dissipated as heat.

Additionally, the electrons accumulated in the ETC during this reaction must be terminally donated to oxygen at complex IV in order to facilitate incoming oxidized substrates. In isolated mitochondrial preparations, oxygen consumption during the presence of ADP is referred to as 'active' (or state 3) respiration, whereas oxygen consumption in the absence of ADP phosphorylation is 'passive' (or state 4) respiration. State 4 respiration is essentially a measure of uncoupled respiration, and thus the ratio of state 3/state 4 respiration is a good indicator of ETC coupling, providing a crude assessment of the sample's bioenergetic status. When compared to SS mitochondria, isolated IMF subfractions have approximately three-fold and two-fold higher rates of state 3 respiration and ATP synthesis, respectively (42). This discrepancy in OXPHOS-

related measures may be a reflection of their localized function, and this is important to acknowledge since respiration is coupled to many mitochondrial processes including protein import.

Mitochondrial oxygen consumption is a good measure of overall organelle function, as the transfer of electrons from complex IV to oxygen is dependent on the successive completion of previous enzymatic reactions. Alternatively, other measures such as the maximal activity of Krebs' Cycle or respiratory chain enzymes may also be used to gauge mitochondrial function. Furthermore, Ψ_m is a critical reflection of organelle viability and subsequent function/dysfunction. Proper mitochondrial function is critical for post mitotic cell cycle proliferation, iron sulfur biosynthesis and calcium signaling/storage (34; 137). Mitochondria with high Ψ_m are conducive to mitochondrial events important for mitochondrial biogenesis, such as organelle fusion and protein import (38; 161). On the other hand, mitochondria with low Ψ_m display poor coupling of the ETC, generate less ATP, are more likely to undergo fission events and are generally considered dysfunctional.

2.3.2 ROS production

Normally, during OXPHOS, oxygen accepts a pair of electrons at the COX complex and combines with protons in the matrix to form water. As referred to earlier, it is possible for electrons passing down the ETC to form highly unstable molecules called reactive oxygen species (ROS), as a result of oxygen picking up an electron in a non-terminal fashion. A small percentage of total oxygen consumption is always leaking out

of complexes I and III on both the matrix side and the IMS side of the ETC. However, the presence of antioxidants such as manganese superoxide dismutase (MnSOD), catalase and glutathione peroxidase (GPx) serve to neutralize the toxic effects of ROS on cellular components (11).

There is an inverse relationship between mitochondrial ROS generation and oxygen consumption, as ROS generation is lower during state 3 respiration when compared to state 4 oxygen consumption (70). Additionally, comparing the two subfractions of mitochondria reveals higher rates of ROS production in the SS sub-population, which also display lower rates of respiration. Greater rates of basal ROS production and fluctuations to physiological perbutations may contribute to the lability of SS mitochondria in adapting to different stimuli.

Increased ROS production by dysfunctional mitochondria has been implicated in mitochondrial myopathies, sarcopenia, cell death pathways, neurodegenerative diseases and conditions of chronic muscle disuse. A common feature among all of these detrimental conditions is oxidative stress, a state when the cell's anti-oxidant mechanisms are unable to neutralize a sudden increase in ROS. Increased intracellular ROS can alter the conformation and activity of proteins by oxidizing vulnerable residues. Redox-sensitive proteins which contain thiol residues are susceptible to ROS-mediated modifications (51). Alternatively, ROS can directly damage protein structures and lipid bilayers through carbonylation and peroxidation reactions. ROS-mediated oxidation of nucleic acids has also been known to cause DNA mutations (23). mtDNA is more

susceptible to oxidative stress-induced mutations because unlike nuclear DNA, they lack histones and are also closer to the site of ROS production.

Overall, ROS are involved in nearly every instance of mitochondrial dysfunction. Dysfunctional mitochondria have poor coupling of the ETC and ATP production, which are more likely to generate ROS. Due to the close interaction of mitochondria and ER in regulating cellular Ca^{2+} levels, dysfunctional mitochondria are usually accompanied by impaired Ca^{2+} storage and functioning, which can lead to cell death (31). Increases in ROS and Ca^{2+} promote the opening of the mitochondrial permeability transition port (mtPTP), which leads to Ψ_m dissipation and mitochondrial swelling. Both of these processes inactivate the ATP synthase, which leads to necrosis. Additionally, the swelling of the matrix can dislodge harmful proteins that reside in the IMS, which can exit the mitochondria through the mtPTP and initiate pathways leading to apoptosis (84). Furthermore, ROS-induced increases in Bcl-2 family of pro-apoptotic protein signaling can promote OM permeabilization and the activation of caspase-dependent and independent apoptosis (41). Finally, the removal of mitochondria by autophagy is dependent on the Ψ_m of mitochondria. Since dysfunctional mitochondria have poor mitochondrial function, they are more likely to undergo mitophagy (83; 127).

2.4 Chronic muscle disuse-evoked changes in mitochondria

Chronic disuse models like denervation are effective in rapidly reducing muscle mass and force production. Another characteristic feature of long-term disuse is a reduction in mitochondrial content and function. Electron microscope pictures of

chronically disused muscle reveal a disruption of the mitochondrial reticulum, and increased occurrences of fragmented mitochondria (35). Furthermore, key mitochondrial enzymes such as COX, MDH and SDH are diminished in denervated muscle, illustrating a reduction in oxidative capacity. Also, functional assays performed on isolated mitochondria from denervated muscle show reduced rates of respiration along with high levels of ROS production (3; 126). To help elucidate the mechanisms regulating these changes, it is useful to identify alterations in the regulation of mitochondrial biogenesis.

Due to the lack of contractile activity in skeletal muscle, the normal signaling events regulating mitochondrial biogenesis are not activated. Reduced ATP turnover is apparent during muscle disuse since the contractile apparatus is not active. Although there is an increase in cytoplasmic calcium, these ions are involved in promoting calpain-mediated proteolysis (158), instead of activating kinases involved in mitochondrial proliferation. Finally, the increase in oxidative stress is evident during dysfunction, and negates any signaling effects directed toward mitochondrial transcriptional activation which are observed with modest increases in ROS.

At the transcriptional level, important mediators of mitochondrial biogenesis such as Tfam and PGC-1α are severely affected. The mRNA expression of PGC-1α has been shown to decrease by as much as 70% after just two days of denervation (142). This drop is critical because of its importance in regulating so many other transcription factors and NUGEMPs. Restoring PGC-1α in denervated muscle has been shown to prevent muscle atrophy during disuse. Additionally, the lowered protein content of Tfam is not favourable for mtDNA replication and transcription (3). Other events regulating

mitochondrial biogenesis downstream of transcription such as adaptations in the protein import pathway have not been well elucidated, and require more investigation.

Denervation of skeletal muscle produces higher rates of mitochondrial degradation which outweigh the rate of mitochondrial synthesis in atrophying muscle. Increased ROS production contributes to protein degradation, cell death pathways and organelle dysfunction (4). When comparing SS and IMF mitochondria isolated from denervated muscle, there is a greater reduction in SS, compared to IMF, mitochondrial content. Also, SS mitochondria generate higher amounts of ROS after denervation (3). The effect of prior contractile activity or the administration of antioxidants, do not attenuate most pro-apoptotic and other detrimental effects observed with denervation (126).

3.0 MITOCHONDRIAL PROTEIN IMPORT MACHINERY

New mitochondria cannot be produced by *de novo* synthesis. Mitochondria contain about 1500 different proteins, of which only 1% are synthesized on ribosomes found within the mitochondrial matrix. The majority of proteins found in this organelle are encoded by nuclear genes which are translated by cytosolic ribosomes, and subsequently imported and assembled into existing mitochondria (123).

Recent findings have also linked the processes of mitochondrial protein import and assembly to that of mitochondrial morphology and dynamics (161). Additionally, this system may play a key role during the mediation of mitochondrially-mediated apoptosis (129). The mitochondrial protein import system is adaptable, and can be altered by

physiological perbutations in energy status and hormones (69; 71). Also, errors in the molecular mechanisms of protein import can lead to several diseases (98).

All nuclear-encoded proteins enter mitochondria via the translocase machinery of the outer membrane (TOM complex), and are then sorted to one of the four sub-compartments of mitochondria by the interaction of the targeting information encoded within the imported protein and the translocation machinery (36). The components of the import machinery actively interact with each other during import, processing and assembly.

3.1 Mitochondrial protein unfolding and trafficking

Before being assimilated into existing organelles, mitochondrial preproteins synthesized in the cytosol are termed precursor proteins. All precursor proteins contain targeting and sorting signals which direct them to different sorting machineries of the import apparatus. Furthermore, precursor proteins cannot pass the translocase machinery while they are folded, and require cytosolic chaperones which help unfold them into import competent states, and even guide them toward import receptors.

3.1.1 Mitochondrial targeting signals

Approximately 40% of mitochondrial precursor proteins possess a positively charged α-helix at the N-terminus which is cleaved after import (59). This portion of the precursor includes crucial mitochondrial targeting signals (MTS), whereas the remainder of precursor proteins that lack this α-helix have their targeting information within the

mature part (123). The MTS helps guide precursor proteins towards the organelle and contains information that will sort them into the outer membrane (OM), inner membrane (IM), intermembrane space (IMS) or the matrix.

Cleavable presequences are typically 15-100 amino acids long and were the first class of presequences to be discovered (25). All precursor proteins destined to the matrix contain this signal. Several IM and IMS proteins also contain presequences, but they are not completely cleaved off (36). The targeting and sorting signals of precursor proteins may be further differentiated if they possess two (bipartite) or more signals, which require further processing. The nature of these additional second sorting signal may also determine the sorting of the precursor protein. For instance, proteins destined for the IM and IMS contain almost identical MTS and are sorted very similarly, except for a hydrophobic sorting signal which differentiates the two subsets (123). Finally, mitochondrial IMS proteins contain a special variety of internal signals rich in cysteine residues, which are particularly important as these proteins undergo several redox steps during import (169).

Signal anchor proteins such as the OM receptors, Tom20 and Tom70, contain a non-cleavable MTS at the C-terminus. Unlike the precursor variants of the IM and IMS mentioned earlier, it is possible to have a presequence-like internal signal present after the hydrophobic region (123).

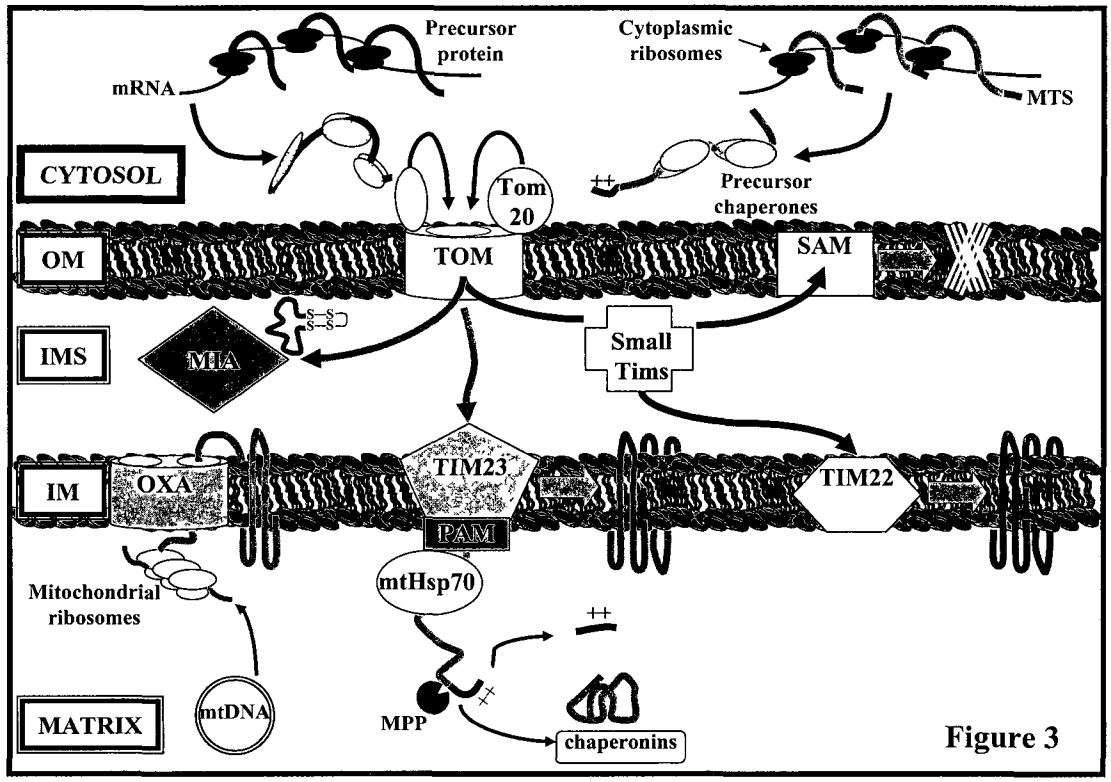

Figure 3: Protein import and sorting in mitochondria. Nuclear gene-encoded mitochondrial proteins (NUGEMPs) and are synthesized on cytosolic ribosomes as precursor proteins. They contain targeting signals that are either internalized or located at the N-terminus of the precursor. These signals guide precursor proteins to one of the four mitochondrial compartments: outer membrane (OM), intermembrane space (IMS), inner membrane (IM) or the matrix. Precursor proteins form complexes with cytosolic chaperones which transport them to the mitochondrial surface. Preproteins possessing N-terminal mitochondrial targeting sequences (MTS) interact with Tom20. The translocase of the outer membrane (TOM complex) is the general entry gate for all NUGEMPS. The sorting and assembly machinery (SAM complex) is committed to the insertion of β-barrel proteins in the OM, after they are chaperoned through the IMS by small Tim proteins. Hydrophobic inner membrane proteins with internal targeting sequences are guided through the IMS by small Tim proteins towards the TIM22 complex, where they are inserted into the inner membrane. Proteins encoded by mitochondrial DNA (mtDNA) are synthesized on ribosomes found in the matrix, and are incorporated into the inner membrane via the OXA complex. The majority of imported proteins are processed by the TIM23 complex, which either translocates precursor proteins into the matrix or laterally sorts preproteins into the inner membrane. Matrix-destined proteins are actively translocated into the compartment by the ATP-driven import motor (PAM), where mtHsp70 is the central component. Upon arrival in the matrix, the MTS is cleaved off by mitochondrial processing peptidases (MPP). The processed mature protein is then refolded to its native state by matrix chaperonins.

3.1.2 Cytosolic chaperones

As stated previously, precursor proteins need to be in proximity to the mitochondria, and in an import-competent state, in order to successfully transverse the outer membrane. The translocation and unfolding of preproteins is performed by one or more cytosolic chaperones, which include the cytosolic heat shock protein 90 (Hsp90), heat shock protein 70 (Hsp70), and the mitochondrial import stimulation factor (MSF) (90; 120).

Hsp90 is believed to exclusively chaperone preproteins that only contain an internal targeting sequence (71). On the other hand, Hsp70 has the ability to bind to precursors with, or without, the N-terminal targeting sequence. Hsp70 activity is determined, in part, by its interactions with additional cytosolic factors that act as co-chaperones (173). For instance, the type I DnaJ homologues, DjA1 and DjA2, enhance the binding of Hsp70 to presequence containing precursors, and subsequently transfer them to the mitochondrial outer membrane. Interestingly, Hsp70 acts in conjunction with Hsp90 when guiding proteins without a presequence (56). The role of chaperones in guiding proteins with C-terminal targeting sequences is not known.

Both Hsp70 and Hsp90 require ATP to actively unfold and guide substrates to the mitochondria, although there is some debate surrounding the energy requirements for matrix-destined precursor translocation (13). Finally, MSF also acts in an ATP-dependent process, and has been suggested to have a higher affinity for precursor proteins with an internal targeting sequence (128). However, unlike Hsp70 and Hsp90, its properties have not been well documented.

3.2 Protein import machinery of the outer membrane

At the outer mitochondrial surface, all precursor proteins must interact with protein translocases located on the outer membrane in order to enter the organelle. The outer membrane houses the translocase of the outer membrane (TOM) complex, which is the entry gate for almost all precursor proteins, along with the sorting and assembly machinery (SAM) responsible for aggregating β-barreled proteins into the outer membrane. The outer membrane also contains a few proteins such as Mim1, Tom37 and Tom34 which are involved in import and sorting, but are not components of the SAM and TOM complexes.

3.2.1 TOM complex

The TOM complex is composed of the general import pore (GIP) and the primary receptors, Tom20 and Tom70 (25). Tom40 and Tom22 form the major foundation of the GIP as a highly stable structure with unusual resistance to cytosolic perturbations such as urea and alkaline pH (104). The inclusion of three small Tom proteins: Tom7, Tom6 and Tom5, completes the composition of the GIP (71; 123).

At the outer mitochondrial membrane, precursor proteins with cleavable presequences interact with Tom20, whereas Tom70 acts as a receptor for preporteins with internal signals (36; 159). Both Tom20 and Tom70 transfer precursors to Tom22 and eventually Tom40, but do so using different mechanisms. In the first instance, precursors with cleavable presequences undergo a series of sequential binding reactions: Tom20-Tom22-Tom5-Tom40-Tom7-Tom22 (IMS domain). This chain of binding events

continues with the translocase proteins of the inner membrane. This series of events is referred to as the "binding chain" hypothesis (57). Alternatively, with OM and IMS proteins, there is a second mechanism called the "translocation in loop formation", where the series of transfers is simply Tom70-Tom22-Tom40. However, both the C- and N-termini of precursors of carrier proteins are exposed to the cytosol, whereas the middle portion reaches the IMS first (185).

It is important to note that Tom22 possesses receptors for preproteins at both the outer and inner sides of the outer membrane (194). Additionally, its membrane domain regulates the organization and integrity of the TOM complex by interacting with Tom40. Tom40 is the core of the TOM complex, and it forms the channel used by precursors to enter the organelle (36; 123; 161). Finally, Tom5, Tom6 and Tom7 are believed to participate in the assembly and dynamics of the TOM complex, along with the transfer of precursors from the receptor to Tom40.

3.2.2 SAM complex

The SAM complex is responsible for the insertion and sorting of β-barrel proteins and possibly α-helical proteins into the outer membrane. β-barrel proteins such as VDAC and Tom40 have segments that transverse the outer membrane, and its insertion is dependent on a number of protein complexes that mediate its insertion (91). The SAM complex is composed of Sam50, Sam35, Sam37 and Mdm10.

Sam50 is the central component of the SAM complex, which is responsible for the insertion of β-barrel proteins into the lipid bilayer (89). β-barrel proteins designated for the outer membrane interact with Sam35 (metaxin2), which has a recognition site for

the C-terminals of these proteins (110). The integrity of the SAM complex is maintained by Sam37 (metaxin1), which stabilizes Sam50. Additionally, Sam37 has been shown to serve as a docking site for MSF-mediated precursor proteins (88). Mdm10 is an assembly protein which is especially important in the assembly of the TOM complex (103).

β-barrel proteins initially enter the IMS via the TOM complex, where IMS chaperones direct precursors to the SAM complex (91). However the mechanisms regulating other α-helical proteins with N-signal and C-terminal anchors, as well as multiple transmembrane segments, are not well elucidated, and there is no evidence linking them to SAM activity.

3.2.3 Other receptors

Translocases involved in the import and assembly of outer membrane proteins which are not members of either the TOM or SAM complex include Mim1, Tom37 and Tom34. Mim1 plays an important role in the efficient assembly of the TOM complex (97; 178). Specifically it is required for the insertion of Tom20 and Tom70, α-helical proteins whose assembly into the TOM complex has not been fully elucidated (21; 72). Additionally, Mim1 also associates with the SAM complex during Tom40 biogenesis where it supports the integration of the Tom40 precursor into the outer membrane.

Tom37 is believed to be a docking site for precursors chaperoned by MSF (71), whereas Tom34 is portrayed as a peripheral OM protein with a primarily cytosolic domain (88; 116). Furthermore, Tom34 contains a tetratricopeptide domain, similar to that found in Tom70 (39), and may influence the import of Tom70-dependent proteins

like metabolite carriers. However, Tom34$^{-/-}$ mice showed no differences in mitochondrial import when compared to wild type mice, and thus this protein does not appear to be a critical regulator of the import process (167).

3.3 Presequence pathway and translocase coupling

The majority of mitochondrial proteins are found in the matrix, and are co-ordinately imported by the TOM complex and the TIM23 complex. This was also the first discovered mitochondrial import pathway. Matrix-destined protein import utilizes both ATP and Ψ_m as driving forces for translocation. The TIM23 complex translocates all matrix proteins, most IM proteins along with several IMS proteins (177). All of the preproteins imported by the TIM23 complex contain a cleavable presequence. In addition to being one of the major sorting complexes in mitochondria, the TIM23 complex is arguably the most dynamic and sophisticated amalgamation within the entire protein import and assembly system.

When inactive, the TIM23 complex is simply composed of four components: Tim23, Tim50, Tim17 and Tim21. However, the introduction of precursor proteins with cleavable N-terminal sequences from the IMS to the IM activates the TIM23 complex, which culminates in the formation of a TOM-TIM super-complex (37). Here, the TIM23 complex is capable of assuming one of two distinct forms: 1) association with the motor apparatus, dedicated to driving preproteins into the matrix, and 2) association with complexes III and IV of the ETC for the lateral sorting of precursors into the inner

membrane. The TIM23 complex has the capacity to dynamically switch from one state to another (112).

Tim50 is the IMS receptor of the TIM23 complex, and it acts as a gateway to the Tim23 channel, keeping it closed in the absence of precursor proteins to prevent the leakage of ions across the inner membrane (102; 191). Tim23 is the main translocase protein of this complex, and all the precursor proteins pass through its channel pore. Tim17 is involved during both lateral sorting of preproteins, as well as during motor recruitment of the PAM complex (37; 99).

Precursor proteins containing a hydrophobic sorting signal downstream of the matrix-targeting signal get arrested during transit by Tim17, and are released into the inner membrane by the lateral opening of the Tim23 channel (99). Tim21 modulates Tim23 activity by interacting with the TOM complex, as well as complexes III and IV of the respiratory chain. Interestingly, Tim21 acts as a link connecting the TIM23 complex to the respiratory chain during the lateral sorting of precursors, and is also the only fully dissociated protein during matrix translocation (111). The import pathway of inner membrane and matrix proteins is distinguished by the presence of a hydrophobic sequence within the precursor.

3.3.1 Association with import motor (TIM23-PAM)

Most proteins entering the TIM23 complex are imported into the matrix, which is mediated by the matrix import motor. The ATP-driven import motor (PAM) consists of the mitochondrial matrix chaperone Hsp70 (mtHsp70) which is associated with the

adaptor protein Tim44. The family of J-proteins: Pam18, Pam16 and Pam17, along with the nucleotide exchange factor, mtGrpE complete the motor (36).

Protein translocation into the matrix is mediated by mtHsp70, which binds to precursor proteins in an ATP-dependent and sequential manner (147). There are two models proposed for how mtHsp70 drives protein translocation into the matrix. In the Brownian ratchet model, mtHsp70 molecules bind to the precursor protein during import to prevent retrograde transport (193). This is followed by another mtHsp70 molecule which directs an inward movement of the protein. Alternatively, the power stroke model states that mtHsp70 is tethered to Tim44, which changes its conformation every time mtHsp70 actively pulls the preprotein into the matrix (146). This model also uses several mtHsp70 molecules to import proteins into the matrix. Functional studies using yeast mutants to verify the two hypotheses have provided sound evidence for each hypothesis (170; 174). It is likely that a combination of pulling and trapping mechanisms govern the matrix motor during import.

J-proteins are a class of molecular chaperones that serve to stimulate the activity of Hsp70s and are abundant in locations where Hsp70 is needed in performing cellular functions (81; 190). Pam16 is a J-like protein, which forms a module with and controls DnaJC19 (Pam18) activity (182). In mammals, the ortholog of Pam16 has been reported as mitochondria-associated granulocyte macrophage colony stimulating factor signalling molecule (or Magmas). Magmas plays a critical role in positioning J-proteins with Pam18, and thereby potentially regulating the import motor activity in mammalian

systems (151). Magmas has been proposed to function as a signalling molecule that may also control anaerobic metabolism and apoptotic susceptibility (77).

Recently, a protein called Tam41 has been identified near the TIM23-PAM complex which may be important for the maintenance of the motor complex (90). Additionally, Tam41 is involved in cardiolipin biosynthesis. The TIM23 complex is embedded within a cardiolipin-rich lipid bilayer, and is an important determinant of protein import (67).

One example of a mitochondrial protein that is imported through the TIM23-PAM complex is ornithine transcarbamylase (OCT). OCT is part of an enzyme system that converts ammonia, a toxic by-product of amino acid metabolism, to urea. Specifically, OCT catalyzes the reaction of ornithine with carbomyl phosphate to form citrulline (165). The OCT precursor protein has a N-terminal extension of 32 amino acids, which is cleaved off by a matrix protease to a transient intermediate, and eventually to the mature protein (124).

3.3.2 Association with ETC (TIM23-SORT)

Precursor proteins traveling through the TIM23 complex containing a presequence-like internal signal are sorted through Tim23 into the inner membrane. As alluded to earlier, the hydrophobic sorting signal present in this presequence arrests matrix import, and causes a conformational switch from the TIM23-PAM to the TIM23-SORT pathway (37). Tim21 serves as a gateway to the respiratory chain and the lateral opening of the Tim23 channel subsequently delivers precursor protein into the inner

membrane (132). This mechanism also supports the hypothesis of protein import being coupled to ETC activity.

3.4 Inner membrane carrier pathway (TIM22 complex)

Proteins responsible for the exchange of metabolites are found in the inner membrane. The import and consequent insertion of these precursor proteins are different than the presequence-containing proteins (116; 159). After being recognized by Tom70 and subsequently entering the TOM complex, the small Tim chaperones of the IMS shuttle the preproteins toward the TIM22 complex (71). This complex consists of Tim18, Tim22, Tim54, and a membrane-bound chaperone complex composed of Tim9, Tim10, and Tim12. The precursor proteins are inserted into the inner membrane by the channel-forming Tim22 protein in a membrane potential ($\Delta\Psi$)-dependent manner.

Several metabolite carrier proteins, such as the phosphate carrier (PiC) can be sorted to either the TIM22 pathway or the TIM23 pathway for its import (192). Normally the import of PiC requires the Tim9-Tim10 and TIM22 complex in order to be inserted into the inner membrane. However, the presence of a conserved internal latent signal allows for sorting through the TIM23 pathway in the event of reduced interactions with Tim9-Tim10 complex, or when the import competence of the TIM22 complex is compromised (56).

3.5 Mitochondrial intermembrane space chaperones and import

The intermembrane space between the outer and inner mitochondrial membranes mainly functions as a reservoir for protons as they are pumped across the matrix during oxidative phosphorylation (67). Additionally, during protein import, several hydrophobic precursor proteins are guided through the IMS by a group of small redox-sensitive Tim chaperones (169). These IMS chaperones, along with other resident redox proteins, contain disulfide bonds. The formation of disulfide bonds is mediated by the import of cysteine-rich proteins by the mitochondrial intermembrane space assembly (MIA) pathway (36).

3.5.1 Intermembrane space import chaperones

There are several Tim proteins organized in complexes which mediate intermembrane space import. The main chaperone complexes include Tim9-Tim10, Tim8-Tim13 and Tim12-Tim9-Tim10 (184). Both the Tim9-Tim10 and Tim8-Tim13 complexes are involved in guiding hydrophobic inner membrane proteins with internal targeting sequences, such as metabolite carrier proteins, through the IMS.

Additionally, Tim9-Tim10 is the major chaperone complex facilitating β-barrel precursors to the SAM complex (91). Finally, the complex composed of Tim9, Tim10 and Tim12 is bound to the TIM22 complex, and it guides the insertion of proteins into the channel-forming Tim22 protein in a ψ_m-dependent manner (37; 123). The Tim9-Tim10 and Tim12-Tim9-Tim10 chaperone complexes are essential in mediating protein import, and are assembled by the MIA pathway (109).

3.5.2 Mitochondrial intermembrane space assembly (MIA) pathway

The import of intermembrane space proteins with disulfide bonds relies on the mitochondrial intermembrane space assembly (MIA) pathway (169). Precursors are imported via a disulfide exchange relay with two main components, Mia40 and Erv1, along with the support of Hot13, a zinc-binding protein (105). However, this pathway has never been characterized in mammalian cells.

Proteins containing cysteine-rich residues are imported into the IMS, oxidized by Mia40, which forms disulfide bonds in these IMS precursors. This substrate then participates in a series of disulfide exchange reactions through Erv1, where electrons are donated to different acceptors (117). Eventually this cycle is terminated when the exchange reactions generate an assembled complex, and Mia is re-oxidized by Erv1, which is mediated by Hot13 (160).

Additionally, the electrons generated in this pathway may either be shuttled to cytochrome *c*, and eventually to the ETC, or the electrons may bypass the requirement of the ETC, and instead be directly donated to oxygen to generate ROS. The eventual outcome is dependent on the protein being processed and function of the ETC. This feature of the MIA pathway is particularly intriguing, as organelle redox status and intermembrane space proteins are important for apoptosis (4), and have been implicated in oxidative-stress related disorders such as Parkinson's disease (17; 155) and Human Deafness Dystonia Syndrome (5).

3.6 Mitochondrial export machinery

All 13 proteins encoded by mtDNA are subunits of components of the ETC or the ATP synthase (179). These proteins are embedded in a hydrophobic environment, which necessitates a route of export from the matrix in order to reach their final destination. Additionally, a number of nuclear-encoded proteins are imported into the matrix where they are processed, but unlike most other matrix proteins, they are subsequently exported into other compartments of the mitochondria. These proteins also require an export route to exit the matrix.

The Oxa complex mediates protein export in mitochondria, and Oxa1 is the core chaperone of this machinery (36). Oxa1 assembles proteins translated from mitochondrial ribosomes and can incorporate them into the inner membrane in a co-translational manner (121). Oxa1 relies on other intermediates such as Oxa2 for facilitating membrane insertion and interactions with matrix ribosomes. This complex is particularly crucial for the assembly of the cytochrome *c* oxidase and NADH dehydrogenase holoenzymes (8; 157).

3.7 Mitochondrial processing peptidases and protein folding

After being driven into the matrix by the TIM23-PAM complex, N-terminal targeting signals are proteolytically cleaved by the matrix-processing peptidase (MPP) (59). Additionally, since preproteins are unravelled during the import process, they need to be subsequently refolded in order to be functional components of the organelle. A family of matrix chaperones which includes mtHsp70, and the Hsp60/Hsp10 chaperonins

perform this function (71). It must also be noted that not all imported preproteins are refolded by these proteins in the matrix, but they are nevertheless essential components of the organelle.

4.0 PURPOSES OF THE PRESENT STUDY

Skeletal muscle adaptations in the mitochondrial protein import system in response to chronic muscle disuse are not known. Characterizing the role of this pathway during blunted mitochondrial biogenesis requires measuring changes in the rates of protein import, along with the underlying mechanisms which govern this process. Therefore, the purposes of this study were to 1) establish whether denervation-induced decrements in contractile activity elicit a differential response in protein import kinetics, and 2) relate changes in protein import to alterations in mitochondrial respiration and content within the mitochondrial subfractions. The protein content of several components of the protein import machinery was also determined to characterize any underlying alterations in import during reduced contractile activity. Finally, in an effort to provide a more comprehensive assessment of the import system's function during oxidative stress, protein kinetics were evaluated in the presence of hydrogen peroxide, since denervated muscle generates higher levels of ROS than control.

4.1 Hypothesis

We hypothesized that denervation will diminish protein import kinetics in both mitochondrial subfractions, with the decrease being greater in SS mitochondria. We base

this hypothesis on previously reported accounts of relative lability in response to various physiological perbutations among the two subfractions. We also hypothesize that the protein expression of various components of the import machinery will be diminished. Furthermore, we hypothesize a close association between alterations in mitochondrial function, characterized by respiration and ROS production, with protein import kinetics. Finally, we also hypothesize that if protein import function is altered by muscle disuse, corresponding changes in COX activity will be demonstrated.

References

1. **Adhihetty PJ, Ljubicic V and Hood DA**. Effect of chronic contractile activity on SS and IMF mitochondrial apoptotic susceptibility in skeletal muscle. *Am J Physiol Endocrinol Metab* 292: E748-E755, 2007.
2. **Adhihetty PJ, Ljubicic V, Menzies KJ and Hood DA**. Differential susceptibility of subsarcolemmal and intermyofibrillar mitochondria to apoptotic stimuli. *Am J Physiol Cell Physiol* 289: C994-C1001, 2005.
3. **Adhihetty PJ, O'Leary MF, Chabi B, Wicks KL and Hood DA**. Effect of denervation on mitochondrially mediated apoptosis in skeletal muscle. *J Appl Physiol* 102: 1143-1151, 2007.
4. **Adhihetty PJ, O'Leary MF and Hood DA**. Mitochondria in skeletal muscle: adaptable rheostats of apoptotic susceptibility. *Exerc Sport Sci Rev* 36: 116-121, 2008.
5. **Aguirre LA, del C, I, Macaya A, Meda C, Villamar M, Moreno-Pelayo MA and Moreno F**. A novel mutation in the gene encoding TIMM8a, a component of the mitochondrial protein translocase complexes, in a Spanish familial case of deafness-dystonia (Mohr-Tranebjaerg) syndrome. *Am J Med Genet A* 140: 392-397, 2006.
6. **Allen DL, Roy RR and Edgerton VR**. Myonuclear domains in muscle adaptation and disease. *Muscle Nerve* 22: 1350-1360, 1999.
7. **Almon RR and Dubois DC**. Fiber-type discrimination in disuse and glucocorticoid-induced atrophy. *Med Sci Sports Exerc* 22: 304-311, 1990.
8. **Altamura N, Capitanio N, Bonnefoy N, Papa S and Dujardin G**. The Saccharomyces cerevisiae OXA1 gene is required for the correct assembly of cytochrome c oxidase and oligomycin-sensitive ATP synthase. *FEBS Lett* 382: 111-115, 1996.
9. **Ament W and Verkerke GJ**. Exercise and fatigue. *Sports Med* 39: 389-422, 2009.
10. **Amirouche A, Durieux AC, Banzet S, Koulmann N, Bonnefoy R, Mouret C, Bigard X, Peinnequin A and Freyssenet D**. Down-regulation of Akt/mammalian target of rapamycin signaling pathway in response to myostatin overexpression in skeletal muscle. *Endocrinology* 150: 286-294, 2009.
11. **Andreyev AY, Kushnareva YE and Starkov AA**. Mitochondrial metabolism of reactive oxygen species. *Biochemistry (Mosc)* 70: 200-214, 2005.
12. **Ariano MA, Armstrong RB and Edgerton VR**. Hindlimb muscle fiber populations of five mammals. *J Histochem Cytochem* 21: 51-55, 1973.
13. **Asai T, Takahashi T, Esaki M, Nishikawa S, Ohtsuka K, Nakai M and Endo T**. Reinvestigation of the requirement of cytosolic ATP for mitochondrial protein import. *J Biol Chem* 279: 19464-19470, 2004.
14. **Attaix D, Aurousseau E, Combaret L, Kee A, Larbaud D, Ralliere C, Souweine B, Taillandier D and Tilignac T**. Ubiquitin-proteasome-dependent proteolysis in skeletal muscle. *Reprod Nutr Dev* 38: 153-165, 1998.

15. **Attaix D, Taillandier D, Temparis S, Larbaud D, Aurousseau E, Combaret L and Voisin L**. Regulation of ATP-ubiquitin-dependent proteolysis in muscle wasting. *Reprod Nutr Dev* 34: 583-597, 1994.
16. **Attaix D, Ventadour S, Codran A, Bechet D, Taillandier D and Combaret L**. The ubiquitin-proteasome system and skeletal muscle wasting. *Essays Biochem* 41: 173-186, 2005.
17. **Banerjee R, Starkov AA, Beal MF and Thomas B**. Mitochondrial dysfunction in the limelight of Parkinson's disease pathogenesis. *Biochim Biophys Acta* 1792: 651-663, 2009.
18. **Bar-Shai M, Carmeli E, Coleman R and Reznick AZ**. Mechanisms in muscle atrophy in immobilization and aging. *Ann N Y Acad Sci* 1019: 475-478, 2004.
19. **Barja G and Herrero A**. Oxidative damage to mitochondrial DNA is inversely related to maximum life span in the heart and brain of mammals. *FASEB J* 14: 312-318, 2000.
20. **Bechet D, Tassa A, Taillandier D, Combaret L and Attaix D**. Lysosomal proteolysis in skeletal muscle. *Int J Biochem Cell Biol* 37: 2098-2114, 2005.
21. **Becker T, Pfannschmidt S, Guiard B, Stojanovski D, Milenkovic D, Kutik S, Pfanner N, Meisinger C and Wiedemann N**. Biogenesis of the mitochondrial TOM complex: Mim1 promotes insertion and assembly of signal-anchored receptors. *J Biol Chem* 283: 120-127, 2008.
22. **Benard G, Bellance N, James D, Parrone P, Fernandez H, Letellier T and Rossignol R**. Mitochondrial bioenergetics and structural network organization. *J Cell Sci* 120: 838-848, 2007.
23. **Bennett MR**. Reactive oxygen species and death: oxidative DNA damage in atherosclerosis. *Circ Res* 88: 648-650, 2001.
24. **Bergeron R, Ren JM, Cadman KS, Moore IK, Perret P, Pypaert M, Young LH, Semenkovich CF and Shulman GI**. Chronic activation of AMP kinase results in NRF-1 activation and mitochondrial biogenesis. *Am J Physiol Endocrinol Metab* 281: E1340-E1346, 2001.
25. **Bohnert M, Pfanner N and van der LM**. A dynamic machinery for import of mitochondrial precursor proteins. *FEBS Lett* 581: 2802-2810, 2007.
26. **Booth FW**. Effect of limb immobilization on skeletal muscle. *J Appl Physiol* 52: 1113-1118, 1982.
27. **Booth FW, Lou W, Hamilton MT and Yan Z**. Cytochrome c mRNA in skeletal muscles of immobilized limbs. *J Appl Physiol* 81: 1941-1945, 1996.
28. **Brand MD**. Regulation analysis of energy metabolism. *J Exp Biol* 200: 193-202, 1997.
29. **Brand MD and Esteves TC**. Physiological functions of the mitochondrial uncoupling proteins UCP2 and UCP3. *Cell Metab* 2: 85-93, 2005.
30. **Brennan CM and Steitz JA**. HuR and mRNA stability. *Cell Mol Life Sci* 58: 266-277, 2001.
31. **Brookes PS, Yoon Y, Robotham JL, Anders MW and Sheu SS**. Calcium, ATP, and ROS: a mitochondrial love-hate triangle. *Am J Physiol Cell Physiol* 287: C817-C833, 2004.

32. **Burnham R, Martin T, Stein R, Bell G, MacLean I and Steadward R.** Skeletal muscle fibre type transformation following spinal cord injury. *Spinal Cord* 35: 86-91, 1997.
33. **Cann RL, Stoneking M and Wilson AC.** Mitochondrial DNA and human evolution. *Nature* 325: 31-36, 1987.
34. **Carafoli E.** Calcium signaling: a tale for all seasons. *Proc Natl Acad Sci U S A* 99: 1115-1122, 2002.
35. **Carlson BM.** Denervation, reinnervation, and regeneration of skeletal muscle. *Otolaryngol Head Neck Surg* 89: 192-196, 1981.
36. **Chacinska A, Koehler CM, Milenkovic D, Lithgow T and Pfanner N.** Importing mitochondrial proteins: machineries and mechanisms. *Cell* 138: 628-644, 2009.
37. **Chacinska A, van der LM, Mehnert CS, Guiard B, Mick DU, Hutu DP, Truscott KN, Wiedemann N, Meisinger C, Pfanner N and Rehling P.** Distinct forms of mitochondrial TOM-TIM supercomplexes define signal-dependent states of preprotein sorting. *Mol Cell Biol* 30: 307-318, 2010.
38. **Chan DC.** Mitochondrial fusion and fission in mammals. *Annu Rev Cell Dev Biol* 22: 79-99, 2006.
39. **Chewawiwat N, Yano M, Terada K, Hoogenraad NJ and Mori M.** Characterization of the novel mitochondrial protein import component, Tom34, in mammalian cells. *J Biochem* 125: 721-727, 1999.
40. **Chin ER.** Role of Ca2+/calmodulin-dependent kinases in skeletal muscle plasticity. *J Appl Physiol* 99: 414-423, 2005.
41. **Chipuk JE, Bouchier-Hayes L and Green DR.** Mitochondrial outer membrane permeabilization during apoptosis: the innocent bystander scenario. *Cell Death Differ* 13: 1396-1402, 2006.
42. **Cogswell AM, Stevens RJ and Hood DA.** Properties of skeletal muscle mitochondria isolated from subsarcolemmal and intermyofibrillar regions. *Am J Physiol* 264: C383-C389, 1993.
43. **Cohen S, Brault JJ, Gygi SP, Glass DJ, Valenzuela DM, Gartner C, Latres E and Goldberg AL.** During muscle atrophy, thick, but not thin, filament components are degraded by MuRF1-dependent ubiquitylation. *J Cell Biol* 185: 1083-1095, 2009.
44. **Combaret L, Dardevet D, Bechet D, Taillandier D, Mosoni L and Attaix D.** Skeletal muscle proteolysis in aging. *Curr Opin Clin Nutr Metab Care* 12: 37-41, 2009.
45. **Connor MK, Bezborodova O, Escobar CP and Hood DA.** Effect of contractile activity on protein turnover in skeletal muscle mitochondrial subfractions. *J Appl Physiol* 88: 1601-1606, 2000.
46. **Copeland WC.** Inherited mitochondrial diseases of DNA replication. *Annu Rev Med* 59: 131-146, 2008.
47. **Csordas G and Hajnoczky G.** SR/ER-mitochondrial local communication: calcium and ROS. *Biochim Biophys Acta* 1787: 1352-1362, 2009.

48. **Decker CJ and Parker R.** Mechanisms of mRNA degradation in eukaryotes. *Trends Biochem Sci* 19: 336-340, 1994.
49. **Dedkov EI, Kostrominova TY, Borisov AB and Carlson BM.** Resistance vessel remodeling and reparative angiogenesis in the microcirculatory bed of long-term denervated skeletal muscles. *Microvasc Res* 63: 96-114, 2002.
50. **Detmer SA and Chan DC.** Functions and dysfunctions of mitochondrial dynamics. *Nat Rev Mol Cell Biol* 8: 870-879, 2007.
51. **Droge W.** Free radicals in the physiological control of cell function. *Physiol Rev* 82: 47-95, 2002.
52. **Echtay KS.** Mitochondrial uncoupling proteins--what is their physiological role? *Free Radic Biol Med* 43: 1351-1371, 2007.
53. **Edgerton VR, Roy RR, Allen DL and Monti RJ.** Adaptations in skeletal muscle disuse or decreased-use atrophy. *Am J Phys Med Rehabil* 81: S127-S147, 2002.
54. **Eisenberg HA and Hood DA.** Blood flow, mitochondria, and performance in skeletal muscle after denervation and reinnervation. *J Appl Physiol* 76: 859-866, 1994.
55. **Eley HL and Tisdale MJ.** Skeletal muscle atrophy, a link between depression of protein synthesis and increase in degradation. *J Biol Chem* 282: 7087-7097, 2007.
56. **Endo T and Yamano K.** Multiple pathways for mitochondrial protein traffic. *Biol Chem* 390: 723-730, 2009.
57. **Esaki M, Shimizu H, Ono T, Yamamoto H, Kanamori T, Nishikawa S and Endo T.** Mitochondrial protein import. Requirement of presequence elements and tom components for precursor binding to the TOM complex. *J Biol Chem* 279: 45701-45707, 2004.
58. **Franch HA and Price SR.** Molecular signaling pathways regulating muscle proteolysis during atrophy. *Curr Opin Clin Nutr Metab Care* 8: 271-275, 2005.
59. **Gakh O, Cavadini P and Isaya G.** Mitochondrial processing peptidases. *Biochim Biophys Acta* 1592: 63-77, 2002.
60. **Glass DJ.** Signalling pathways that mediate skeletal muscle hypertrophy and atrophy. *Nat Cell Biol* 5: 87-90, 2003.
61. **Gray MW, Burger G and Lang BF.** Mitochondrial evolution. *Science* 283: 1476-1481, 1999.
62. **Hajnoczky G, Csordas G, Das S, Garcia-Perez C, Saotome M, Sinha RS and Yi M.** Mitochondrial calcium signalling and cell death: approaches for assessing the role of mitochondrial Ca2+ uptake in apoptosis. *Cell Calcium* 40: 553-560, 2006.
63. **Hatefi Y.** The mitochondrial electron transport and oxidative phosphorylation system. *Annu Rev Biochem* 54: 1015-1069, 1985.
64. **Hawke TJ and Garry DJ.** Myogenic satellite cells: physiology to molecular biology. *J Appl Physiol* 91: 534-551, 2001.
65. **Hock MB and Kralli A.** Transcriptional control of mitochondrial biogenesis and function. *Annu Rev Physiol* 71: 177-203, 2009.
66. **Holt CE and Bullock SL.** Subcellular mRNA localization in animal cells and why it matters. *Science* 326: 1212-1216, 2009.

67. **Hood DA**. Invited Review: contractile activity-induced mitochondrial biogenesis in skeletal muscle. *J Appl Physiol* 90: 1137-1157, 2001.
68. **Hood DA**. Mechanisms of exercise-induced mitochondrial biogenesis in skeletal muscle. *Appl Physiol Nutr Metab* 34: 465-472, 2009.
69. **Hood DA, Adhihetty PJ, Colavecchia M, Gordon JW, Irrcher I, Joseph AM, Lowe ST and Rungi AA**. Mitochondrial biogenesis and the role of the protein import pathway. *Med Sci Sports Exerc* 35: 86-94, 2003.
70. **Hood DA, Irrcher I, Ljubicic V and Joseph AM**. Coordination of metabolic plasticity in skeletal muscle. *J Exp Biol* 209: 2265-2275, 2006.
71. **Hood DA and Joseph AM**. Mitochondrial assembly: protein import. *Proc Nutr Soc* 63: 293-300, 2004.
72. **Hulett JM, Lueder F, Chan NC, Perry AJ, Wolynec P, Likic VA, Gooley PR and Lithgow T**. The transmembrane segment of Tom20 is recognized by Mim1 for docking to the mitochondrial TOM complex. *J Mol Biol* 376: 694-704, 2008.
73. **Huo L and Scarpulla RC**. Mitochondrial DNA instability and peri-implantation lethality associated with targeted disruption of nuclear respiratory factor 1 in mice. *Mol Cell Biol* 21: 644-654, 2001.
74. **Irrcher I and Hood DA**. Regulation of Egr-1, SRF, and Sp1 mRNA expression in contracting skeletal muscle cells. *J Appl Physiol* 97: 2207-2213, 2004.
75. **Irrcher I, Ljubicic V and Hood DA**. Interactions between ROS and AMP kinase activity in the regulation of PGC-1alpha transcription in skeletal muscle cells. *Am J Physiol Cell Physiol* 296: C116-C123, 2009.
76. **Jorgensen SB and Rose AJ**. How is AMPK activity regulated in skeletal muscles during exercise? *Front Biosci* 13: 5589-5604, 2008.
77. **Jubinsky PT, Short MK, Mutema G, Morris RE, Ciraolo GM and Li M**. Magmas expression in neoplastic human prostate. *J Mol Histol* 36: 69-75, 2005.
78. **Kandarian SC and Jackman RW**. Intracellular signaling during skeletal muscle atrophy. *Muscle Nerve* 33: 155-165, 2006.
79. **Kang D, Kim SH and Hamasaki N**. Mitochondrial transcription factor A (TFAM): roles in maintenance of mtDNA and cellular functions. *Mitochondrion* 7: 39-44, 2007.
80. **Kaufman BA, Durisic N, Mativetsky JM, Costantino S, Hancock MA, Grutter P and Shoubridge EA**. The mitochondrial transcription factor TFAM coordinates the assembly of multiple DNA molecules into nucleoid-like structures. *Mol Biol Cell* 18: 3225-3236, 2007.
81. **Kaul SC, Yaguchi T, Taira K, Reddel RR and Wadhwa R**. Overexpressed mortalin (mot-2)/mthsp70/GRP75 and hTERT cooperate to extend the in vitro lifespan of human fibroblasts. *Exp Cell Res* 286: 96-101, 2003.
82. **Kerner J and Hoppel C**. Fatty acid import into mitochondria. *Biochim Biophys Acta* 1486: 1-17, 2000.
83. **Kim I, Rodriguez-Enriquez S and Lemasters JJ**. Selective degradation of mitochondria by mitophagy. *Arch Biochem Biophys* 462: 245-253, 2007.

84. **Kim JS, He L, Qian T and Lemasters JJ**. Role of the mitochondrial permeability transition in apoptotic and necrotic death after ischemia/reperfusion injury to hepatocytes. *Curr Mol Med* 3: 527-535, 2003.
85. **Kirkwood SP, Munn EA and Brooks GA**. Mitochondrial reticulum in limb skeletal muscle. *Am J Physiol* 251: C395-C402, 1986.
86. **Kirkwood SP, Packer L and Brooks GA**. Effects of endurance training on a mitochondrial reticulum in limb skeletal muscle. *Arch Biochem Biophys* 255: 80-88, 1987.
87. **Knowles MK, Guenza MG, Capaldi RA and Marcus AH**. Cytoskeletal-assisted dynamics of the mitochondrial reticulum in living cells. *Proc Natl Acad Sci U S A* 99: 14772-14777, 2002.
88. **Komiya T and Mihara K**. Protein import into mammalian mitochondria. Characterization of the intermediates along the import pathway of the precursor into the matrix. *J Biol Chem* 271: 22105-22110, 1996.
89. **Kozjak V, Wiedemann N, Milenkovic D, Lohaus C, Meyer HE, Guiard B, Meisinger C and Pfanner N**. An essential role of Sam50 in the protein sorting and assembly machinery of the mitochondrial outer membrane. *J Biol Chem* 278: 48520-48523, 2003.
90. **Kutik S, Rissler M, Guan XL, Guiard B, Shui G, Gebert N, Heacock PN, Rehling P, Dowhan W, Wenk MR, Pfanner N and Wiedemann N**. The translocator maintenance protein Tam41 is required for mitochondrial cardiolipin biosynthesis. *J Cell Biol* 183: 1213-1221, 2008.
91. **Kutik S, Stojanovski D, Becker L, Becker T, Meinecke M, Kruger V, Prinz C, Meisinger C, Guiard B, Wagner R, Pfanner N and Wiedemann N**. Dissecting membrane insertion of mitochondrial beta-barrel proteins. *Cell* 132: 1011-1024, 2008.
92. **Lal A, Mazan-Mamczarz K, Kawai T, Yang X, Martindale JL and Gorospe M**. Concurrent versus individual binding of HuR and AUF1 to common labile target mRNAs. *EMBO J* 23: 3092-3102, 2004.
93. **Lamb GD**. Mechanisms of excitation-contraction uncoupling relevant to activity-induced muscle fatigue. *Appl Physiol Nutr Metab* 34: 368-372, 2009.
94. **Lister R, Hulett JM, Lithgow T and Whelan J**. Protein import into mitochondria: origins and functions today (review). *Mol Membr Biol* 22: 87-100, 2005.
95. **Ljubicic V and Hood DA**. Kinase-specific responsiveness to incremental contractile activity in skeletal muscle with low and high mitochondrial content. *Am J Physiol Endocrinol Metab* 295: E195-E204, 2008.
96. **Lu DX, Huang SK and Carlson BM**. Electron microscopic study of long-term denervated rat skeletal muscle. *Anat Rec* 248: 355-365, 1997.
97. **Lueder F and Lithgow T**. The three domains of the mitochondrial outer membrane protein Mim1 have discrete functions in assembly of the TOM complex. *FEBS Lett* 583: 1475-1480, 2009.
98. **MacKenzie JA and Payne RM**. Mitochondrial protein import and human health and disease. *Biochim Biophys Acta* 1772: 509-523, 2007.

99. **Martinez-Caballero S, Grigoriev SM, Herrmann JM, Campo ML and Kinnally KW**. Tim17p regulates the twin pore structure and voltage gating of the mitochondrial protein import complex TIM23. *J Biol Chem* 282: 3584-3593, 2007.
100. **Matsakas A and Patel K**. Skeletal muscle fibre plasticity in response to selected environmental and physiological stimuli. *Histol Histopathol* 24: 611-629, 2009.
101. **McKinnell IW and Rudnicki MA**. Molecular mechanisms of muscle atrophy. *Cell* 119: 907-910, 2004.
102. **Meinecke M, Wagner R, Kovermann P, Guiard B, Mick DU, Hutu DP, Voos W, Truscott KN, Chacinska A, Pfanner N and Rehling P**. Tim50 maintains the permeability barrier of the mitochondrial inner membrane. *Science* 312: 1523-1526, 2006.
103. **Meisinger C, Rissler M, Chacinska A, Szklarz LK, Milenkovic D, Kozjak V, Schonfisch B, Lohaus C, Meyer HE, Yaffe MP, Guiard B, Wiedemann N and Pfanner N**. The mitochondrial morphology protein Mdm10 functions in assembly of the preprotein translocase of the outer membrane. *Dev Cell* 7: 61-71, 2004.
104. **Meisinger C, Ryan MT, Hill K, Model K, Lim JH, Sickmann A, Muller H, Meyer HE, Wagner R and Pfanner N**. Protein import channel of the outer mitochondrial membrane: a highly stable Tom40-Tom22 core structure differentially interacts with preproteins, small tom proteins, and import receptors. *Mol Cell Biol* 21: 2337-2348, 2001.
105. **Mesecke N, Bihlmaier K, Grumbt B, Longen S, Terziyska N, Hell K and Herrmann JM**. The zinc-binding protein Hot13 promotes oxidation of the mitochondrial import receptor Mia40. *EMBO Rep* 9: 1107-1113, 2008.
106. **Michel RN and Gardiner PF**. To what extent is hindlimb suspension a model of disuse? *Muscle Nerve* 13: 646-653, 1990.
107. **Midrio M**. The denervated muscle: facts and hypotheses. A historical review. *Eur J Appl Physiol* 98: 1-21, 2006.
108. **Mignone F, Gissi C, Liuni S and Pesole G**. Untranslated regions of mRNAs. *Genome Biol* 3: REVIEWS0004, 2002.
109. **Milenkovic D, Gabriel K, Guiard B, Schulze-Specking A, Pfanner N and Chacinska A**. Biogenesis of the essential Tim9-Tim10 chaperone complex of mitochondria: site-specific recognition of cysteine residues by the intermembrane space receptor Mia40. *J Biol Chem* 282: 22472-22480, 2007.
110. **Milenkovic D, Kozjak V, Wiedemann N, Lohaus C, Meyer HE, Guiard B, Pfanner N and Meisinger C**. Sam35 of the mitochondrial protein sorting and assembly machinery is a peripheral outer membrane protein essential for cell viability. *J Biol Chem* 279: 22781-22785, 2004.
111. **Milenkovic D, Ramming T, Muller JM, Wenz LS, Gebert N, Schulze-Specking A, Stojanovski D, Rospert S and Chacinska A**. Identification of the signal directing Tim9 and Tim10 into the intermembrane space of mitochondria. *Mol Biol Cell* 20: 2530-2539, 2009.
112. **Mokranjac D and Neupert W**. The many faces of the mitochondrial TIM23 complex. *Biochim Biophys Acta* 2010.

113. **Morey-Holton E, Globus RK, Kaplansky A and Durnova G.** The hindlimb unloading rat model: literature overview, technique update and comparison with space flight data. *Adv Space Biol Med* 10: 7-40, 2005.
114. **Morey-Holton ER and Globus RK.** Hindlimb unloading of growing rats: a model for predicting skeletal changes during space flight. *Bone* 22: 83S-88S, 1998.
115. **Morey-Holton ER and Globus RK.** Hindlimb unloading rodent model: technical aspects. *J Appl Physiol* 92: 1367-1377, 2002.
116. **Mori M and Terada K.** Mitochondrial protein import in animals. *Biochim Biophys Acta* 1403: 12-27, 1998.
117. **Muller JM, Milenkovic D, Guiard B, Pfanner N and Chacinska A.** Precursor oxidation by Mia40 and Erv1 promotes vectorial transport of proteins into the mitochondrial intermembrane space. *Mol Biol Cell* 19: 226-236, 2008.
118. **Murphy MP.** How mitochondria produce reactive oxygen species. *Biochem J* 417: 1-13, 2009.
119. **Murton AJ, Constantin D and Greenhaff PL.** The involvement of the ubiquitin proteasome system in human skeletal muscle remodelling and atrophy. *Biochim Biophys Acta* 1782: 730-743, 2008.
120. **Musacchia XJ, Steffen JM and Fell RD.** Disuse atrophy of skeletal muscle: animal models. *Exerc Sport Sci Rev* 16: 61-87, 1988.
121. **Nargang FE, Preuss M, Neupert W and Herrmann JM.** The Oxa1 protein forms a homooligomeric complex and is an essential part of the mitochondrial export translocase in Neurospora crassa. *J Biol Chem* 277: 12846-12853, 2002.
122. **Neupert W.** Protein import into mitochondria. *Annu Rev Biochem* 66: 863-917, 1997.
123. **Neupert W and Herrmann JM.** Translocation of proteins into mitochondria. *Annu Rev Biochem* 76: 723-749, 2007.
124. **Nguyen M, Argan C, Sheffield WP, Bell AW, Shields D and Shore GC.** A signal sequence domain essential for processing, but not import, of mitochondrial pre-ornithine carbamyl transferase. *J Cell Biol* 104: 1193-1198, 1987.
125. **NODA L and KUBY SA.** Adenosine triphosphate-adenosine monophosphate transphosphorylase (myokinase). II. Homogeneity measurements and physicochemical properties. *J Biol Chem* 226: 551-558, 1957.
126. **O'Leary MF and Hood DA.** Effect of prior chronic contractile activity on mitochondrial function and apoptotic protein expression in denervated muscle. *J Appl Physiol* 105: 114-120, 2008.
127. **O'Leary MF and Hood DA.** Denervation-induced oxidative stress and autophagy signaling in muscle. *Autophagy* 5: 230-231, 2009.
128. **Omura T.** Mitochondria-targeting sequence, a multi-role sorting sequence recognized at all steps of protein import into mitochondria. *J Biochem* 123: 1010-1016, 1998.
129. **Paschen SA, Weber A and Hacker G.** Mitochondrial protein import: a matter of death? *Cell Cycle* 6: 2434-2439, 2007.

130. **Pette D**. The adaptive potential of skeletal muscle fibers. *Can J Appl Physiol* 27: 423-448, 2002.
131. **Pierno S, Desaphy JF, Liantonio A, De LA, Zarrilli A, Mastrofrancesco L, Procino G, Valenti G and Conte CD**. Disuse of rat muscle in vivo reduces protein kinase C activity controlling the sarcolemma chloride conductance. *J Physiol* 584: 983-995, 2007.
132. **Popov-Celeketic D, Mapa K, Neupert W and Mokranjac D**. Active remodelling of the TIM23 complex during translocation of preproteins into mitochondria. *EMBO J* 27: 1469-1480, 2008.
133. **Powers SK, Kavazis AN and McClung JM**. Oxidative stress and disuse muscle atrophy. *J Appl Physiol* 102: 2389-2397, 2007.
134. **Rappaport L, Oliviero P and Samuel JL**. Cytoskeleton and mitochondrial morphology and function. *Mol Cell Biochem* 184: 101-105, 1998.
135. **Reid MB**. Free radicals and muscle fatigue: Of ROS, canaries, and the IOC. *Free Radic Biol Med* 44: 169-179, 2008.
136. **Rone MB, Fan J and Papadopoulos V**. Cholesterol transport in steroid biosynthesis: role of protein-protein interactions and implications in disease states. *Biochim Biophys Acta* 1791: 646-658, 2009.
137. **Rouault TA and Tong WH**. Iron-sulphur cluster biogenesis and mitochondrial iron homeostasis. *Nat Rev Mol Cell Biol* 6: 345-351, 2005.
138. **Russell ST, Eley H and Tisdale MJ**. Role of reactive oxygen species in protein degradation in murine myotubes induced by proteolysis-inducing factor and angiotensin II. *Cell Signal* 19: 1797-1806, 2007.
139. **Ryan MT and Hoogenraad NJ**. Mitochondrial-nuclear communications. *Annu Rev Biochem* 76: 701-722, 2007.
140. **Sacheck JM, Hyatt JP, Raffaello A, Jagoe RT, Roy RR, Edgerton VR, Lecker SH and Goldberg AL**. Rapid disuse and denervation atrophy involve transcriptional changes similar to those of muscle wasting during systemic diseases. *FASEB J* 21: 140-155, 2007.
141. **Sandri M**. Signaling in muscle atrophy and hypertrophy. *Physiology (Bethesda)* 23: 160-170, 2008.
142. **Sandri M, Lin J, Handschin C, Yang W, Arany ZP, Lecker SH, Goldberg AL and Spiegelman BM**. PGC-1alpha protects skeletal muscle from atrophy by suppressing FoxO3 action and atrophy-specific gene transcription. *Proc Natl Acad Sci U S A* 103: 16260-16265, 2006.
143. **Sandri M, Sandri C, Gilbert A, Skurk C, Calabria E, Picard A, Walsh K, Schiaffino S, Lecker SH and Goldberg AL**. Foxo transcription factors induce the atrophy-related ubiquitin ligase atrogin-1 and cause skeletal muscle atrophy. *Cell* 117: 399-412, 2004.
144. **Scarpulla RC**. Transcriptional paradigms in mammalian mitochondrial biogenesis and function. *Physiol Rev* 88: 611-638, 2008.
145. **Schatz G**. The magic garden. *Annu Rev Biochem* 76: 673-678, 2007.
146. **Schiller D**. Pam17 and Tim44 act sequentially in protein import into the mitochondrial matrix. *Int J Biochem Cell Biol* 41: 2343-2349, 2009.

147. **Schneider HC, Berthold J, Bauer MF, Dietmeier K, Guiard B, Brunner M and Neupert W**. Mitochondrial Hsp70/MIM44 complex facilitates protein import. *Nature* 371: 768-774, 1994.
148. **Schwartz LM**. Atrophy and programmed cell death of skeletal muscle. *Cell Death Differ* 15: 1163-1169, 2008.
149. **Servais S, Couturier K, Koubi H, Rouanet JL, Desplanches D, Sornay-Mayet MH, Sempore B, Lavoie JM and Favier R**. Effect of voluntary exercise on H2O2 release by subsarcolemmal and intermyofibrillar mitochondria. *Free Radic Biol Med* 35: 24-32, 2003.
150. **Shenkman BS and Nemirovskaya TL**. Calcium-dependent signaling mechanisms and soleus fiber remodeling under gravitational unloading. *J Muscle Res Cell Motil* 29: 221-230, 2008.
151. **Sinha D, Joshi N, Chittoor B, Samji P and D'Silva P**. Role of Magmas in protein transport and human mitochondria biogenesis. *Hum Mol Genet* 2010.
152. **Siu PM and Alway SE**. Response and adaptation of skeletal muscle to denervation stress: the role of apoptosis in muscle loss. *Front Biosci* 14: 432-452, 2009.
153. **Siu PM, Pistilli EE and Alway SE**. Apoptotic responses to hindlimb suspension in gastrocnemius muscles from young adult and aged rats. *Am J Physiol Regul Integr Comp Physiol* 289: R1015-R1026, 2005.
154. **Solandt DY, Partridge RC and Hunter J**. The effect of skeletal fixation on skeletal muscle. *Journal of Neurophysiology* 6: 17-22, 1943.
155. **Starkov AA and Beal FM**. Portal to Alzheimer's disease. *Nat Med* 14: 1020-1021, 2008.
156. **Steinmetz AC, Renaud JP and Moras D**. Binding of ligands and activation of transcription by nuclear receptors. *Annu Rev Biophys Biomol Struct* 30: 329-359, 2001.
157. **Stiburek L, Hansikova H, Tesarova M, Cerna L and Zeman J**. Biogenesis of eukaryotic cytochrome c oxidase. *Physiol Res* 55 Suppl 2: S27-S41, 2006.
158. **Stockholm D, Herasse M, Marchand S, Praud C, Roudaut C, Richard I, Sebille A and Beckmann JS**. Calpain 3 mRNA expression in mice after denervation and during muscle regeneration. *Am J Physiol Cell Physiol* 280: C1561-C1569, 2001.
159. **Stojanovski D, Johnston AJ, Streimann I, Hoogenraad NJ and Ryan MT**. Import of nuclear-encoded proteins into mitochondria. *Exp Physiol* 88: 57-64, 2003.
160. **Stojanovski D, Muller JM, Milenkovic D, Guiard B, Pfanner N and Chacinska A**. The MIA system for protein import into the mitochondrial intermembrane space. *Biochim Biophys Acta* 1783: 610-617, 2008.
161. **Stojanovski D, Rissler M, Pfanner N and Meisinger C**. Mitochondrial morphology and protein import--a tight connection? *Biochim Biophys Acta* 1763: 414-421, 2006.
162. **Swynghedauw B**. Developmental and functional adaptation of contractile proteins in cardiac and skeletal muscles. *Physiol Rev* 66: 710-771, 1986.

163. **Takahashi M, Chesley A, Freyssenet D and Hood DA**. Contractile activity-induced adaptations in the mitochondrial protein import system. *Am J Physiol* 274: C1380-C1387, 1998.
164. **Takahashi M and Hood DA**. Protein import into subsarcolemmal and intermyofibrillar skeletal muscle mitochondria. Differential import regulation in distinct subcellular regions. *J Biol Chem* 271: 27285-27291, 1996.
165. **Takiguchi M and Mori M**. Transcriptional regulation of genes for ornithine cycle enzymes. *Biochem J* 312 (Pt 3): 649-659, 1995.
166. **Taylor RW and Turnbull DM**. Mitochondrial DNA mutations in human disease. *Nat Rev Genet* 6: 389-402, 2005.
167. **Terada K, Ueno S, Yomogida K, Imai T, Kiyonari H, Takeda N, Yano M, Abe S, Aizawa S and Mori M**. Expression of Tom34 splicing isoforms in mouse testis and knockout of Tom34 in mice. *J Biochem* 133: 625-631, 2003.
168. **Thomason DB and Booth FW**. Atrophy of the soleus muscle by hindlimb unweighting. *J Appl Physiol* 68: 1-12, 1990.
169. **Tienson HL, Dabir DV, Neal SE, Loo R, Hasson SA, Boontheung P, Kim SK, Loo JA and Koehler CM**. Reconstitution of the mia40-erv1 oxidative folding pathway for the small tim proteins. *Mol Biol Cell* 20: 3481-3490, 2009.
170. **Tomkiewicz D, Nouwen N and Driessen AJ**. Pushing, pulling and trapping--modes of motor protein supported protein translocation. *FEBS Lett* 581: 2820-2828, 2007.
171. **Tupling AR**. The decay phase of Ca2+ transients in skeletal muscle: regulation and physiology. *Appl Physiol Nutr Metab* 34: 373-376, 2009.
172. **Tyml K and Mathieu-Costello O**. Structural and functional changes in the microvasculature of disused skeletal muscle. *Front Biosci* 6: D45-D52, 2001.
173. **Tzankov S, Wong MJ, Shi K, Nassif C and Young JC**. Functional divergence between co-chaperones of Hsc70. *J Biol Chem* 283: 27100-27109, 2008.
174. **Ungermann C, Neupert W and Cyr DM**. The role of Hsp70 in conferring unidirectionality on protein translocation into mitochondria. *Science* 266: 1250-1253, 1994.
175. **Van GD, Damrauer JS, Jackman RW and Kandarian SC**. The IkappaB kinases IKKalpha and IKKbeta are necessary and sufficient for skeletal muscle atrophy. *FASEB J* 23: 362-370, 2009.
176. **Ventura-Clapier R, Garnier A and Veksler V**. Transcriptional control of mitochondrial biogenesis: the central role of PGC-1alpha. *Cardiovasc Res* 79: 208-217, 2008.
177. **Wagner K, Mick DU and Rehling P**. Protein transport machineries for precursor translocation across the inner mitochondrial membrane. *Biochim Biophys Acta* 1793: 52-59, 2009.
178. **Waizenegger T, Schmitt S, Zivkovic J, Neupert W and Rapaport D**. Mim1, a protein required for the assembly of the TOM complex of mitochondria. *EMBO Rep* 6: 57-62, 2005.
179. **Wallace DC**. Mitochondrial diseases in man and mouse. *Science* 283: 1482-1488, 1999.

180. **Wallace DC, Fan W and Procaccio V.** Mitochondrial energetics and therapeutics. *Annu Rev Pathol* 5: 297-348, 2010.
181. **Walsh C, Barrow S, Voronina S, Chvanov M, Petersen OH and Tepikin A.** Modulation of calcium signalling by mitochondria. *Biochim Biophys Acta* 1787: 1374-1382, 2009.
182. **Walsh P, Bursac D, Law YC, Cyr D and Lithgow T.** The J-protein family: modulating protein assembly, disassembly and translocation. *EMBO Rep* 5: 567-571, 2004.
183. **Wicks KL and Hood DA.** Mitochondrial adaptations in denervated muscle: relationship to muscle performance. *Am J Physiol* 260: C841-C850, 1991.
184. **Wiedemann N, Pfanner N and Chacinska A.** Chaperoning through the mitochondrial intermembrane space. *Mol Cell* 21: 145-148, 2006.
185. **Wiedemann N, Pfanner N and Ryan MT.** The three modules of ADP/ATP carrier cooperate in receptor recruitment and translocation into mitochondria. *EMBO J* 20: 951-960, 2001.
186. **Winder WW, Holmes BF, Rubink DS, Jensen EB, Chen M and Holloszy JO.** Activation of AMP-activated protein kinase increases mitochondrial enzymes in skeletal muscle. *J Appl Physiol* 88: 2219-2226, 2000.
187. **Wright DC, Geiger PC, Han DH, Jones TE and Holloszy JO.** Calcium induces increases in peroxisome proliferator-activated receptor gamma coactivator-1alpha and mitochondrial biogenesis by a pathway leading to p38 mitogen-activated protein kinase activation. *J Biol Chem* 282: 18793-18799, 2007.
188. **Wright DC, Han DH, Garcia-Roves PM, Geiger PC, Jones TE and Holloszy JO.** Exercise-induced mitochondrial biogenesis begins before the increase in muscle PGC-1alpha expression. *J Biol Chem* 282: 194-199, 2007.
189. **Wu Z, Puigserver P, Andersson U, Zhang C, Adelmant G, Mootha V, Troy A, Cinti S, Lowell B, Scarpulla RC and Spiegelman BM.** Mechanisms controlling mitochondrial biogenesis and respiration through the thermogenic coactivator PGC-1. *Cell* 98: 115-124, 1999.
190. **Yaguchi T, Aida S, Kaul SC and Wadhwa R.** Involvement of mortalin in cellular senescence from the perspective of its mitochondrial import, chaperone, and oxidative stress management functions. *Ann N Y Acad Sci* 1100: 306-311, 2007.
191. **Yamamoto H, Esaki M, Kanamori T, Tamura Y, Nishikawa S and Endo T.** Tim50 is a subunit of the TIM23 complex that links protein translocation across the outer and inner mitochondrial membranes. *Cell* 111: 519-528, 2002.
192. **Yamano K, Ishikawa D, Esaki M and Endo T.** The phosphate carrier has an ability to be sorted to either the TIM22 pathway or the TIM23 pathway for its import into yeast mitochondria. *J Biol Chem* 280: 10011-10017, 2005.
193. **Yamano K, Kuroyanagi-Hasegawa M, Esaki M, Yokota M and Endo T.** Step-size analyses of the mitochondrial Hsp70 import motor reveal the Brownian ratchet in operation. *J Biol Chem* 283: 27325-27332, 2008.
194. **Yano M, Terada K and Mori M.** Mitochondrial import receptors Tom20 and Tom22 have chaperone-like activity. *J Biol Chem* 279: 10808-10813, 2004.

195. **Yu J and Auwerx J**. Protein deacetylation by SIRT1: An emerging key post-translational modification in metabolic regulation. *Pharmacol Res* 2009.

MANUSCRIPT

The writing of this manuscript, the data collection and statistical analyses, the experiments and preparation of the animals used in this study were all performed by Kaustabh Singh. In addition to proposing this study, David Hood was the research director and editor of the manuscript.

May 1, 2010

Effect of denervation on mitochondrial protein import in skeletal muscle

Kaustabh Singh [1, 2] and David A. Hood [1, 2, 3]

[1] Muscle Health Research Center, [2] School of Kinesiology and Health Science, and [3] Department of Biology, York University, Toronto, Ontario M3J 1P3, Canada

To whom correspondence should be addressed:
David A. Hood,
Muscle Health Research Center,
York University,
Toronto, Ontario,
M3J 1P3, Canada
Tel: (416) 736-2100 ext. 66640
Fax: (416) 736-5698
E-mail: dhood@yorku.ca

ABSTRACT

This study was conducted to determine whether chronic muscle disuse affects the mitochondrial protein import system, which is vital for the assembly of nuclear-derived proteins into existing organelles. We measured adaptations in protein import using a model of unilateral peroneal nerve denervation in rats for 3, 7 or 14 days. We compared the import of preproteins into the matrix of subsarcolemmal (SS) and intermyofibrillar (IMF) mitochondria, isolated from the denervated and the contralateral control tibialis anterior muscles. Denervation led to 50% and 29% reductions in protein import after 14 days of disuse in SS and IMF mitochondria, respectively. This was accompanied by significant decreases in mitochondrial state 3 respiration, muscle mass and whole muscle cytochrome *c* oxidase activity. To investigate the mechanisms involved, we assessed disuse-related changes in 1) protein import machinery components and 2) mitochondrial function, reflected by reactive oxygen species (ROS) production. Denervation reduced the expression of Tim23, Tom20 and mtHsp70, especially in the SS subfraction. Chronic disuse also resulted in elevated ROS generation, and exogenous ROS was found to markedly reduce protein import. Thus, our data indicate that protein import kinetics are closely related to alterations in mitochondrial respiratory capacity, and are negatively impacted by ROS. Changes in the protein import system likely facilitate the reduction in mitochondrial content and the increase in organelle dysfunction during chronic disuse, ultimately contributing to muscle atrophy.

INTRODUCTION

Chronic muscle disuse results in biochemical alterations that affect the endurance performance of muscle, which is particularly dependent on mitochondrial content (4; 20; 30). Skeletal muscle mitochondrial content is determined by the net synthesis and degradation of organellar proteins. Muscle disuse accelerates the rate of protein degradation, with concomitant decreases in the synthesis of mitochondrial proteins (29). The principle pathway for mitochondrial assembly involves the import of newly synthesized preproteins from the cytosol into existing mitochondria (7; 21; 26). These preproteins are actively transported into existing organelles by the protein import machinery (PIM). The important components of the import pathway include the translocases, which aid in the movement of preproteins across membranes (16). These translocases are localized in the outer membrane (TOM complex), or the inner membrane (TIM complex). During mitochondrial import, Tom20 is important for the recognition and binding of cytosolic preproteins possessing targeting presequences, as well as for transferring them into the general import pore (17). Matrix-destined proteins have to be channeled through Tim23 (5; 40), and they are actively pulled into the matrix by the mitochondrial heat shock protein 70 (mtHsp70) motor complex in an ATP-dependent fashion (39).

In skeletal muscle, mitochondria exist as a reticular membrane network. The subsarcolemmal (SS) and intermyofibrillar (IMF) mitochondria are located in distinct subcellular regions, and they possess subtle differences in biochemical and functional properties which are characterized by their anatomical locations (2; 10; 38). Furthermore,

alterations in contractile activity exert a differential response within these two subpopulations of mitochondria. In the case of chronic muscle disuse, these changes include reductions in mitochondrial oxygen consumption and increased reactive oxygen species (ROS) production (3; 28), which may have an impact on muscle performance (15; 31; 41), apoptosis (14; 28; 36) or gene expression (27; 33). However, it remains to be determined if muscle inactivity regulates the activity of precursor protein import.

We recently showed that the protein content of mitochondrial Tim23 decreased significantly after 7 days of denervation (28). Given the prominent role of this protein in regulating the import of matrix proteins (7; 21), a reduction in Tim23 might suggest a decline in the kinetics of protein import in denervated muscle. This is consistent with evidence of higher protein import rates observed in skeletal muscle when PIM expression is increased during conditions of increased mitochondrial biogenesis, such as during chronic contractile activity (18; 23; 37), thyroid hormone treatment (11; 12; 34) and the onset of muscle differentiation (19).

Thus, the overall purpose of this study was to evaluate the relationship between mitochondrial content and the protein import system during chronic muscle disuse. We hypothesized that protein import dynamics would correlate closely with alterations in mitochondrial content and function. Our results indicate that the components and kinetics of the import machinery in skeletal muscle are subject to adaptations under conditions of inactivity, and that the altered mitochondrial phenotype evident in denervated muscle may be partially attributed to a reduced capacity to import proteins.

METHODS

In vivo denervation protocol. Male Sprague-Dawley rats were anesthetized with an intraperitoneal injection of Ketamine-Xylazine (0.2 mls/100g of body weight). The tibialis anterior (TA) and extensor digitorum longus (EDL) muscles were denervated by exposing the left common peroneal nerve and excising a 5-mm section. The incision was sutured after administration of sterile ampicillin. The contralateral leg served as an internal control for each animal. After surgery, the skin was closed with metal clips and the day of surgery represented *day 0* of the time course. Denervated animals were given amoxicillin in their drinking water for 1 week after surgery (0.025% w/v). All procedures involving animals were approved by the York University Animal Care Committee, in accordance with the Canadian Council on Animal Care.

Cytochrome c oxidase (COX) activity. Pulverized EDL muscles were diluted in muscle extraction buffer (100 mM KH_2PO_4, 100 mM Na_2HPO_4, 2mM EDTA, pH 7.2) and sonicated 3x5 seconds on ice. Supernatant fractions were added to a test solution containing fully reduced cytochrome *c*, and this reaction was carried out within a 96-well plate at 30 °C using a Synergy-HT microplate reader. COX activity was assessed by the maximal rate of reduction in absorbance at 550nm.

Tissue extraction and mitochondrial isolation. Animals were anesthetized, and both denervated and contralateral TA muscles were excised, minced, and briefly homogenized using an Ultra-Turrax polytron at 40% power output. The intermyofibrillar (IMF) and subsarcolemmal (SS) mitochondrial subfractions were isolated by differential centrifiguation as described previously (10). Freshly isolated mitochondria were used for

protein import, respiration and ROS emission assays. Aliquots of each mitochondrial sample were also frozen for future use in immunoblotting assays. The EDL muscles were clamp frozen in liquid nitrogen and used for cytochrome-*c* oxidase (COX) activity measurements.

In vitro transcription, translation and import of OCT. The full length cDNA clone for ornithine transcarbamylase (OCT) was a generous gift from Dr. Gordon Shore (McGill University, Montreal, Canada). This cDNA was transcribed and translated in vitro as previously described (12). Briefly, the vector containing the OCT cDNA was linearized using *SacI* and subsequently phenol extracted and ethanol precipitated. OCT was *in vitro* transcribed at 40 °C for 90 minutes using SP6 RNA polymerase, followed by *in vitro* translation in the presence of ^{35}S-methionine within a rabbit reticulocyte lysate system.

The mitochondrial protein import assay was performed as outlined previously (34; 38). Briefly, mitochondria were preincubated for 10 min at 30 °C prior to the import assay. For experiments investigating the effect of ROS on protein import, the appropriate volume of H_2O_2 was added to the reaction so that the final concentration of H_2O_2 was either 5μM or 10μM. For 0 μM of ROS, H_2O_2 was substituted with water. Translation mix (12 μL per 25 μg of mitochondrial protein) was added to the mitochondria and the import incubation was allowed to proceed at 30 °C for 20 minutes. After 20 minutes, import was halted by adding an aliquot of the mitochondrial-translation mix to an ice-cold sucrose cushion (600 mM sucrose, 100 mM KCl, 20 mM HEPES, 2 mM $MgCl_2$). Mitochondria were pelleted by centrifugation for 15 minutes at 16,000 g (4°C) and

resuspended in 20 μL of ice-cold breaking buffer (600 mM sorbitol, 20 mM HEPES, pH 7.4). The samples were then denatured at 95°C in the presence of lysis buffer for 5 minutes, quick cooled on ice, and then resolved through a 12% SDS-polyacrylamide gel. Gels were processed and dried as described elsewhere (12; 34). Images and subsequent quantification were obtained with electronic autoradiography (Quantity One, BioRad, Hercules, CA). Imported mature OCT was distinguished from precursor OCT because of its lower molecular weight. The percentage of available protein that was imported was calculated based on ratio of the intensity of the mature OCT and total OCT (sum of mature and precursor bands).

Mitochondrial respiration assay. Fifty microliters of isolated mitochondrial samples were incubated with 250 μL of VO_2 buffer (250 mM sucrose, 50 mM KCl, 25 mM Tris, 10 mM K_2HPO_4, pH 7.4) in a Clark oxygen electrode respiratory chamber (Strathkelvin Instruments, North Lanarkshire, Scotland) with continuous stirring at 30°C. Mitochondrial oxygen consumption was measured in the presence of exogenously added 10 mM glutamate to assess state 4 respiration, followed by 0.44 mM ADP to elicit state 3 respiration. In addition, NADH was added during state 3 measurements to evaluate the integrity of the inner mitochondrial membrane.

Mitochondrial ROS production. SS and IMF mitochondria (75 μg) were incubated with 50 μM dichlorodihydroflurescein diacetate (H_2DCDA) and VO_2 buffer at 37°C for 30 minutes in a 96-well plate. ROS production is directly proportional to fluorescence emission between 480 and 520 nm measured using a multidetection microplate reader (Synergy HT; Bio-Tek Instruments, Winooski, VT). ROS emission was assessed during

state 4 and state 3 respiration, and the microplate data were compiled and analyzed using KC4 (v 3.0).

Immunoblotting. Isolated SS and IMF mitochondrial protein extracts were separated by performing 15% SDS-PAGE and subsequently electroblotted onto nitrocellulose membranes. After transfer, membranes were blocked for 1 hour in 1X TBST containing 5% skim milk. Blots were then incubated in blocking buffer with antibodies detected against Tim23 (1:500), Tom20 (1:500), mtHSP70 (1:1000) and ANT (1:2000) overnight at 4°C. Antibodies were obtained from Santa Cruz (Tom20, sc-11415), BD Biosciences (Tim23, 611222) and Assay Designs (mtHSP70, SPS-825F). The ANT antibody was generously provided by Dr. K.B. Freeman (McMaster University, Hamilton, Ontario). After three washes for 5 minutes, blots were incubated for 1 hour at room temperature with the appropriate secondary antibody coupled to horseradish peroxidase and washed again three times for 5 minutes each. Antibody-bound protein was revealed using the ECL method. Films were scanned and analyzed using SigmaScan Pro 5.0 software (Aspire Software, Ashburn, VA).

Statistical Analysis. Data were expressed as means ± SEM. Paired Student's t-tests were used for comparisons between IMF and SS mitochondria isolated from control muscle. A one-way or two-way analysis of variance was used for all denervation time points, followed by Bonferroni's post hoc test to assess differences within groups. Statistical differences were considered significant if $P < 0.05$.

RESULTS

Relationship of mitochondrial function and protein expression to protein import in mitochondrial subfractions. State 3 respiration was 2.5-fold greater in IMF mitochondria ($P < 0.05$; Fig. 1*A*). In contrast, ROS production during state 3 respiration was 4.3-fold higher in SS mitochondria, compared to the IMF subfraction ($P < 0.05$; Fig. 1*B*). pOCT import was two-fold greater in IMF mitochondria than those observed in the SS mitochondrial subfraction ($P < 0.05$; Fig. 1*C*). mtHSP70 protein levels were 30% lower in IMF mitochondria, compared to the SS subfraction ($P < 0.05$; Fig. 1*D*), while levels of Tim23 and Tom20 expression were not different between IMF and SS mitochondria (data not shown).

Effect of denervation on muscle mass and mitochondrial content. Denervation of the TA muscle resulted in significant reductions of muscle mass by 7, 33, and 65% after 3, 7 and 14 days respectively, compared to control muscle ($P < 0.05$; Fig. 2*A*). COX activity, a typical marker of mitochondrial content, decreased by 32, 35 and 48%, respectively, during the same time frame ($P < 0.05$; Fig. 2*B*). These data confirm that denervation effectively reduced mitochondrial content per gram of muscle.

Effect of denervation on mitochondrial respiration. Mitochondrial function from denervated muscle was assessed by measuring oxygen consumption in the presence (state 3) or absence (state 4) of ADP in SS and IMF subfractions. There was a main effect of denervation in both SS and IMF mitochondrial state 3 respiration. State 3 respiration was reduced by 40-45% in SS mitochondria, whereas IMF mitochondrial oxygen consumption was decreased by 16, 39 and 45% following 3, 7 and 14 days respectively

($P < 0.05$; Fig. 3*A*). State 4 respiration was not affected by denervation in IMF mitochondria, but was decreased by 17% and 26% at 3 and 7 days respectively in SS mitochondria ($P < 0.05$; Fig. 3*B*).

Effect of denervation on ROS production. Mitochondrial ROS production was assessed in SS and IMF subfractions during state 3 and state 4 respiration. State 3 ROS production was increased by 3.7-fold in SS mitochondria after 14 days of denervation, whereas IMF mitochondria generated 4.2-, 2.8- and 5.5-fold higher levels of ROS after 3, 7 and 14 days respectively ($P < 0.05$; Fig. 4*A*). State 4 ROS emission in SS mitochondria was elevated by 1.8- and 3.9-fold following 7 and 14 days respectively. Finally IMF mitochondrial state 4 ROS emission was enhanced by 1.9- and 2.9 fold after 3 and 14 days of denervation ($P < 0.05$; Fig. 4*B*).

Effect of denervation on mitochondrial protein import. OCT import was blunted in both the SS and IMF subfractions during all three time periods of denervation. Protein import in SS mitochondria from denervated muscle was reduced by 29, 42 and 50%, whereas IMF mitochondrial protein import was reduced by 13, 19 and 29% at 3, 7 and 14 days, respectively ($P < 0.05$; Fig. 5).

Effect of denervation on mitochondrial protein import machinery expression. Corresponding to the deceleration of OCT import in denervated muscle, there was a decrease in the protein expression of mitochondrial import machinery components, Tim23, Tom20 and mtHSP70. Tim23 levels were reduced by 40% following 14 days of denervation in IMF mitochondria, whereas SS Tim23 expression was decreased by 45, 46 and 21% after 3, 7 and 14 days respectively ($P < 0.05$; Fig. 6). In contrast, Tom20 was

not affected by denervation in IMF mitochondria, but was reduced by 45 and 33% at 7 and 14 days respectively in SS mitochondria ($P < 0.05$; Fig. 7). Finally, mtHSP70 was decreased in SS mitochondria by 49, 40 and 66% following 3, 7 and 14 days respectively, whereas IMF mitochondrial mtHSP70 protein levels had declined by 37 and 68% subsequent to 3 and 14 days of denervation respectively ($P < 0.05$; Fig. 8).

Assessment of ROS on protein import. To investigate the effect of ROS on protein import, we incubated mitochondria and OCT preprotein in the presence of either 5 or 10 μM hydrogen peroxide. **Protein import in SS mitochondria was reduced by 36 and 64%, whereas IMF mitochondrial protein import was reduced by 33 and 67% in the presence of 5 and 10** μM of hydrogen peroxide **respectively** ($P < 0.05$; Fig. 9).

DISCUSSION

A hallmark feature of skeletal muscle disuse-induced atrophy is a decrease in mitochondrial biogenesis (3; 36). Our previous work has characterized reduced muscle performance and mitochondrial enzyme activity (41), altered blood flow (15), and increased mitochondrially-mediated cell death during denervation (3; 27; 28). The majority of mitochondrial proteins are nuclear-encoded, and mitochondrial biogenesis requires the protein import machinery to transport these cytosolic proteins into the organelle (7; 21). Our previous work has illustrated the adaptability of this pathway in skeletal muscle mitochondria responding to various physiological perbutations such as chronic contractile activity (18; 22; 37), ageing (13; 22), thyroid hormone treatment (11; 12; 34) and muscle differentiation (19). However, the adaptation of the protein import system in response to chronic muscle disuse has never been previously investigated. In addition, skeletal muscle comprise two subpopulations of mitochondria, subsarcolemmal (SS) and intermyofibrillar (IMF), which are found in different cellular compartments, possessing subtle differences in functional and biochemical properties. These characteristics could be accounted for, in part, by divergent rates of protein import within the two subfractions (20). Thus, the main purposes of the present study were to 1) evaluate denervation-induced adaptations in protein import within skeletal muscle SS and IMF mitochondria, and 2) to relate these changes to alterations in the expression of import machinery components and mitochondrial function.

First, we wanted to relate any basal differences in SS and IMF mitochondrial protein import to organelle function and the expression of import machinery components.

Current results confirm higher rates of state 3 respiration along with lower ROS generation in IMF, compared to SS mitochondria, in agreement with previously reported values (3; 28; 41). Enhanced ETC activity in IMF mitochondria was accompanied by a two-fold higher rate of OCT import in the IMF subfraction. We also measured the protein expression of Tim23, Tom20 and mtHsp70, which are critical components of the import machinery governing matrix-destined proteins (8). Although, we found no differences in SS and IMF mitochondrial Tom20 and Tim23 content, mtHsp70 protein levels were significantly higher in the SS subfraction. This pattern of PIM expression is similar to our previous observations (18; 19; 38). Clearly, this lower expression of mtHsp70 in IMF mitochondria could not account for the higher rate of import in this subfraction, but other components of the import machinery, not measured in this study, may be higher in IMF mitochondria to compensate for this effect.

Next, our goal was to characterize denervation-induced changes in mitochondrial content in relation to alterations in protein import and organelle respiration. The application of a cell-free *in vitro* import assay permitted the conclusion that impaired matrix protein import occurs independent of precursor protein availability. Additionally, the import of radiolabelled pOCT into muscle mitochondria, where the background of processed OCT is negligible, provides a useful model to study the import of matrix-destined proteins. Once imported into the matrix, the 39kDa translation product of OCT is cleaved and processed to the mature 36kDa form of the enzyme (6). OCT protein import was blunted in both SS and IMF mitochondria from denervated muscle, and the extent of reduction closely paralleled the denervation-induced decline in whole muscle

cytochrome c oxidase (COX) activity, which was measured to confirm an overall reduction in muscle oxidative capacity. This is supported by the close correlation between the rate of protein import and whole muscle COX activity (Fig 10*A*). Of the two mitochondrial subfractions, import kinetics were reduced to the greatest extent in SS mitochondria, confirming the concept that this subpopulation of mitochondria is more labile during conditions of chronic muscle use and disuse (1; 3; 4; 25). Additionally, differences in import rates between IMF and SS mitochondria from denervated muscle were well matched with alterations in state 3 respiration (Fig 10*B*). These data reinforce the contention (38) that protein import is closely related to the rate of ATP formed by respiration, which is used to internally to drive the translocation of the precursor into the matrix.

Our data also suggest the existence of a dissociation between the rate of muscle atrophy and changes in mitochondrial content during different periods of muscle disuse. For example, after 3 days of denervation, COX activity was reduced by 30% but there was only a 9% decline in muscle mass. This early adaptation in mitochondrial content may be necessary to initiate the catabolic activities that are associated with denervation (9). In addition, the extent of muscle atrophy was greater than the reduction in oxidative capacity during 7 and 14 days of denervation. These data demonstrate that changes in mitochondrial content are not critical determinants of muscle mass during disuse atrophy (29; 32). This reduced mitochondrial content was coupled with mitochondrial dysfunction in denervated muscle, as demonstrated by reduced state 3 respiration in both subfractions. This is indicative of a lower capacity for ATP synthesis as a result of altered

mitochondrial components. Mitochondrial dysfunction was also reflected by an increase in ROS production in both SS and IMF mitochondria. Mitochondrial ROS generation is inversely related to mitochondrial respiration (2; 35), and this increase in oxidative stress is likely caused by a combination of reduced antioxidant activity, as well as impaired function of complexes within the ETC. These alterations in respiration and ROS production were more pronounced in SS mitochondria, suggesting a greater sensitivity and response to denervation in this mitochondrial subfraction.

Since the protein import machinery mediates the import process, we also determined the expression of selected components within SS and IMF mitochondria from denervated muscle to evaluate their potential roles in disuse-mediated changes in protein import. The content of all components investigated (Tim23, Tom20 and mtHsp70) decreased in SS mitochondria during the time course of denervation. This response was different in IMF mitochondria, where mtHsp70 and Tim23 were significantly reduced at specific time points. Clearly, components of SS mitochondrial import machinery were more vulnerable to denervation-induced organelle remodelling, and these heterogenous adaptations could be related to altered cardiolipin content, since this phospholipid is critical for embedding components of the import machinery (20). A greater loss of cardiolipin in SS mitochondria could account for the reduced topology of import proteins. However, this mechanism requires further investigation.

One important implication of the present study relates to the potential redox modulation of the mitochondrial protein import machinery during oxidative stress. Since large quantities of ROS are responsible for initiating several harmful events within cells,

they may inappropriately signal the arrest of precursor protein import. Indeed, the greater ROS production evident in SS mitochondria (2) may serve to attenuate protein import compared to IMF mitochondria under steady state conditions. In addition, because denervated muscle mitochondria produce more ROS and display reduced protein import, we hypothesized that exogenous ROS would inhibit protein import in mitochondria. Wright and colleagues have previously used a superoxide generating agent to inhibit OCT import in liver mitochondria, and promote subsequent precursor degradation (42). Our data illustrate that muscle mitochondria incubated in the presence of H_2O_2 exhibited reduced protein import in a dose-dependent manner. In all likelihood, this reduction in import is related to the redox-modulation of import machinery components with cysteine- or thiol-rich residues. The mitochondrial intermembrane space machinery, which imports and assembles cysteine-rich proteins in a disulfide relay system inside the intermembrane space, is highly susceptible to oxidative stress (24). Other constituents of the import pathway are also likely to be affected by oxidative stress, but future studies are required to identify the mechanisms governing the inhibition of protein import by ROS.

In summary, we have shown for the first time that skeletal muscle responds to chronic muscle disuse by reducing the rate of mitochondrial precursor protein import, which is mediated in part by a reduced capacity for ATP production, as well as modifications in the expression of critical components of the import machinery (Fig 11). Decreased protein import is likely a strong contributor to the reduction in mitochondrial content evident with denervation. In addition, we have provided some evidence for the inhibition of mitochondrial precursor protein import by oxidative stress in muscle

mitochondria. This work sets the stage for future studies designed to evaluate the physiological role of the protein import pathway during oxidative stress conditions in skeletal muscle.

ACKNOWLEDGEMENTS

This work was supported by Canadian Institutes of Health Research (CIHR) and Natural Sciences and Engineering Research Council of Canada (NSERC) grants to D.A Hood. D.A Hood is the holder of a Canada Research Chair in cell physiology.

References

1. **Adhihetty PJ, Ljubicic V, Menzies KJ and Hood DA**. Differential susceptibility of subsarcolemmal and intermyofibrillar mitochondria to apoptotic stimuli. *Am J Physiol Cell Physiol* 289: C994-C1001, 2005.
2. **Adhihetty PJ, O'Leary MF, Chabi B, Wicks KL and Hood DA**. Effect of denervation on mitochondrially mediated apoptosis in skeletal muscle. *J Appl Physiol* 102: 1143-1151, 2007.
3. **Adhihetty PJ, Ljubicic V and Hood DA**. Effect of chronic contractile activity on SS and IMF mitochondrial apoptotic susceptibility in skeletal muscle. *Am J Physiol Endocrinol Metab* 292: E748-E755, 2007.
4. **Adhihetty PJ, O'Leary MF and Hood DA**. Mitochondria in skeletal muscle: adaptable rheostats of apoptotic susceptibility. *Exerc Sport Sci Rev* 36: 116-121, 2008.
5. **Ahting U, Floss T, Uez N, Schneider-Lohmar I, Becker L, Kling E, Iuso A, Bender A, de Angelis MH, Gailus-Durner V, Fuchs H, Meitinger T, Wurst W, Prokisch H and Klopstock T**. Neurological phenotype and reduced lifespan in heterozygous Tim23 knockout mice, the first mouse model of defective mitochondrial import. *Biochim Biophys Acta* 1787: 371-376, 2009.
6. **Argan C, Lusty CJ and Shore GC**. Membrane and cytosolic components affecting transport of the precursor for ornithine carbamyltransferase into mitochondria. *J Biol Chem* 258: 6667-6670, 1983.
7. **Chacinska A, Koehler CM, Milenkovic D, Lithgow T and Pfanner N**. Importing mitochondrial proteins: machineries and mechanisms. *Cell* 138: 628-644, 2009.
8. **Chacinska A, van der LM, Mehnert CS, Guiard B, Mick DU, Hutu DP, Truscott KN, Wiedemann N, Meisinger C, Pfanner N and Rehling P**. Distinct forms of mitochondrial TOM-TIM supercomplexes define signal-dependent states of preprotein sorting. *Mol Cell Biol* 30: 307-318, 2010.
9. **Chen YW, Gregory CM, Scarborough MT, Shi R, Walter GA and Vandenborne K**. Transcriptional pathways associated with skeletal muscle disuse atrophy in humans. *Physiol Genomics* 31: 510-520, 2007.
10. **Cogswell AM, Stevens RJ and Hood DA**. Properties of skeletal muscle mitochondria isolated from subsarcolemmal and intermyofibrillar regions. *Am J Physiol* 264: C383-C389, 1993.
11. **Colavecchia M, Christie LN, Kanwar YS and Hood DA**. Functional consequences of thyroid hormone-induced changes in the mitochondrial protein import pathway. *Am J Physiol Endocrinol Metab* 284: E29-E35, 2003.
12. **Craig EE and Hood DA**. Influence of aging on protein import into cardiac mitochondria. *Am J Physiol* 272: H2983-H2988, 1997.
13. **Craig EE, Chesley A and Hood DA**. Thyroid hormone modifies mitochondrial phenotype by increasing protein import without altering degradation. *Am J Physiol* 275: C1508-C1515, 1998.

14. **Csukly K, Ascah A, Matas J, Gardiner PF, Fontaine E and Burelle Y**. Muscle denervation promotes opening of the permeability transition pore and increases the expression of cyclophilin D. *J Physiol* 574: 319-327, 2006.
15. **Eisenberg HA and Hood DA**. Blood flow, mitochondria, and performance in skeletal muscle after denervation and reinnervation. *J Appl Physiol* 76: 859-866, 1994.
16. **Endo T, Yamamoto H and Esaki M** . Functional cooperation and separation of translocators in protein import into mitochondria, the double-membrane bounded organelles. *J Cell Sci* 116: 3259-3267, 2003.
17. **Esaki M, Shimizu H, Ono T, Yamamoto H, Kanamori T, Nishikawa S and Endo T**. Mitochondrial protein import. Requirement of presequence elements and tom components for precursor binding to the TOM complex. *J Biol Chem* 279: 45701-45707, 2004.
18. **Gordon JW, Rungi AA, Inagaki H and Hood DA**. Effects of contractile activity on mitochondrial transcription factor A expression in skeletal muscle. *J Appl Physiol* 90: 389-396, 2001.
19. **Grey JY, Connor MK, Gordon JW, Yano M, Mori M and Hood DA**. Tom20-mediated mitochondrial protein import in muscle cells during differentiation. *Am J Physiol Cell Physiol* 279: C1393-C1400, 2000.
20. **Hood DA**. Invited Review: contractile activity-induced mitochondrial biogenesis in skeletal muscle. *J Appl Physiol* 90: 1137-1157, 2001.
21. **Hood DA and Joseph AM**. Mitochondrial assembly: protein import. *Proc Nutr Soc* 63: 293-300, 2004.
22. **Huang JH, Joseph AM, Ljubicic V, Iqbal S and Hood DA**. Effect of Age on the Processing and Import of Matrix-Destined Mitochondrial Proteins in Skeletal Muscle. *J Gerontol A Biol Sci Med Sci* 2010.
23. **Joseph AM, Ljubicic V, Adhihetty PJ and Hood DA**. Biogenesis of the mitochondrial Tom40 channel in skeletal muscle from aged animals and its adaptability to chronic contractile activity. *Am J Physiol Cell Physiol* 2010.
24. **Koehler CM and Tienson HL**. Redox regulation of protein folding in the mitochondrial intermembrane space. *Biochim Biophys Acta* 1793: 139-145, 2009.
25. **Krieger DA, Tate CA, Millin-Wood J and Booth FW**. Populations of rat skeletal muscle mitochondria after exercise and immobilization. *J Appl Physiol* 48: 23-28, 1980.
26. **Neupert W and Herrmann JM**. Translocation of proteins into mitochondria. *Annu Rev Biochem* 76: 723-749, 2007.
27. **O'Leary MF and Hood DA**. Effect of prior chronic contractile activity on mitochondrial function and apoptotic protein expression in denervated muscle. *J Appl Physiol* 105: 114-120, 2008.
28. **O'Leary MF and Hood DA**. Denervation-induced oxidative stress and autophagy signaling in muscle. *Autophagy* 5: 230-231, 2009.
29. **Phillips SM, Glover EI and Rennie MJ**. Alterations of protein turnover underlying disuse atrophy in human skeletal muscle. *J Appl Physiol* 107: 645-654, 2009.

30. **Powers SK, Kavazis AN and McClung JM**. Oxidative stress and disuse muscle atrophy. *J Appl Physiol* 102: 2389-2397, 2007.
31. **Rezvani M, Ornatsky OI, Connor MK, Eisenberg HA and Hood DA**. Dystrophin, vinculin, and aciculin in skeletal muscle subject to chronic use and disuse. *Med Sci Sports Exerc* 28: 79-84, 1996.
32. **Saini A, Faulkner S, Al-Shanti N and Stewart C**. Powerful signals for weak muscles. *Ageing Res Rev* 8: 251-267, 2009.
33. **Sandri M, Lin J, Handschin C, Yang W, Arany ZP, Lecker SH, Goldberg AL and Spiegelman BM**. PGC-1alpha protects skeletal muscle from atrophy by suppressing FoxO3 action and atrophy-specific gene transcription. *Proc Natl Acad Sci U S A* 103: 16260-16265, 2006.
34. **Schneider JJ and Hood DA**. Effect of thyroid hormone on mtHsp70 expression, mitochondrial import and processing in cardiac muscle. *J Endocrinol* 165: 9-17, 2000.
35. **Servais S, Couturier K, Koubi H, Rouanet JL, Desplanches D, Sornay-Mayet MH, Sempore B, Lavoie JM and Favier R** . Effect of voluntary exercise on H2O2 release by subsarcolemmal and intermyofibrillar mitochondria. *Free Radic Biol Med* 35: 24-32, 2003.
36. **Siu PM and Alway SE**. Response and adaptation of skeletal muscle to denervation stress: the role of apoptosis in muscle loss. *Front Biosci* 14: 432-452, 2009.
37. **Takahashi M and Hood DA**. Protein import into subsarcolemmal and intermyofibrillar skeletal muscle mitochondria. Differential import regulation in distinct subcellular regions. *J Biol Chem* 271: 27285-27291, 1996.
38. **Takahashi M, Chesley A, Freyssenet D and Hood DA**. Contractile activity-induced adaptations in the mitochondrial protein import system. *Am J Physiol* 274: C1380-C1387, 1998.
39. **Tomkiewicz D, Nouwen N and Driessen AJ**. Pushing, pulling and trapping--modes of motor protein supported protein translocation. *FEBS Lett* 581: 2820-2828, 2007.
40. **Wagner K, Mick DU and Rehling P**. Protein transport machineries for precursor translocation across the inner mitochondrial membrane. *Biochim Biophys Acta* 1793: 52-59, 2009.
41. **Wicks KL and Hood DA**. Mitochondrial adaptations in denervated muscle: relationship to muscle performance. *Am J Physiol* 260: C841-C850, 1991.
42. **Wright G, Terada K, Yano M, Sergeev I and Mori M**. Oxidative stress inhibits the mitochondrial import of preproteins and leads to their degradation. *Exp Cell Res* 263: 107-117, 2001.

Figure 1

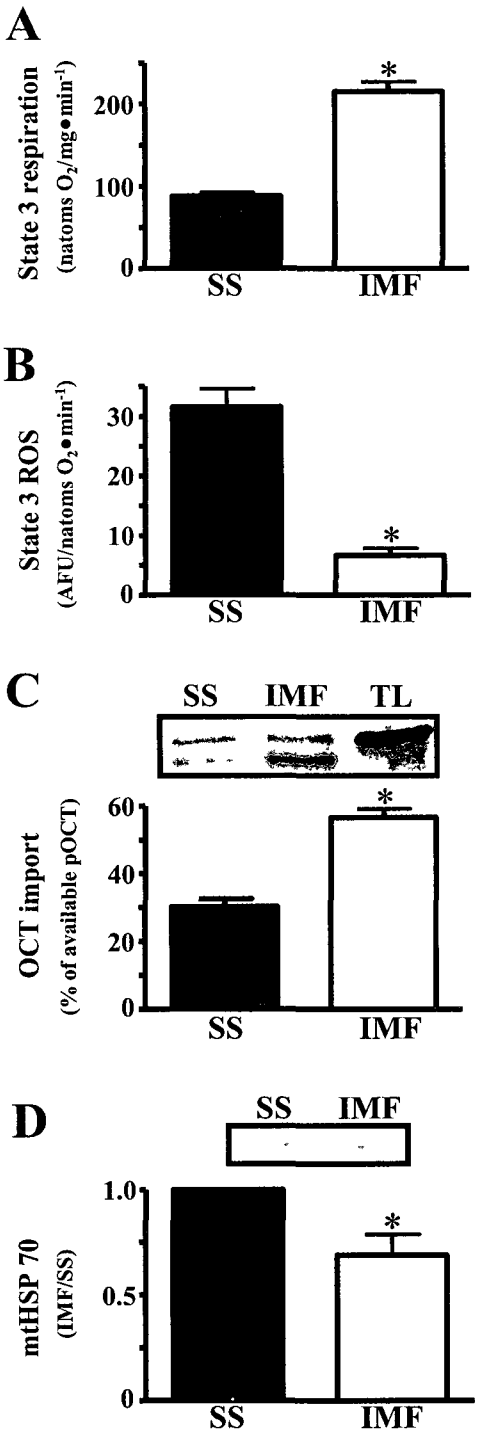

Fig. 1. Differences in subsarcolemmal (SS) and intermyofibrillar (IMF) mitochondrial function and protein import. *A:* Oxygen consumption during ADP stimulated respiration (state 3). *B:* ROS production during state 3 respiration. *C:* Rate of pOCT protein import. A representative autoradiograph is shown. and *D:* expression of mitochondrial heat shock protein 70 (mtHSP70) protein levels. A typical western blot is illustrated. (n=23-26). *P<0.05 SS vs. IMF. Values are means ± SEM.

Figure 2

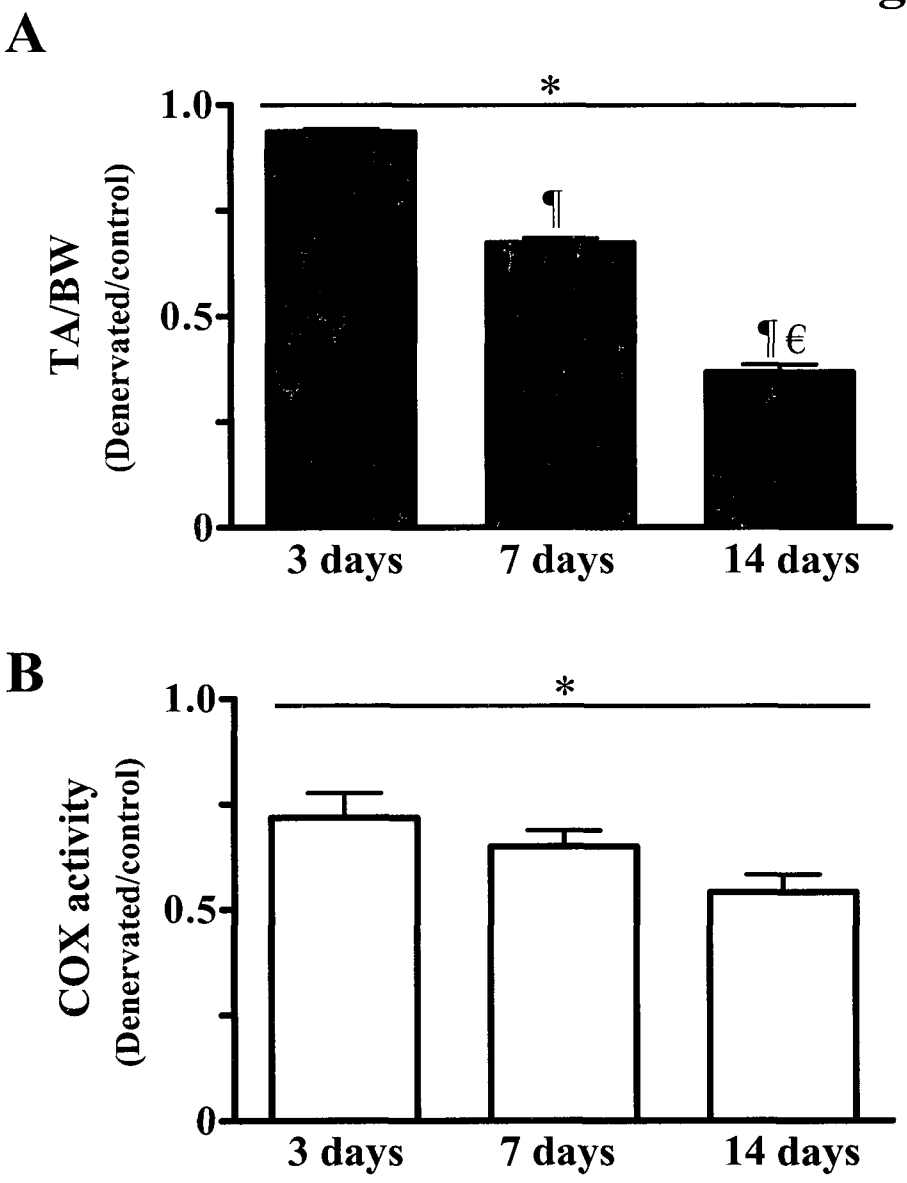

Fig. 2. Effect of 3, 7 and 14 days of denervation on muscle atrophy and mitochondrial content. *A*: Tibialis anterior (TA) muscle mass corrected for body weight (BW) (n=10-14 per group) . *B*: Cytochrome *c* oxidase (COX) activity in response to different periods of denervation (n=8-10 per group). * $P<0.05$ control vs. denervated; ¶ $P < 0.05$ vs. 3 day, € $P < 0.05$ vs. 7 day. Values are means ± SEM.

Figure 3

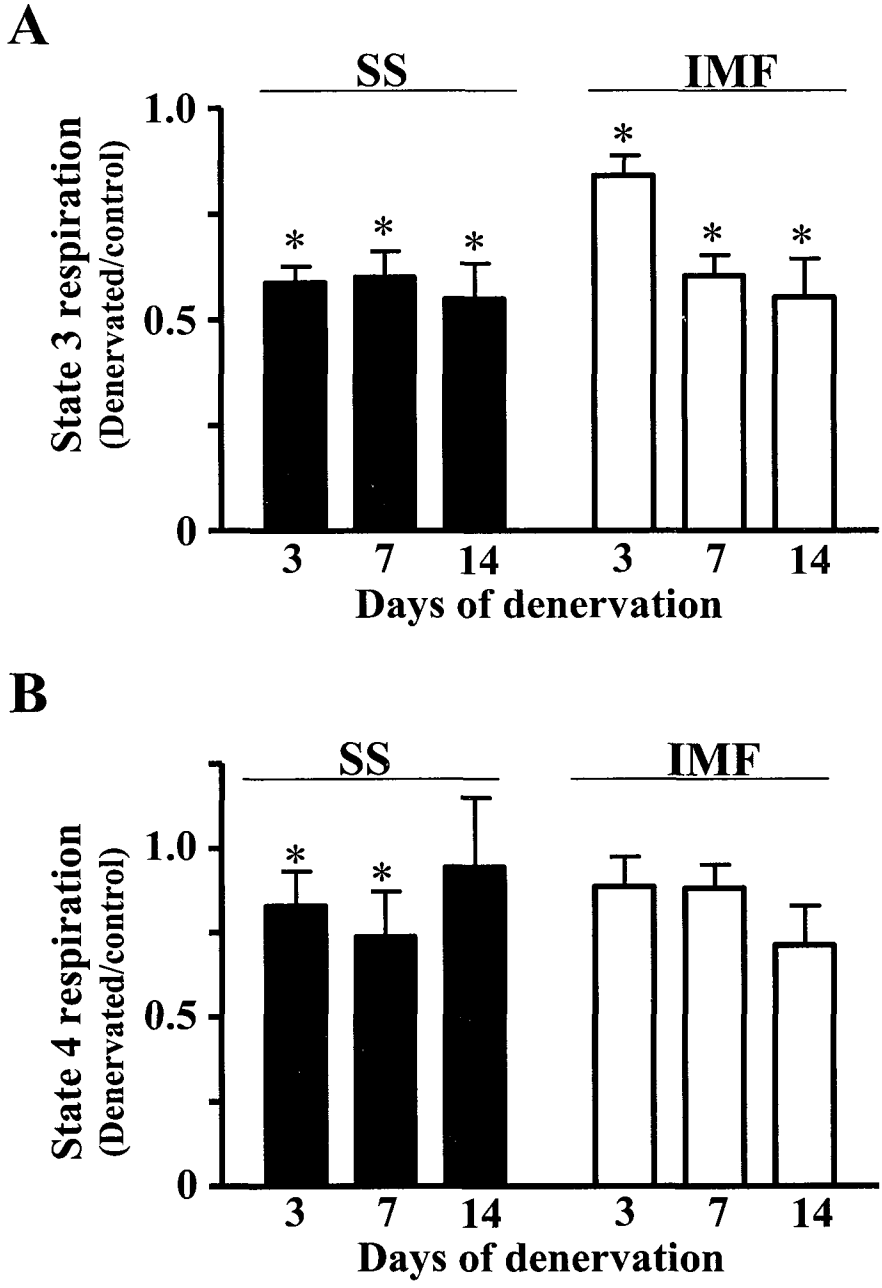

Fig. 3. SS and IMF oxygen consumption following 3, 7 and 14 days of muscle denervation. Oxygen consumption was measured in the presence of 10mM glutamate (State 4) and 0.44 mM ADP (state 3) in a clark oxygen electrode. Graphical representation of (A) state 3 respiration and (B) state 4 respiration, which was expressed as a fraction of control, non-denervated muscle mitochondria. (n=6-12). Values are means ± SEM. *$P < 0.05$, control vs. denervated.

Figure 4

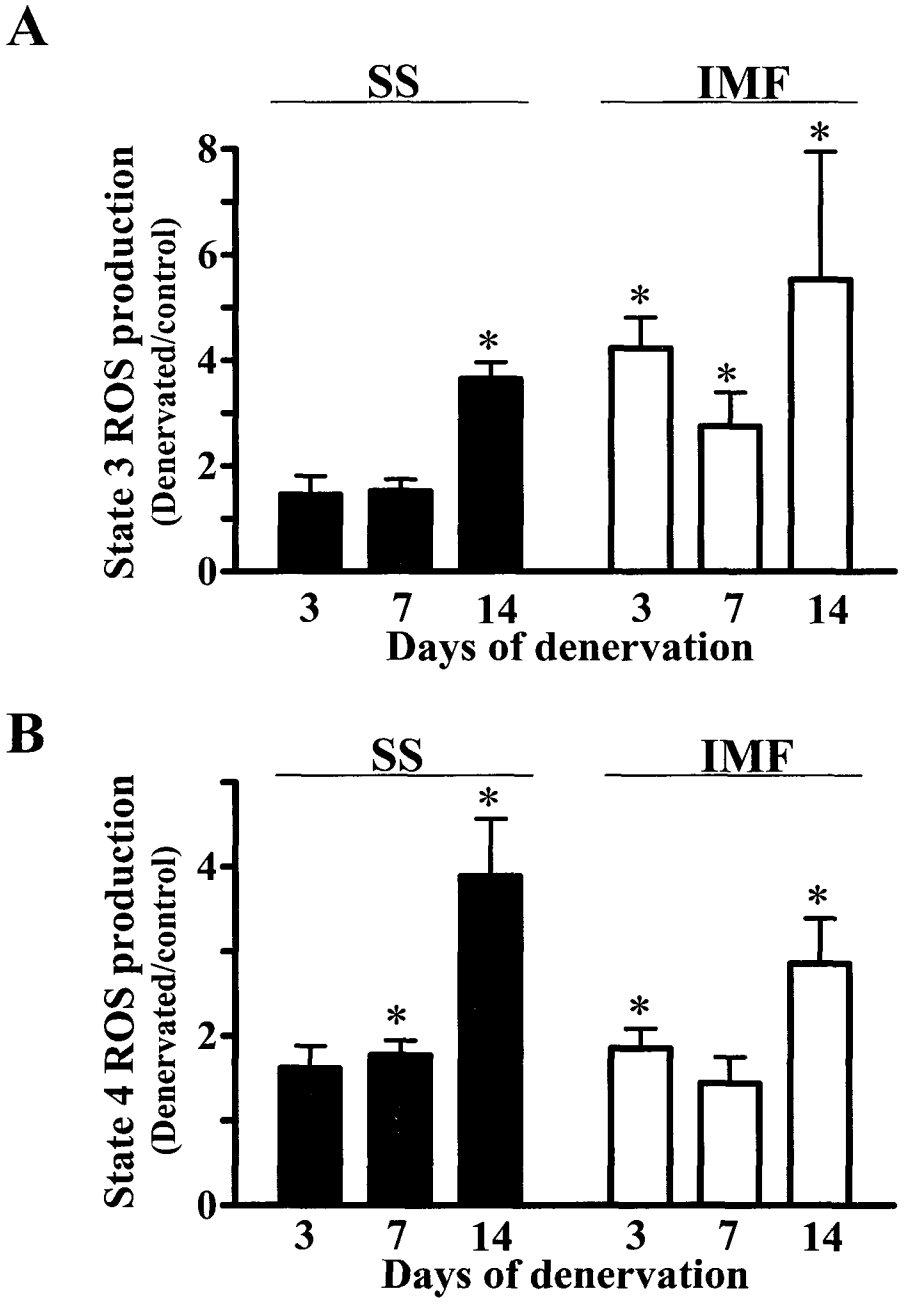

Fig. 4. Fold increase in SS and IMF ROS production over control following 3, 7 and 14 days of muscle denervation. ROS (arbitrary fluorescence units) per natom of oxygen consumed per minute was measured during (A) state 3 respiration and (B) state 4 respiration, which was expressed as a fraction of control, non-denervated muscle mitochondria.. (n=6-8). Values are means ± SEM. *$P < 0.05$, control vs. denervated.

Figure 5

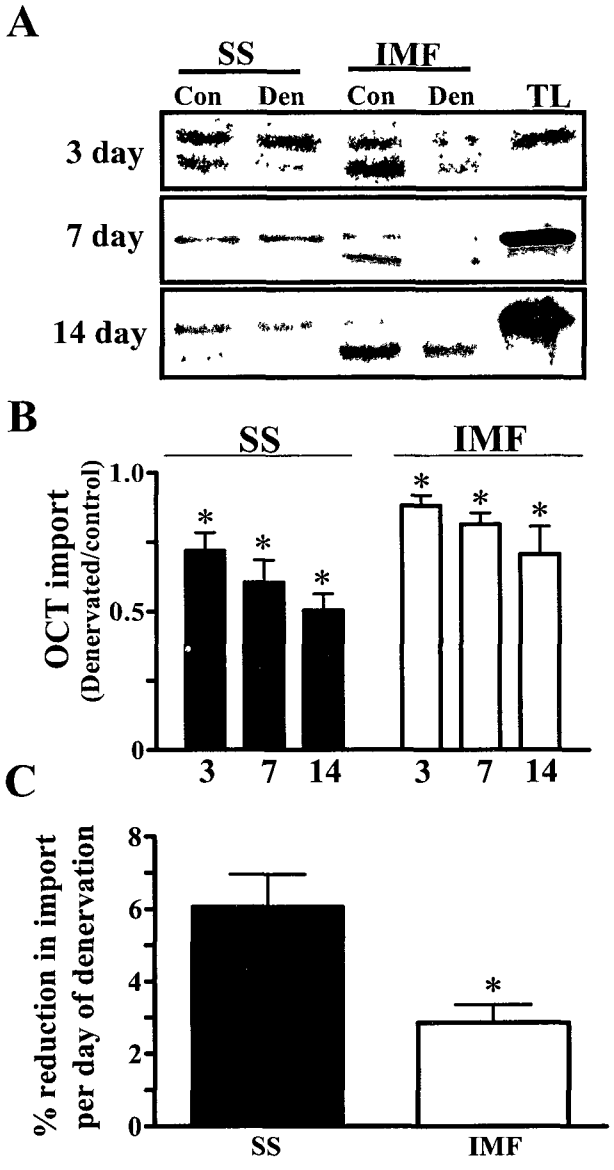

Fig. 5. Mitochondrial protein import of OCT in skeletal muscle denervated for 3, 7 and 14 days. A: Representative autoradiograms from the mitochondrial protein import assay for 3, 7 and 14 days of denervation. SS, subsarcolemmal mitochondria; IMF, intermyofibrillar mitochondria; Con, control; Den, denervated; TL, 5 μL of translation product. Below, *B*: quantification of protein import was expressed as a ratio of control/non-denervated muscle mitochondria in SS and IMF subfractions (n=7-8 per group). *C*: Reduced protein import in denervated muscle SS and IMF mitochondria expressed as a ratio of percentage reduction of OCT import/days of denervation (n = 23) Values are means ± SEM.

Figure 6

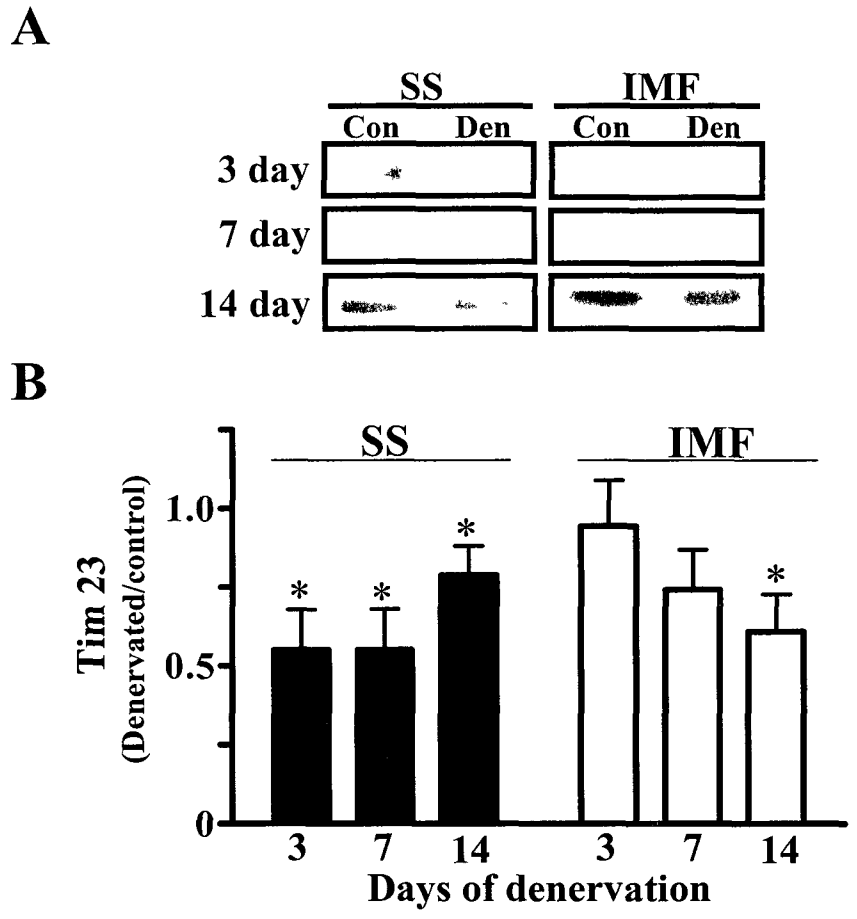

Fig. 6. Effect of denervation on Tim23 protein content in subsarcolemmal and intermyofibrillar mitochondria. *A*: Typical western blots (30 μg protein/lane) comparing SS and IMF mitochondria from 3-, 7- and 14 day denervated TA muscles. SS, subsarcolemmal mitochondria; IMF, intermyofibrillar mitochondria; Con, control; Den, denervated. Below, *B*: Associated quantification of repeated experiments (n=8-10) $*P < 0.05$, control vs. denervated. Values are means ± SEM.

Figure 7

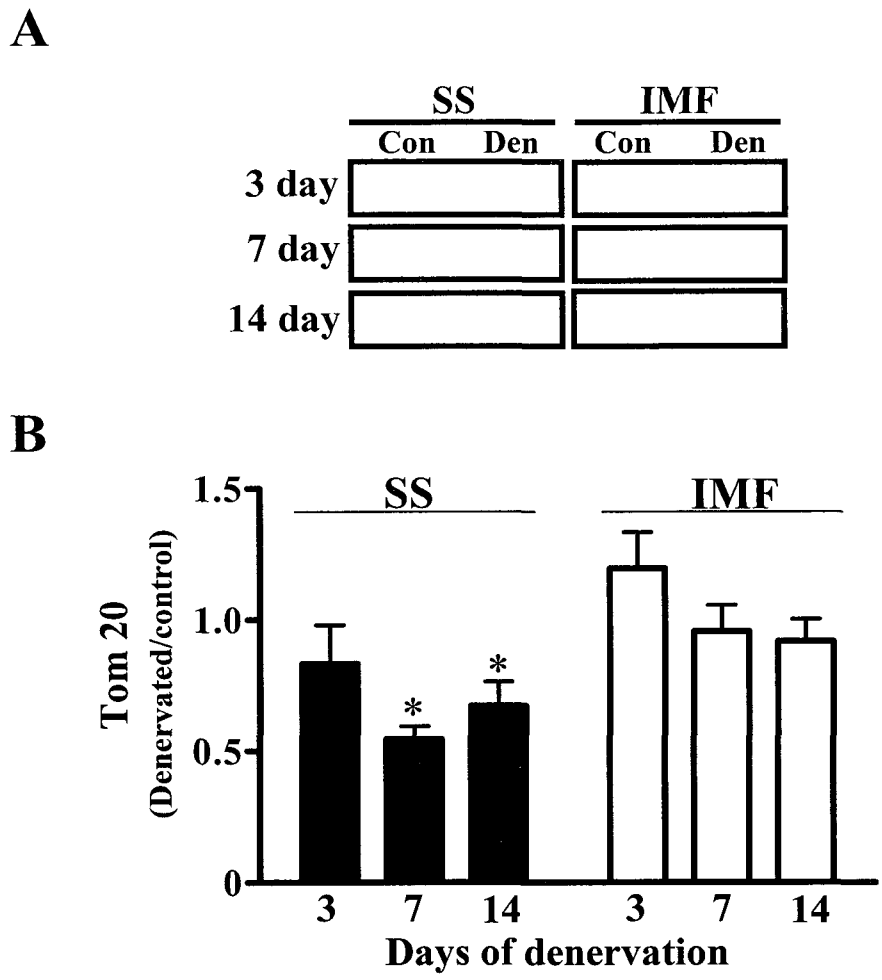

Fig. 7. Effect of denervation on Tom20 protein content in subsarcolemmal and intermyofibrillar mitochondria. *A*: Typical western blots (30 μg protein/lane) comparing SS and IMF mitochondria from 3-, 7- and 14 day denervated TA muscles. SS, subsarcolemmal mitochondria; IMF, intermyofibrillar mitochondria; Con, control; Den, denervated. Below, *B*: Associated quantification of repeated experiments (n=6-8) $*P < 0.05$, control vs. denervated. Values are means ± SEM.

Figure 8

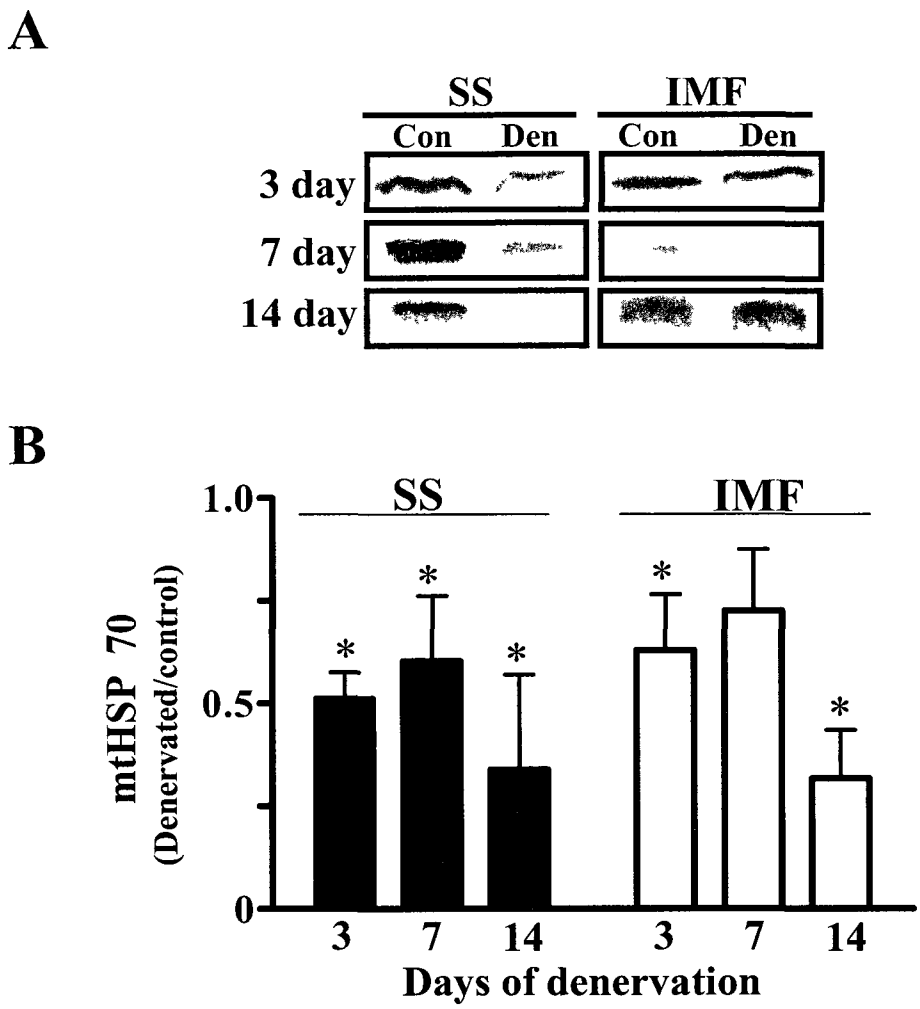

Fig. 8. Effect of denervation on mtHsp70 protein content in subsarcolemmal and intermyofibrillar mitochondria. *A*: Typical western blots (30 μg protein/lane) comparing SS and IMF mitochondria from 3-, 7- and 14 day denervated TA muscles. SS, subsarcolemmal mitochondria; IMF, intermyofibrillar mitochondria; Con, control; Den, denervated. Below, *B*: Associated quantification of repeated experiments (n=8) $*P <$ 0.05, control vs. denervated. Values are means ± SEM.

Figure 9

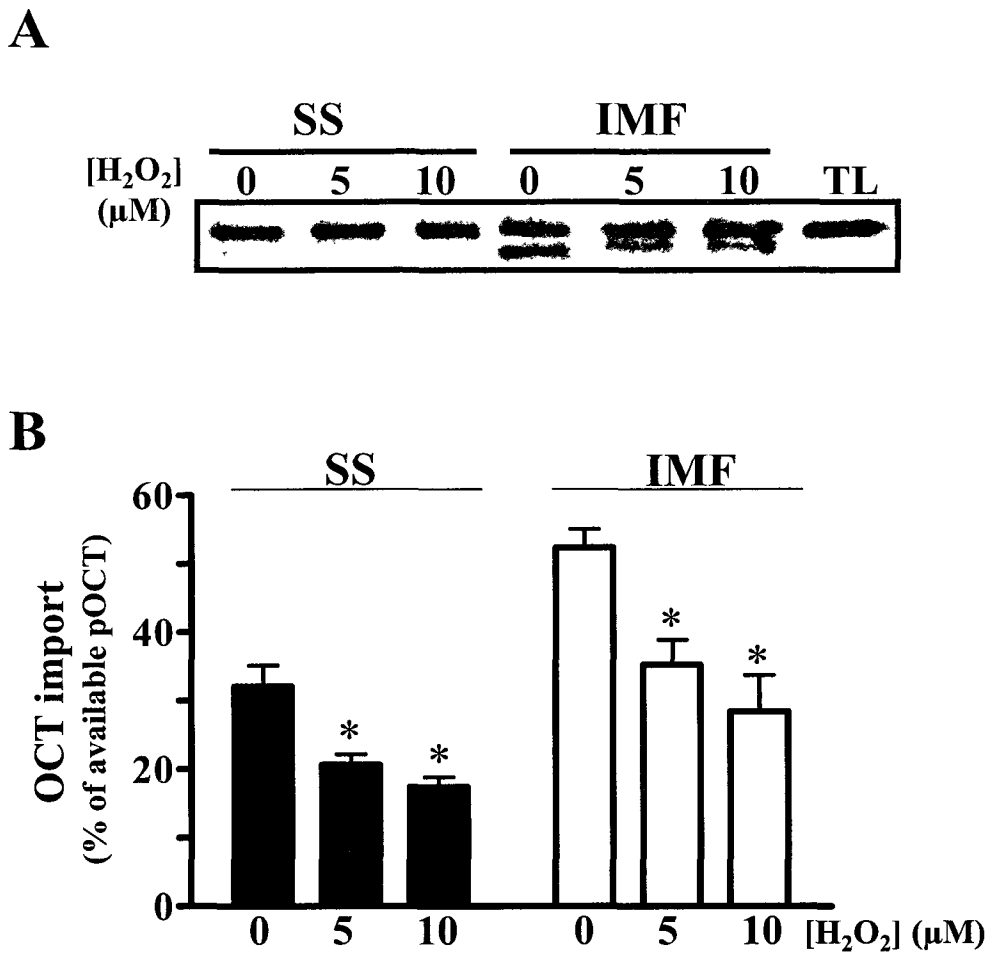

Fig. 9. Effect of ROS on pOCT protein import in SS and IMF mitochondria. *A*: Mitochondria from control muscles were incubated with 5 or 10μM of H2O2 during the import reaction. A representative autoradiogram is shown for the import assay. SS, subsarcolemmal mitochondria; IMF, intermyofibrillar mitochondria; TL, translation product. Below, *B*: graphical representation of repeated experiments where protein import was expressed as a percentage of mature protein over total protein imported. *P<0.05 vs. 0μM (n=4-7). Values are means ± SEM.

Figure 10

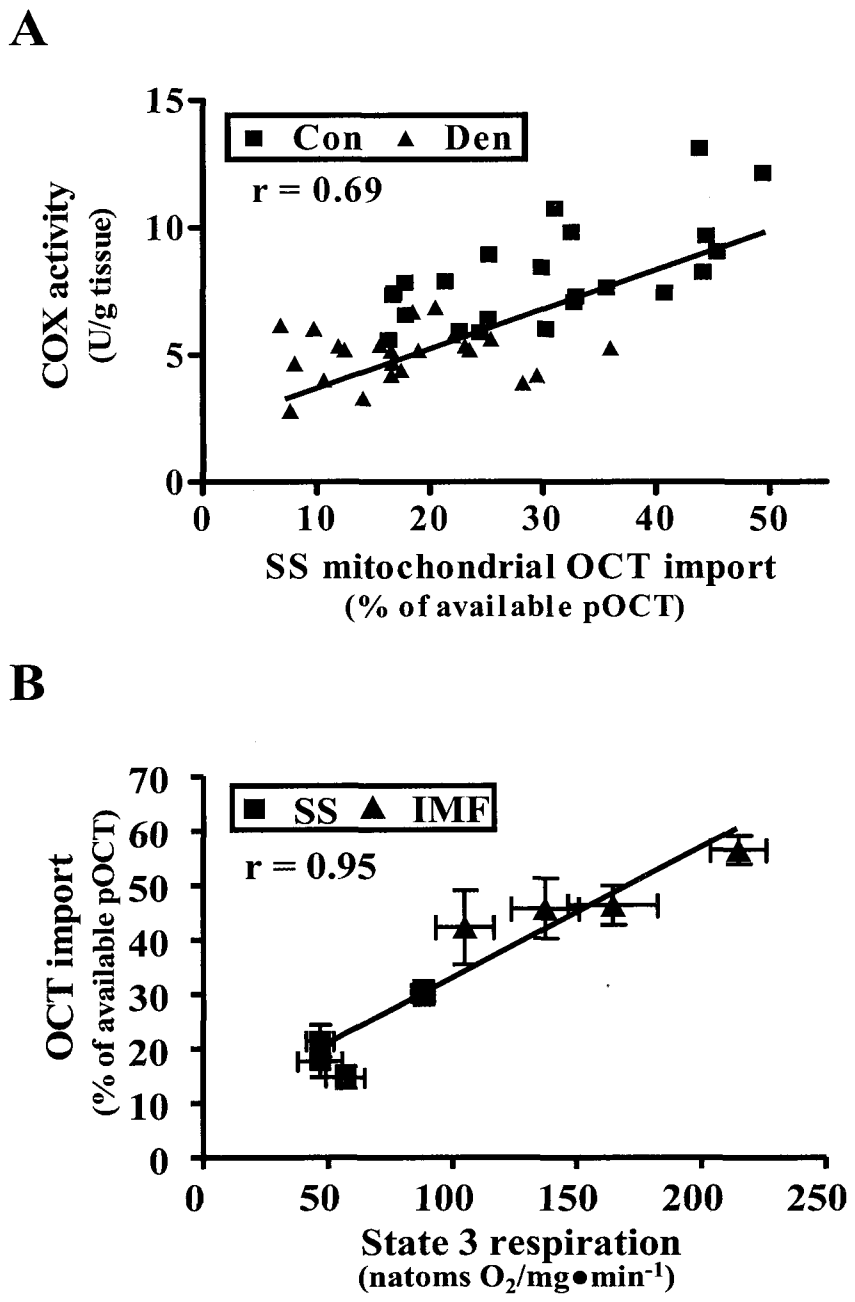

Fig. 10. Correlation between mitochondrial content, protein import and state 3 respiration. *A*: Relationship between whole muscle COX activity and SS mitochondrial protein import (n=23) and *B*: SS and IMF mitochondrial OCT import and state 3 respiration (n=21) from control and denervated muscles, on the basis of acquired data. Values are means ± SEM.

Figure 11

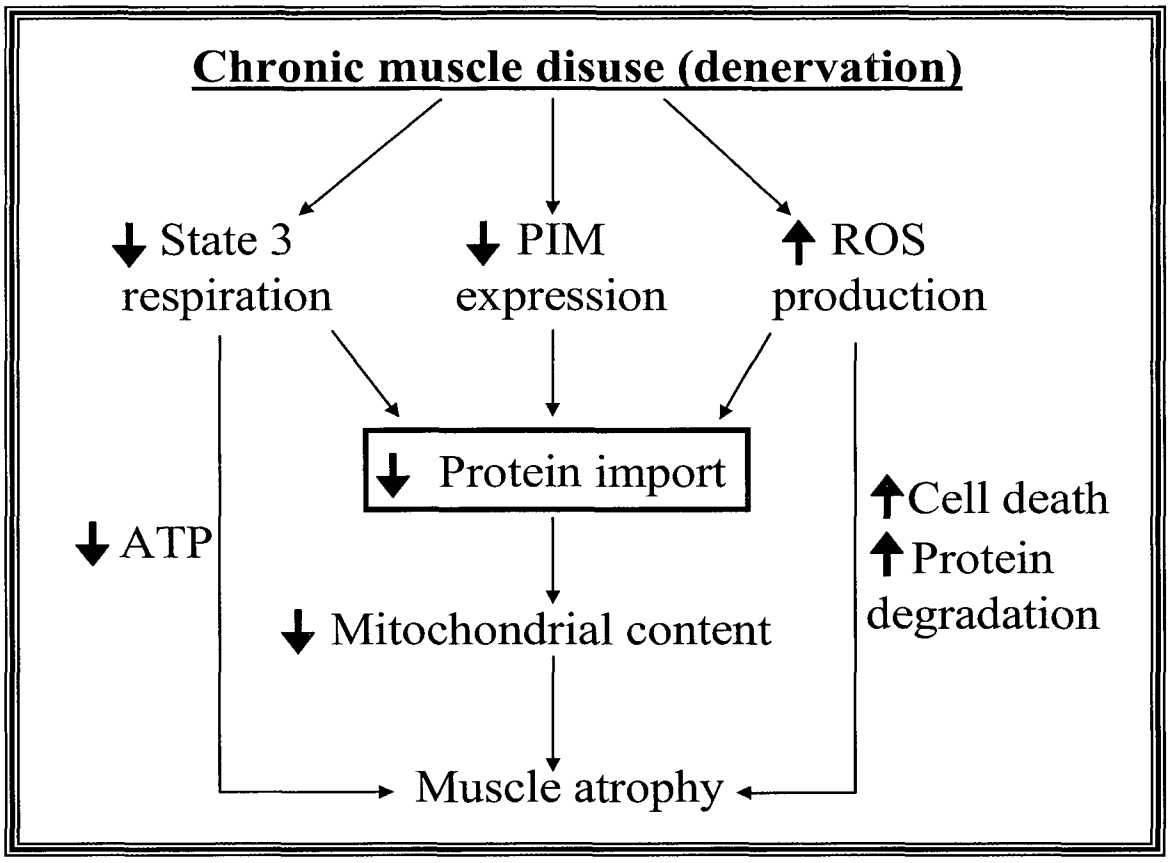

Figure 11: Summary of chronic disuse-related events leading to alterations in muscle mitochondria and atrophy. Protein import kinetics are mediated by components of the protein import machinery (PIM) complex and mitochondrial function. Denervation reduces the rate of protein import in mitochondria by decreasing the expression of various PIM components, as well as state 3 respiration. Furthermore, denervation-induced decreases in antioxidant enzymes, along with alterations in electron transport chain activity simultaneously elevate ROS generation in muscle. This increase in oxidative stress further reduces mitochondrial protein import. An overall decline in the assembly of nuclear-encoded proteins in the mitochondria lowers whole muscle mitochondrial content which contributes towards muscle atrophy. Furthermore, alterations in organelle function, denoted by mitochondrial respiration and ROS production, can also directly affect muscle mass. Reduced state 3 respiration lowers ATP content in the cell, which condenses cytoplasmic volume per myonucleus. Excessive ROS production promotes the activation of proteolytic pathways that culminate in myofibrillar degradation. Alternatively, higher levels of intracellular ROS can also initiate a cascade of pro-apoptotic events which lead to myonuclear apoptosis. All of these factors contribute towards chronic muscle disuse-induced fiber atrophy.

SUMMARY AND FUTURE WORK

The results obtained from this thesis are important for our understanding of 1) the molecular mechanisms which regulate mitochondrial protein import, as well as 2) the pathophysiology of muscle inactivity-related ailments such as spinal muscular atrophy. While many studies have demonstrated that mitochondrial content and function are reduced by chronic muscle disuse, these changes have been mainly attributed to alterations in the transcriptional activity of genes involved in mitochondrial biogenesis, or catabolic events such as apoptosis, which are associated with muscle atrophy. There have not been many investigations into the post-translational processes governing mitochondrial synthesis during muscle disuse, which includes adaptations in the protein import complex.

Therefore, the purposes of this thesis were to establish whether denervation induces a differential response in modulating protein import between subsarcolemmal (SS) and intermyofibrillar (IMF) mitochondria, and to relate how changes in mitochondrial function affect import kinetics in determining mitochondrial content. Since protein import is conducted by the import machinery, the protein expression of several important components involved in this pathway were also investigated. Our results provide evidence of a partial role for the protein import pathway in the dysregulation of mitochondrial biogenesis in SS and IMF subfractions. This decrease in import kinetics is mediated by the combination of reduced import machinery expression, increased oxidative stress and impaired mitochondrial respiration. Given the present findings, future studies should focus on the following:

1. A determination of whether denervation-induced adaptations in import kinetics are protein specific. Our experiments should be validated with the use of preproteins other than OCT. Furthermore, using proteins such as the mitochondrial transcription factor A (Tfam), which decreases with muscle disuse, as well as the apoptosis inducing factor (AIF), which increases in expression will allow us to establish if the import process adapts in a protein-specific manner.
2. The role of cytosolic factors in mediating protein import may be demonstrated *in vitro* by supplementing our import reaction with cytosolic extracts from control and denervated muscles. Using western blot analysis, alterations in import may be attributed to expression of key chaperones such as Hsp70 and MSF, or mediators of protein degradation such as the proteosome.
3. A third research path that deserves exploration is the investigation of specific PIM components in the regulating protein import during basal conditions as well as circumstances of altered contractile activity. This may be demonstrated by measuring precursor import in mitochondria isolated from transgenic mice such as the recently characterized Tim23 heterozygous knockout mouse. The *in vitro* cell culture model of C2C12 myotubes may be alternatively employed to knockdown the expression of various components of the PIM using siRNA to complement the *in vivo* results.
4. Previous work, along with the results in this thesis, have demonstrated that precursor import activity is affected by alterations in ROS and respiration. To

further elucidate the mechanisms by which mitochondrial function regulates protein import, the following experiments should be conducted:

a. The reactions where protein import is inhibited by ROS should be supplemented with an antioxidant such as N-acetyl-L-cysteine (NAC) to see if the effect of ROS is attenuated;

b. The redox status of PIM components with cysteine-rich thiol residues should be examined by the incorporation of radiolabelled PIM into mitochondria, which are then subjected to oxidative stress *in vitro* as performed in our experiments. Alterations in S-thiolation as visualized by autoradiography following SDS-PAGE would then be used to link protein oxidation status to the inhibition of import by ROS;

c. The Ψ_m and ATP synthesis in mitochondria are controlled by respiration, and have been previously linked to precursor protein import. However, the relative contribution of cardiolipin content and state 3 respiration in altering import has never been functionally characterized. The use of adriamycin to inhibit cardiolipin, and varying the concentration of ADP in the import reaction could be used to achieve this.

APPENDIX A

Data tables and statistical analyses

Table 1. *A*

IMF and SS mitochondrial state 3 respiration rates (natoms O_2/min•mg)			
N	**SS control**	**IMF control**	**IMF control/ SS control**
1	74.21	246.51	3.32
2	89.54	162.23	1.81
3	63.28	218.98	3.46
4	87.14	124.25	1.43
5	57.33	113.35	1.98
6	102.40	178.22	1.74
7	89.26	312.26	3.50
8	65.56	245.86	3.75
9	64.90	196.32	3.02
10	114.83	338.19	2.95
11	141.15	239.42	1.70
12	124.83	208.30	1.67
13	98.91	214.53	2.17
14	71.49	176.23	2.47
15	74.13	277.17	3.74
16	66.19	249.87	3.78
17	135.91	172.59	1.27
18	86.43	235.56	2.73
19	102.85	253.40	2.46
20	75.32	188.52	2.50
21	94.14	177.82	1.89
22	106.22	164.22	1.55
23	71.01	179.34	2.53
24	70.53	179.73	2.55
25	68.81	334.12	4.86
26	92.12	200.29	2.17
X ± SE	**88.02 ± 4.47**	**214.90± 11.24**	**2.58 ± 0.18**

Paired t test
SS control vs. IMF control
Two-tailed P value < 0.0001
t = 10.70
df = 25

Table. 1. *B*

IMF and SS mitochondrial ROS production during state 3 respiration (AFU/natoms $O_2 \bullet min^{-1}$)			
n	**SS control**	**IMF control**	**IMF control/ SS control**
1	17	3	0.18
2	19	2	0.11
3	43	3	0.07
4	17	7	0.41
5	57	11	0.19
6	43	6	0.14
7	23	4	0.15
8	21	2	0.08
9	13	3	0.20
10	40	10	0.25
11	30	26	0.88
12	36	10	0.28
13	24	4	0.15
14	30	9	0.29
15	63	7	0.11
16	17	11	0.65
17	46	6	0.13
18	38	3	0.08
19	32	2	0.06
20	21	3	0.14
X ± SE	**31.50 ± 3.14**	**6.60± 1.24**	**0.23 ± 0.05**

Paired t test
SS control vs. IMF control
Two-tailed P value < 0.0001
t = 7.93
df = 19

Table 1. *C*

pOCT protein import in isolated mitochondrial subfractions (% of mature protein/available pOCT)			
n	**SS control**	**IMF control**	**IMF control/ SS control**
1	29.85	63.42	2.12
2	44.34	54.34	1.23
3	35.62	67.3	1.89
4	17.84	44.31	2.48
5	24.43	61.45	2.52
6	32.76	46.23	1.41
7	25.16	34.23	1.36
8	17.75	43.11	2.43
9	16.78	39.43	2.35
10	16.71	32.97	1.97
11	31.04	72.4	2.33
12	21.28	58.51	2.75
13	44.04	67.89	1.54
14	32.47	75.25	2.32
15	25.2	59.25	2.35
16	45.29	69.36	1.53
17	30.25	46.74	1.55
18	49.35	57.38	1.16
19	16.33	64.52	3.95
20	22.59	43.63	1.93
21	43.79	66.7	1.52
22	40.72	63.53	1.56
23	32.93	66.93	2.03
X ± SE	**30.28 ± 2.18**	**56.47 ± 2.62**	**2.01 ± 0.13**

Paired t test
SS control vs. IMF control
Two-tailed P value < 0.0001
t = 11.24
df = 22

Table 1. *D*

mtHSP70 protein expression in isolated mitochondrial subfractions (AU)			
n	**SS control**	**IMF control**	**IMF control/ SS control**
1	0.51	0.21	0.41
2	0.70	0.56	0.79
3	0.97	0.90	0.92
4	1.36	2.34	1.72
5	3.47	0.59	0.17
6	0.93	0.50	0.54
7	2.74	0.65	0.24
8	2.31	0.86	0.37
9	1.90	1.00	0.52
10	0.79	0.83	1.05
11	1.63	0.66	0.40
12	1.73	0.81	0.47
13	0.85	0.61	0.72
14	1.75	0.68	0.39
15	1.58	0.27	0.17
16	1.35	0.70	0.52
17	1.52	1.53	1.01
18	1.46	1.89	1.29
19	1.25	1.28	1.03
20	0.47	0.96	2.06
21	1.64	0.74	0.45
22	1.63	0.67	0.41
23	1.50	0.42	0.28
24	1.11	0.68	0.61
X ± SE	**1.47 ± 0.14**	**0.85 ± 0.10**	**0.69 ± 0.09**

Paired t test
SS control vs. IMF control
Two-tailed P value = 0.002
t = 3.59
df = 23

Table 2. *A*

Tibialis anterior muscle mass / body weight (mg/g)			
n	**3 day control**	**3 day denervated**	**3 day den/con**
1	1.68	1.64	0.98
2	1.66	1.55	0.94
3	1.88	1.77	0.94
4	1.84	1.70	0.93
5	1.90	1.74	0.92
6	1.75	1.60	0.91
7	1.65	1.58	0.96
8	1.85	1.70	0.92
9	1.86	1.73	0.93
10	1.81	1.66	0.92
X ± SE	**1.79 ± 0.03**	**1.67 ± 0.02**	**0.94 ± 0.01**

Paired t test
Control vs. 3 day denervated
Two-tailed P value = 0.002
t = 4.28
df = 9

Tibialis anterior muscle mass / body weight (mg/g)			
n	**7 day control**	**7 day denervated**	**7 day den/con**
1	1.76	1.14	0.65
2	1.79	1.29	0.72
3	1.82	1.37	0.75
4	1.89	1.38	0.73
5	1.99	1.33	0.67
6	1.98	1.30	0.65
7	1.75	1.21	0.69
8	1.94	1.27	0.65
9	1.85	1.25	0.67
10	1.89	1.20	0.63
11	1.68	1.06	0.63
12	1.66	1.04	0.63
X ± SE	**1.83 ± 0.03**	**1.24 ± 0.03**	**0.67 ± 0.01**

Paired t test
Control vs. 7 day denervated
Two-tailed P value < 0.0001
t = 8.27
df = 8

Table 2. *A (cont)*

Tibialis anterior muscle mass / body weight (mg/g)			
n	**14 day control**	**14 day denervated**	**14 day den/con**
1	1.83	0.47	0.26
2	1.88	0.55	0.29
3	1.89	0.50	0.27
4	1.90	0.80	0.42
5	1.82	0.66	0.36
6	1.87	0.61	0.33
7	1.94	0.71	0.36
8	1.88	0.65	0.35
9	1.83	0.79	0.43
10	1.87	0.86	0.46
11	1.81	0.61	0.34
12	1.78	0.66	0.37
13	2.14	0.91	0.42
14	1.96	0.94	0.48
X ± SE	**1.89 ± 0.02**	**0.69 ± 0.04**	**0.37 ± 0.02**

Paired t test
Control vs. 14 day denervated
Two-tailed P value = 0.001
t = 5.22
df = 7

Tibialis anterior muscle mass (denervated/control)			
n	**3 day**	**7 day**	**14 day**
1	0.98	0.65	0.26
2	0.94	0.72	0.29
3	0.94	0.75	0.27
4	0.93	0.73	0.42
5	0.92	0.67	0.36
6	0.91	0.65	0.33
7	0.96	0.69	0.36
8	0.92	0.65	0.35
9	0.93	0.67	0.43
10	0.92	0.63	0.46
11		0.63	0.34
12		0.63	0.37
13			0.42
14			0.48
X ± SE	**0.94 ± 0.01**	**0.67 ± 0.01**	**0.37 ± 0.02**

One-way ANOVA	Sig?	F (df)
Main effect of days of denervation	Yes	380.7 (2,33)

Bonferroni posttests	t	P
3 day vs. 7 day	12.21	< 0.001
3 day vs. 14 day	27.32	< 0.001
7 day vs. 14 day	15.46	< 0.001

Table 2. *B*

EDL cytochrome c Oxidase activity (U/g muscle)			
n	**3 day control**	**3 day denervated**	**3 day den/con**
1	5.89	5.2	0.88
2	6.42	5.17	0.81
3	6.57	6.69	1.02
4	5.77	3.38	0.59
5	11.92	5.86	0.49
6	8.45	4.39	0.52
7	7.74	5.19	0.67
8	9.68	5.27	0.54
9	7.08	5.21	0.74
10	7.65	5.63	0.74
X ± SE	**7.72 ± 1.90**	**5.20 ± 0.28**	**0.70 ± 0.05**

Paired t test
Control vs. 3 day denervated
Two-tailed P value = 0.002
t = 4.28
df = 9

EDL cytochrome c Oxidase activity (U/g muscle)			
n	**7 day control**	**7 day denervated**	**7 day den/con**
1	7.37	6.15	0.83
2	8.95	6.87	0.77
3	7.89	4.01	0.51
4	8.26	5.18	0.63
5	11.26	8.44	0.75
6	7.84	5.34	0.68
7	9.83	5.36	0.55
8	10.76	6.02	0.56
9	7.45	4.21	0.57
X ± SE	**8.85 ± 0.48**	**5.73 ± 0.45**	**0.65 ± 0.04**

Paired t test
Control vs. 7 day denervated
Two-tailed P value < 0.0001
t = 8.27
df = 8

Table 2. *B (cont)*

EDL cytochrome c Oxidase activity (U/g muscle)			
n	**14 day control**	**14 day denervated**	**14 day den/con**
1	5.94	4.66	0.78
2	6.02	3.3	0.55
3	7.3	3.89	0.53
4	5.6	2.8	0.50
5	9.05	4.19	0.46
6	7.45	4.69	0.63
7	13.11	5.38	0.41
8	12.14	5.74	0.47
X ± SE	**8.32 ± 1.02**	**4.33 ± 0.35**	**0.54 ± 0.04**

Paired t test
Control vs. 14 day denervated
Two-tailed P value = 0.001
t = 5.22
df = 7

EDL muscle cytochrome c oxidase activity (denervated/control)			
n	**3 day**	**7 day**	**14 day**
1	0.88	0.83	0.78
2	0.81	0.77	0.55
3	1.02	0.51	0.53
4	0.59	0.63	0.5
5	0.49	0.75	0.46
6	0.52	0.68	0.63
7	0.67	0.55	0.41
8	0.54	0.56	0.47
9	0.74	0.57	
10	0.92		
X ± SE	**0.70 ± 0.05**	**0.65 ± 0.04**	**0.54 ± 0.04**

One-way ANOVA	Sig?	F (df)
Main effect of days of denervation	No	2.97 (2,24)

Table 3. *A*

Mitochondrial state 3 respiration (natoms O_2/min•mg^{-1})						
n	**3 day SS control**	**3 day SS denervated**	**3 day SS den/con**	**3 day IMF control**	**3 day IMF denervated**	**3 day IMF den/con**
1	74.21	41.19	0.56	246.51	187.25	0.76
2	89.54	36.24	0.40	162.23	174.28	1.07
3	63.28	29.82	0.47	218.98	136.59	0.62
4	87.14	54.22	0.62	124.25	109.29	0.88
5	57.33	33.39	0.58	113.35	108.30	0.96
6	102.40	71.69	0.70	178.22	144.51	0.81
7	89.26	66.29	0.74	312.26	259.65	0.83
8	65.56	41.20	0.63	245.86	197.26	0.80
Average	**78.59 ± 5.59**	**46.76 ± 5.51**	**0.59 ± 0.04**	**200.20 ± 24.04**	**164.60 ± 17.99**	**0.84 ± 0.05**

Paired t test
State 3 control SS vs. 3 day denervated SS
Two-tailed P value < 0.0001
t = 9.25
df = 7

Paired t test
State 3 control IMF vs. 3 day denervated IMF
Two-tailed P value = 0.01
t = 3.22
df = 7

Mitochondrial state 3 respiration (natoms O_2/min•mg^{-1})						
n	**7 day SS control**	**7 day SS denervated**	**7 day SS den/con**	**7 day IMF control**	**7 day IMF denervated**	**7 day IMF den/con**
1	64.90	42.09	0.65	196.32	80.02	0.41
2	114.83	36.36	0.32	338.19	242.76	0.72
3	141.15	117.40	0.83	239.42	118.16	0.49
4	124.83	102.67	0.82	208.30	160.29	0.77
5	98.91	37.56	0.38	214.53	120.09	0.56
6	71.49	65.43	0.92	176.23	124.90	0.71
7	74.13	39.27	0.53	277.17	87.38	0.32
8	66.19	33.89	0.51	249.87	91.09	0.36
9	135.91	43.72	0.32	172.59	116.39	0.67
10	86.43	45.69	0.53	235.56	172.59	0.73
11	102.85	53.43	0.52	253.40	188.82	0.75
12	75.32	66.31	0.88	188.52	145.86	0.77
Average	**96.41 ± 7.94**	**56.99 ± 7.83**	**0.60 ± 0.06**	**229.20 ± 13.69**	**137.40 ± 13.70**	**0.61 ± 0.05**

Paired t test
State 3 control SS vs. 7 day denervated SS
Two-tailed P value = 0.0003
t = 5.12
df = 11

Paired t test
State 3 control IMF vs. 7 day denervated IMF
Two-tailed P value < 0.0001
t = 6.76
df = 11

Table 3. *A (cont)*

Mitochondrial state 3 respiration (natoms O_2/min•mg^{-1})						
n	**14 day SS control**	**14 day SS denervated**	**14 day SS den/con**	**14 day IMF control**	**14 day IMF denervated**	**14 day IMF den/con**
1	94.14	27.85	0.30	177.82	94.28	0.53
2	106.22	78.82	0.74	164.22	116.56	0.71
3	71.01	31.85	0.45	179.34	111.68	0.62
4	70.53	55.19	0.78	179.73	152.98	0.85
5	68.81	24.98	0.36	334.12	80.62	0.24
6	92.12	61.61	0.67	200.29	73.54	0.37
Average	**83.81 ± 6.44**	**46.72 ± 8.90**	**0.55 ± 0.08**	**205.90 ± 26.07**	**104.90 ± 11.80**	**0.55 ± 0.09**

Paired t test
State 3 control SS vs. 14 day denervated SS
Two-tailed P value = 0.003
t = 5.22
df = 5

Paired t test
State 3 control IMF vs. 14 day denervated IMF
Two-tailed P value = 0.03
t = 3.01
df = 5

State 3 mitochondrial respiration (denervated/control)						
	SS mitochondria			**IMF mitochondria**		
n	**3 day**	**7 day**	**14 day**	**3 day**	**7 day**	**14 day**
1	0.56	0.65	0.30	0.76	0.41	0.53
2	0.40	0.32	0.74	1.07	0.72	0.71
3	0.47	0.83	0.45	0.62	0.49	0.62
4	0.62	0.82	0.78	0.88	0.77	0.85
5	0.58	0.38	0.36	0.96	0.56	0.24
6	0.70	0.92	0.67	0.81	0.71	0.37
7	0.74	0.53		0.83	0.32	
8	0.63	0.51		0.80	0.36	
9		0.32			0.67	
11		0.53			0.73	
11		0.52			0.75	
12		0.88			0.77	
X ± SE	**0.59 ± 0.04**	**0.84 ± 0.05**	**0.55 ± 0.08**	**0.61 ± 0.05**	**0.57 ± 0.08**	**0.55 ± 0.09**

Two-way ANOVA		
State 3 respiration (denervated/control)	**Sig?**	**F (df)**
Interaction	Yes	3.44 (2,23)
Main effect of days of denervation	No	2.53 (2, 23)
Main effect of mitochondrial subfraction	No	3.62 (1,23)

Table 3. *B*

Mitochondrial state 4 respiration (natoms O_2/min•mg^{-1})						
n	**3 day SS control**	**3 daySS denervated**	**3 day SS den/con**	**3 day IMF control**	**3 day IMF denervated**	**3 day IMF den/con**
1	16.17	12.39	0.77	28.42	25.41	0.89
2	8.23	10.47	1.27	21.59	27.69	1.28
3	23.56	12.39	0.53	26.38	33.21	1.26
4	30.24	22.54	0.75	39.45	25.18	0.64
5	12.45	10.46	0.84	31.25	22.95	0.73
6	5.87	7.37	1.26	24.09	19.47	0.81
7	9.42	5.80	0.62	42.17	28.39	0.67
8	12.45	7.41	0.60	21.69	17.66	0.81
Average	**14.80 ± 2.93**	**11.10 ± 1.85**	**0.83 ± 0.10**	**29.38 ± 2.76**	**25.00 ± 1.77**	**0.89 ± 0.09**

Paired t test
State 4 control SS vs. 3 day denervated SS
Two-tailed P value = 0.05
t = 2.35
df = 7

Paired t test
State 4 control IMF vs. 3 day denervated IMF
Two-tailed P value = 0.16 (NS)
t = 1.57
df = 7

Mitochondrial state 4 respiration (natoms O_2/min•mg^{-1})						
n	**7 day SS control**	**7 day SS denervated**	**7 day SS den/con**	**7 day IMF control**	**7 day IMF denervated**	**7 day IMF den/con**
1	8.17	15.78	1.93	25.13	33.75	1.34
2	11.67	10.83	0.93	33.24	39.25	1.18
3	28.15	11.24	0.40	28.59	25.90	0.91
4	14.24	7.29	0.51	26.77	23.58	0.88
5	12.25	8.88	0.72	28.85	21.84	0.76
6	22.97	29.82	1.30	24.47	15.14	0.62
7	6.21	4.53	0.73	27.17	32.82	1.21
8	10.67	6.48	0.61	32.91	27.52	0.84
9	24.72	5.48	0.22	38.44	26.06	0.68
10	14.53	4.90	0.34	36.24	28.17	0.78
11	21.42	12.43	0.58	29.92	21.94	0.73
12	18.90	10.80	0.57	21.45	13.87	0.65
Average	**16.16 ± 2.01**	**10.71 ± 2.00**	**0.74 ± 0.14**	**29.43 ± 1.44**	**25.82 ± 2.12**	**0.88 ± 0.07**

Paired t test
State 4 control SS vs. 7 day denervated SS
Two-tailed P value = 0.04
t = 2.33
df = 11

Paired t test
State 4 control IMF vs. 7 day denervated IMF
Two-tailed P value = 0.09 (NS)
t = 1.84
df = 11

Table 3. *B (cont)*

Mitochondrial state 4 respiration (natoms O_2/min•mg^{-1})						
n	**14 day SS control**	**14 day SS denervated**	**14 day SS den/con**	**14 day IMF control**	**14 day IMF denervated**	**14 day IMF den/con**
1	10.91	5.60	0.51	21.94	16.19	0.74
2	14.86	23.04	1.55	27.65	31.99	1.16
3	9.46	14.95	1.58	32.38	15.16	0.47
4	22.17	19.59	0.88	43.19	39.80	0.92
5	26.94	17.58	0.65	44.21	18.47	0.42
6	11.08	5.39	0.49	23.99	13.75	0.57
Average	**15.90 ± 2.90**	**14.36 ± 3.00**	**0.94 ± 0.20**	**32.23 ± 3.91**	**22.56 ± 4.38**	**0.71 ± 0.12**

Paired t test
State 4 control SS vs. 14 day denervated SS
Two-tailed P value = 0.6 (NS)
t = 0.55
df = 5

Paired t test
State 4 control IMF vs. 14 day denervated IMF
Two-tailed P value = 0.07 (NS)
t = 2.22
df = 5

State 4 mitochondrial respiration (denervated/control)						
	SS mitochondria			**IMF mitochondria**		
n	**3 day**	**7 day**	**14 day**	**3 day**	**7 day**	**14 day**
1	0.77	1.93	0.51	0.89	1.34	0.74
2	1.27	0.93	1.55	1.28	1.18	1.16
3	0.53	0.40	1.58	1.26	0.91	0.47
4	0.75	0.51	0.88	0.64	0.88	0.92
5	0.84	0.72	0.65	0.73	0.76	0.42
6	1.26	1.30	0.49	0.81	0.62	0.57
7	0.62	0.73		0.67	1.21	
8	0.60	0.61		0.81	0.84	
9		0.22			0.68	
11		0.34			0.78	
11		0.58			0.73	
12		0.57			0.65	
X ± SE	**0.83 ± 0.10**	**0.74 ± 0.14**	**0.94 ± 0.20**	**0.89 ± 0.09**	**0.88 ± 0.07**	**0.71 ± 0.12**

Two-way ANOVA		
State 4 respiration (denervated/control)	**Sig?**	**F (df)**
Interaction	No	1.77 (2,23)
Main effect of days of denervation	No	0.07 (2, 23)
Main effect of mitochondrial subfraction	No	0.01 (1,23)

Table 4. *A*

Mitochondrial state 3 ROS production (AFU/natoms $O_2 \bullet min^{-1}$)						
n	**3 day SS control**	**3 day SS denervated**	**3 day SS den/con**	**3 day IMF control**	**3 day IMF denervated**	**3 day IMF den/con**
1	17	45	2.65	3	11	3.67
2	19	43	2.26	2	12	6.00
3	43	28	0.65	3	18	6.00
4	17	28	1.65	7	19	2.71
5	57	33	0.58	11	35	3.18
6	43	41	0.95	6	23	3.83
Average	**32.67 ± 7.03**	**36.33 ± 3.12**	**1.46 ± 0.36**	**5.33 ± 1.38**	**19.67 ± 3.58**	**4.23 ± 0.58**

Paired t test
State 3 control SS vs. 3 day denervated SS
Two-tailed P value = 0.6 (NS)
t = 0.43
df = 5

Paired t test
State 3 control IMF vs. 3 day denervated IMF
Two-tailed P value = 0.002
t = 6.11
df = 5

Mitochondrial state 3 ROS production (AFU/natoms $O_2 \bullet min^{-1}$)						
n	**7 day SS control**	**7 day SS denervated**	**7 day SS den/con**	**7 day IMF control**	**7 day IMF denervated**	**7 day IMF den/con**
1	23	35	1.51	4	24	6.86
2	21	60	2.82	2	2	1.17
3	13	19	1.49	3	7	2.76
4	40	32	0.80	10	32	3.18
5	30	30	1.01	26	42	1.62
6	36	41	1.15	10	22	2.16
7	24	39	1.67	4	10	2.94
8	30	52	1.75	9	11	1.30
X ± SE	**27.13 ± 3.06**	**38.50 ± 4.55**	**1.53 ± 0.22**	**8.50 ± 2.75**	**18.75 ± 4.84**	**2.75 ± 0.65**

Paired t test
State 3 control SS vs. 7 day denervated SS
Two-tailed P value = 0.06 (NS)
t = 2.23
df = 7

Paired t test
State 3 control IMF vs. 7 day denervated IMF
Two-tailed P value = 0.01
t = 3.43
df = 7

Table 4. *A (cont)*

Mitochondrial state 3 ROS production (AFU/natoms $O_2 \bullet min^{-1}$)						
n	**14 day SS control**	**14 day SSdenervated**	**14 day SS den/con**	**14 day IMF control**	**14 day IMF denervated**	**14 day IMF den/con**
1	63	157	2.49	7	23	3.29
2	17	75	4.41	11	19	1.73
3	46	135	2.93	6	18	3.00
4	38	157	4.13	3	12	4.00
5	32	122	3.81	2	35	17.50
6	21	87	4.14	3	11	3.67
Average	**36.17 ± 7.03**	**122.20 ± 14.20**	**3.65 ± 0.31**	**5.33 ± 1.38**	**19.67 ± 3.58**	**5.53 ± 2.42**

Paired t test
State 3 control SS vs. 14 day denervated SS
Two-tailed P value = 0.0002
t = 9.69
df = 5

Paired t test
State 3 control IMF vs. 14 day denervated IMF
Two-tailed P value = 0.02
t = 3.64
df = 5

State 3 mitochondrial ROS production (denervated/control)						
	SS mitochondria			**IMF mitochondria**		
n	**3 day**	**7 day**	**14 day**	**3 day**	**7 day**	**14 day**
1	2.65	1.51	2.49	3.67	6.86	3.29
2	2.26	2.82	4.41	6.00	1.17	1.73
3	0.65	1.49	2.93	6.00	2.76	3.00
4	1.65	0.80	4.13	2.71	3.18	4.00
5	0.58	1.01	3.81	3.18	1.62	17.50
6	0.95	1.15	4.14	3.83	2.16	3.67
7		1.67			2.94	
8		1.75			1.30	
X ± SE	**1.46 ± 0.36**	**1.53 ± 0.22**	**3.65 ± 0.31**	**4.23 ± 0.58**	**2.75 ± 0.65**	**5.53 ± 2.42**

Two-way ANOVA		
State 3 ROS (denervated/control)	**Sig?**	**F (df)**
Interaction	No	0.32 (2,23)
Main effect of days of denervation	No	3.30 (2, 23)
Main effect of mitochondrial subfraction	Yes	5.89 (1,23)

Table 4. *B*

Mitochondrial state 4 ROS production (AFU/natoms $O_2 \bullet min^{-1}$)						
n	**3 day SS control**	**3 day SS denervated**	**3 day SS den/con**	**3 day IMF control**	**3 day IMF denervated**	**3 day IMF den/con**
1	112	213	1.90	57	95	1.67
2	309	185	0.60	71	81	1.14
3	153	296	1.93	36	56	1.56
4	119	132	1.11	29	69	2.38
5	216	517	2.39	31	83	2.68
6	308	544	1.77	44	74	1.68
Average	**202.80 ± 36.64**	**314.50 ± 71.74**	**1.62 ± 0.26**	**44.67 ± 6.72**	**76.33 ± 5.44**	**1.85 ± 0.23**

Paired t test
State 4 control SS vs. 3 day denervated SS
Two-tailed P value = 0.1 (NS)
t = 1.78
df = 5

Paired t test
State 4 control IMF vs. 3 day denervated IMF
Two-tailed P value = 0.003
t = 5.16
df = 5

Mitochondrial state 4 ROS production (AFU/natoms $O_2 \bullet min^{-1}$)						
n	**7 day SS control**	**7 day SS denervated**	**7 day SS den/con**	**7 day IMF control**	**7 day IMF denervated**	**7 day IMF den/con**
1	160	421	2.63	22	13	0.61
2	201	366	1.82	48	65	1.37
3	116	162	1.40	27	24	0.89
4	178	392	2.20	62	90	1.44
5	118	222	1.88	32	111	3.45
6	222	222	1.00	30	35	1.18
7	145	254	1.75	32	34	1.06
8	131	198	1.51	34	52	1.52
X ± SE	**158.90 ± 13.76**	**279.60 ± 34.81**	**1.77 ± 0.18**	**35.88 ± 4.57**	**53.00 ± 11.96**	**1.44 ± 0.31**

Paired t test
State 4 control SS vs. 7 day denervated SS
Two-tailed P value = 0.006
t = 3.90
df = 7

Paired t test
State 4 control IMF vs. 7 day denervated IMF
Two-tailed P value = 0.1 (NS)
t = 1.74
df = 7

Table 4. *B (cont)*

Mitochondrial state 4 ROS production (AFU/natoms $O_2 \bullet min^{-1}$)						
n	**14 day SS control**	**14 day SS denervated**	**14 day SS den/con**	**14 day IMF control**	**14 day IMF denervated**	**14 day IMF den/con**
1	306	879	2.87	109	139	1.28
2	129	364	2.82	47	73	1.55
3	317	712	2.25	42	163	3.88
4	119	418	3.51	23	64	2.78
5	74	463	6.26	21	98	4.67
6	137	771	5.63	64	191	2.98
Average	**180.30 ± 42.45**	**601.20 ± 87.03**	**3.89 ± 0.67**	**51.00 ± 13.31**	**121.30 ± 20.87**	**2.86 ± 0.53**

Paired t test
State 4 control SS vs. 14 day denervated SS
Two-tailed P value = 0.001
t = 6.66
df = 5

Paired t test
State 4 control IMF vs. 14 day denervated IMF
Two-tailed P value = 0.01
t = 3.80
df = 5

State 4 mitochondrial ROS production (denervated/control)						
	SS mitochondria			**IMF mitochondria**		
n	**3 day**	**7 day**	**14 day**	**3 day**	**7 day**	**14 day**
1	1.90	2.63	2.87	1.67	0.61	1.28
2	0.60	1.82	2.82	1.14	1.37	1.55
3	1.93	1.40	2.25	1.56	0.89	3.88
4	1.11	2.20	3.51	2.38	1.44	2.78
5	2.39	1.88	6.26	2.68	3.45	4.67
6	1.77	1.00	5.63	1.68	1.18	2.98
7		1.75			1.06	
8		1.51			1.52	
X ± SE	**1.62 ± 0.26**	**1.77 ± 0.18**	**3.89 ± 0.67**	**1.85 ± 0.23**	**1.44 ± 0.31**	**2.86 ± 0.53**

Two-way ANOVA		
State 4 ROS (denervated/control)	**Sig?**	**F (df)**
Interaction	No	2.11 (2,23)
Main effect of days of denervation	Yes	9.08 (2, 23)
Main effect of mitochondrial subfraction	No	2.43 (1,23)

Table 5. *A*

Rate of OCT import in isolated mitochondria (% of available OCT)						
n	**3 day SS control**	**3 day SS denervated**	**3 day SS den/con**	**3 day IMF control**	**3 day IMF denervated**	**3 day IMF den/con**
1	29.85	17.42	0.58	63.42	58.43	0.92
2	44.34	35.98	0.81	54.34	44.93	0.83
3	35.62	25.42	0.71	67.3	53.9	0.80
4	17.84	18.48	1.04	44.31	46.75	1.06
5	24.43	12.45	0.51	61.45	48.97	0.80
6	32.76	23.52	0.72	46.23	43.23	0.94
7	25.16	16.57	0.66	34.23	28.23	0.82
X ± SE	**30.00 ± 3.26**	**21.41± 2.93**	**0.72 ± 0.07**	**53.04 ± 4.53**	**46.35± 3.62**	**0.88 ± 0.04**

Paired t test
Control SS vs. 3 day denervated SS
Two-tailed P value = 0.002
t = 5.21
df = 6

Paired t test
Control IMF vs. 3 day denervated IMF
Two-tailed P value = 0.02
t = 3.18
df = 6

Rate of OCT import in isolated mitochondria (% of available OCT)						
n	**7 day SS control**	**7 day SS denervated**	**7 day SS den/con**	**7 day IMF control**	**7 day IMF denervated**	**7 day IMF den/con**
1	17.75	11.89	0.67	43.11	27.41	0.64
2	16.78	16.58	0.99	39.43	32.25	0.82
3	16.71	6.84	0.41	32.97	31.52	0.96
4	31.04	9.74	0.31	72.4	59.55	0.82
5	21.28	10.58	0.50	58.51	39.6	0.68
6	44.04	18.97	0.43	67.89	51.96	0.77
7	32.47	23.13	0.71	75.25	71.82	0.95
8	25.2	20.5	0.81	59.25	51.56	0.87
X ± SE	**25.66 ± 3.42**	**14.78± 2.06**	**0.60 ± 0.08**	**56.10 ± 5.62**	**45.71± 5.51**	**0.81 ± 0.04**

Paired t test
Control SS vs. 7 day denervated SS
Two-tailed P value = 0.008
t = 3.68
df = 7

Paired t test
Control IMF vs. 7 day denervated IMF
Two-tailed P value = 0.002
t = 4.62
df = 7

Table 5. *A cont*

Rate of OCT import in isolated mitochondria (% of available OCT)						
n	**14 day SS control**	**14 day SS denervated**	**14 day SS den/con**	**14 day IMF control**	**14 day IMF denervated**	**14 day IMF den/con**
1	45.29	29.48	0.65	69.36	53.47	0.77
2	30.25	14.08	0.47	46.74	44.44	0.95
3	49.35	22.08	0.45	57.38	37.61	0.66
4	16.33	7.66	0.47	64.52	8.43	0.13
5	22.59	8.04	0.36	43.63	22.07	0.51
6	43.79	15.6	0.36	66.7	69.13	1.04
7	40.72	16.67	0.41	63.53	50.64	0.80
8	32.93	28.21	0.86	66.93	52.57	0.79
X ± SE	**35.16 ± 4.12**	**17.73 ± 2.93**	**0.50 ± 0.06**	**59.85 ± 3.44**	**42.30 ± 6.81**	**0.71 ± 0.10**

Paired t test
Control SS vs. 14 day denervated SS
Two-tailed P value = 0.0007
t = 5.79
df = 7

Paired t test
Control IMF vs. 14 day denervated IMF
Two-tailed P value = 0.03
t = 2.82
df = 7

OCT protein import in isolated mitochondrial subfractions (denervated/control)						
	SS mitochondria			**IMF mitochondria**		
N	**3 day**	**7 day**	**14 day**	**3 day**	**7 day**	**14 day**
1	0.58	0.67	0.65	0.92	0.64	0.77
2	0.81	0.99	0.47	0.83	0.82	0.95
3	0.71	0.41	0.45	0.8	0.96	0.66
4	1.04	0.31	0.47	1.06	0.82	0.13
5	0.51	0.5	0.36	0.8	0.68	0.51
6	0.72	0.43	0.36	0.94	0.77	1.04
7	0.66	0.71	0.41	0.82	0.95	0.8
8		0.81	0.86		0.87	0.79
X ± SE	**0.72 ± 0.07**	**0.60 ± 0.08**	**0.50 ± 0.06**	**0.88 ± 0.04**	**0.81 ± 0.04**	**0.70 ± 0.10**

Two-way ANOVA		
Mitochondrial OCT import (denervated/control)	**Sig?**	**F (df)**
Interaction	No	0.07 (2,23)
Main effect of days of denervation	No	3.42 (2, 23)
Main effect of mitochondrial subfraction	Yes	13.33 (1,23)

Table 5. *B*

Reduction in import corrected for days of denervation ([1-den/con]/days of denervation%)		
n	**SS mitochondria**	**IMF mitochondria**
1	14.00%	0.03
2	6.33%	0.06
3	9.67%	0.07
4	-1.33%	-0.02
5	16.33%	0.07
6	9.33%	0.02
7	11.33%	0.06
8	4.71%	0.05
9	0.14%	0.03
10	8.43%	0.01
11	9.86%	0.03
12	7.14%	0.05
13	8.14%	0.03
14	4.14%	0.01
15	2.71%	0.02
16	2.50%	0.02
17	3.79%	0.00
18	3.93%	0.02
19	3.79%	0.06
20	4.57%	0.04
21	4.57%	0.00
22	4.21%	0.01
23	1.00%	0.02
X ± SE	**6.06 ± 0.90**	**2.86 ± 0.50**

Paired t test
SS mitochondria vs. IMF mitochondria
Two-tailed P value = 0.0004
t = 4.19
df = 22

Table 6

Tim23 protein expression in isolated mitochondrial subfractions (A.U)						
n	**3 day SS control**	**3 day IMF denervated**	**3 day SS den/con**	**3 day IMF control**	**3 day IMF denervated**	**3 day IMF den/con**
1	0.50	0.47	0.95	0.60	0.48	0.80
2	0.68	0.59	0.87	0.57	0.83	1.45
3	0.88	0.61	0.69	1.56	1.21	0.78
4	0.85	0.25	0.30	1.26	0.59	0.47
5	0.71	0.18	0.25	0.37	0.62	1.67
6	0.60	0.06	0.10	0.77	0.43	0.55
7	0.88	0.96	1.09	1.21	1.89	1.56
8	0.76	0.04	0.06	1.86	0.86	0.46
9	0.42	0.08	0.20	0.25	0.17	0.69
10	0.38	0.38	0.99	0.32	0.33	1.01
X ± SE	**0.67 ± 0.06**	**0.36 ± 0.09**	**0.55 ± 0.13**	**0.88 ± 0.18**	**0.74 ± 0.16**	**0.94 ± 0.15**

Paired t test
Control SS vs. 3 day denervated SS
Two-tailed P value = 0.008
t = 3.37
df = 9

Paired t test
Control IMF vs. 3 day denervated IMF
Two-tailed P value = 0.4 (NS)
t = 0.89
df = 9

Tim23 protein expression in isolated mitochondrial subfractions (A.U)						
n	**7 day SS control**	**7 day IMF denervated**	**7 day SS den/con**	**7 day IMF control**	**7 day IMF denervated**	**7 day IMF den/con**
1	1.23	0.64	0.52	1.09	0.89	0.82
2	1.04	0.35	0.34	1.35	1.03	0.76
3	1.00	0.16	0.16	0.90	0.19	0.21
4	2.14	0.39	0.18	1.56	0.53	0.34
5	1.12	0.93	0.83	1.36	1.09	0.80
6	0.96	0.58	0.60	1.20	1.53	1.28
7	0.80	1.01	1.27	1.08	1.21	1.12
8	1.02	0.51	0.50	1.47	0.89	0.61
X ± SE	**1.16 ± 0.15**	**0.57 ± 0.10**	**0.55 ± 0.13**	**1.21 ± 0.08**	**0.92 ± 0.15**	**0.74 ± 0.13**

Paired t test
Control SS vs. 7 day denervated SS
Two-tailed P value = 0.02
t = 2.94
df = 7

Paired t test
Control IMF vs. 7 day denervated IMF
Two-tailed P value = 0.07 (NS)
t = 2.12
df = 7

Table 6 *(cont)*

Tim23 protein expression in isolated mitochondrial subfractions (A.U)						
n	**14 day SS control**	**14 day IMF denervated**	**14 day SS den/con**	**14 day IMF control**	**14 day IMF denervated**	**14 day IMF den/con**
1	0.72	1.00	1.39	1.02	1.35	1.32
2	1.48	1.28	0.86	0.53	0.25	0.48
3	1.27	1.04	0.82	1.72	0.68	0.40
4	1.59	0.91	0.57	0.78	0.66	0.84
5	2.67	1.60	0.60	0.52	0.17	0.33
6	1.23	0.79	0.64	1.43	0.82	0.57
7	2.71	1.82	0.67	2.17	0.65	0.30
8	2.50	1.90	0.76	0.71	0.45	0.63
X ± SE	**1.77 ± 0.27**	**1.29 ± 0.15**	**0.79 ± 0.09**	**1.11 ± 0.21**	**0.63 ± 0.13**	**0.61 ± 0.12**

Paired t test
Control SS vs. 14 day denervated SS
Two-tailed P value = 0.02
t = 3.15
df = 7

Paired t test
Control IMF vs. 14 day denervated IMF
Two-tailed P value = 0.04
t = 2.37
df = 7

Tim23 protein expression in isolated mitochondrial subfractions (denervated/control)						
	SS mitochondria			**IMF mitochondria**		
n	**3 day**	**7 day**	**14 day**	**3 day**	**7 day**	**14 day**
1	0.95	0.52	1.39	0.80	0.82	1.32
2	0.87	0.34	0.86	1.45	0.76	0.48
3	0.69	0.16	0.82	0.78	0.21	0.40
4	0.30	0.18	0.57	0.47	0.34	0.84
5	0.25	0.83	0.60	1.67	0.80	0.33
6	0.10	0.60	0.64	0.55	1.28	0.57
7	1.09	1.27	0.67	1.56	1.12	0.30
8	0.06	0.50	0.76	0.46	0.61	0.63
9	0.20			0.69		
10	0.99			1.01		
X ± SE	**0.55 ± 0.13**	**0.55 ± 0.13**	**0.79 ± 0.09**	**0.94 ± 0.15**	**0.74 ± 0.13**	**0.61 ± 0.12**

Two-way ANOVA		
Tim23 (denervated/control)	**Sig?**	**F (df)**
Interaction	No	2.62 (2,23)
Main effect of days of denervation	No	1.67 (2,23)
Main effect of mitochondrial subfraction	No	0.32 (1,23)

Table 7

Tom20 protein expression in isolated mitochondrial subfractions (A.U)						
n	**3 day SS control**	**3 day IMF denervated**	**3 day SS den/con**	**3 day IMF control**	**3 day IMF denervated**	**3 day IMF den/con**
1	1.95	1.21	0.62	0.88	1.31	1.49
2	1.35	1.06	0.78	0.96	1.31	1.36
3	0.96	1.15	1.20	1.71	2.75	1.61
4	1.34	1.17	0.87	2.20	1.96	0.89
5	1.09	0.31	0.29	1.56	1.21	0.78
6	1.00	1.24	1.24	1.74	1.81	1.04
X ± SE	**1.28 ± 0.15**	**1.02 ± 0.14**	**0.83 ± 0.15**	**1.51 ± 0.21**	**1.73 ± 0.24**	**1.19 ± 0.14**

Paired t test
Control SS vs. 3 day denervated SS
Two-tailed P value = 0.2 (NS)
t = 1.44
df = 5

Paired t test
Control IMF vs. 3 day denervated IMF
Two-tailed P value = 0.3 (NS)
t = 1.04
df = 5

Tom20 protein expression in isolated mitochondrial subfractions (A.U)						
n	**7 day SS control**	**7 day IMF denervated**	**7 day SS den/con**	**7 day IMF control**	**7 day IMF denervated**	**7 day IMF den/con**
1	1.05	0.72	0.69	0.97	1.01	1.04
2	1.02	0.48	0.48	0.85	0.86	1.00
3	1.71	0.94	0.55	1.51	2.28	1.51
4	2.44	1.06	0.43	2.18	1.53	0.70
5	1.72	1.05	0.61	1.15	1.18	1.03
6	1.33	0.55	0.41	1.04	0.72	0.69
7	1.59	1.24	0.78	1.43	0.92	0.65
8	1.23	0.51	0.41	1.13	1.17	1.03
X ± SE	**1.51 ± 0.16**	**0.82 ± 0.10**	**0.55 ± 0.05**	**1.28 ± 0.15**	**1.21 ± 0.18**	**0.96 ± 0.10**

Paired t test
Control SS vs. 7 day denervated SS
Two-tailed P value = 0.0006
t = 5.95
df = 7

Paired t test
Control IMF vs. 7 day denervated IMF
Two-tailed P value = 0.6 (NS)
t = 0.48
df = 7

Table 7 *cont*

Tom20 protein expression in isolated mitochondrial subfractions (A.U)						
n	**14 day SS control**	**14 day IMF denervated**	**14 day SS den/con**	**14 day IMF control**	**14 day IMF denervated**	**14 day IMF den/con**
1	1.73	1.30	0.75	1.72	1.88	1.09
2	1.90	1.40	0.74	1.97	1.41	0.72
3	1.44	1.67	1.16	1.42	1.03	0.72
4	1.73	0.63	0.37	1.33	0.80	0.60
5	1.92	1.22	0.64	1.50	1.57	1.05
6	2.02	0.68	0.34	1.57	1.56	0.99
7	1.66	1.09	0.66	1.22	1.04	0.85
8	1.23	0.90	0.73	1.19	1.57	1.32
X ± SE	**1.70 ± 0.09**	**1.11 ± 0.13**	**0.67 ± 0.09**	**1.49 ± 0.09**	**1.36 ± 0.13**	**0.92 ± 0.08**

Paired t test
Control SS vs. 14 day denervated SS
Two-tailed P value = 0.01
t = 3.50
df = 7

Paired t test
Control IMF vs. 14 day denervated IMF
Two-tailed P value = 0.3 (NS)
t = 1.10
df = 7

Tom20 protein expression in isolated mitochondrial subfractions (denervated/control)						
	SS mitochondria			**IMF mitochondria**		
n	**3 day**	**7 day**	**14 day**	**3 day**	**7 day**	**14 day**
1	0.62	0.69	0.75	1.49	1.04	1.09
2	0.78	0.48	0.74	1.36	1.00	0.72
3	1.20	0.55	1.16	1.61	1.51	0.72
4	0.87	0.43	0.37	0.89	0.70	0.60
5	0.29	0.61	0.64	0.78	1.03	1.05
6	1.24	0.41	0.34	1.04	0.69	0.99
7		0.78	0.66		0.65	0.85
8		0.41	0.73		1.03	1.32
X ± SE	**0.83 ± 0.14**	**0.55 ± 0.05**	**0.67 ± 0.09**	**1.19 ± 0.13**	**0.96 ± 0.09**	**0.92 ± 0.08**

Two-way ANOVA		
Tom20 (denervated/control)	**Sig?**	**F (df)**
Interaction	No	0.48 (2,19)
Main effect of days of denervation	No	3.09 (2,19)
Main effect of mitochondrial subfraction	Yes	20.41 (1,19)

Table 8

mtHsp70 protein expression in isolated mitochondrial subfractions (A.U)						
n	**3 day SS control**	**3 day IMF denervated**	**3 day SS den/con**	**3 day IMF control**	**3 day IMF denervated**	**3 day IMF den/con**
1	0.51	0.21	0.41	0.21	0.19	0.91
2	0.70	0.45	0.63	0.56	0.77	1.37
3	0.97	0.47	0.48	0.90	0.66	0.74
4	1.36	0.22	0.16	2.34	1.14	0.49
5	3.47	1.46	0.42	0.59	0.36	0.61
6	0.93	0.66	0.71	0.50	0.09	0.18
7	2.74	1.71	0.62	0.65	0.31	0.48
8	2.31	1.52	0.66	0.86	0.22	0.25
X ± SE	**1.62 ± 0.38**	**0.84 ± 0.22**	**0.51 ± 0.06**	**0.83 ± 0.23**	**0.47 ± 0.13**	**0.63 ± 0.14**

Paired t test
Control SS vs. 3 day denervated SS
Two-tailed P value = 0.008
t = 3.68
df = 7

Paired t test
Control IMF vs. 3 day denervated IMF
Two-tailed P value = 0.04
t = 2.39
df = 7

mtHsp70 protein expression in isolated mitochondrial subfractions (A.U)						
n	**7 day SS control**	**7 day IMF denervated**	**7 day SS den/con**	**7 day IMF control**	**7 day IMF denervated**	**7 day IMF den/con**
1	1.90	1.25	0.66	1.00	1.21	1.21
2	0.79	1.05	1.33	0.83	0.72	0.87
3	1.63	1.36	0.84	0.66	0.71	1.08
4	1.73	1.58	0.91	0.81	0.69	0.85
5	0.85	0.62	0.73	0.61	0.42	0.69
6	1.75	0.21	0.12	0.68	0.62	0.91
7	1.58	0.28	0.18	0.27	0.04	0.15
8	1.35	0.07	0.05	0.70	0.03	0.04
X ± SE	**1.45 ± 0.15**	**0.80 ± 0.21**	**0.60 ± 0.16**	**0.70 ± 0.07**	**0.56 ± 0.14**	**0.73 ± 0.15**

Paired t test
Control SS vs. 7 day denervated SS
Two-tailed P value = 0.03
t = 2.78
df = 7

Paired t test
Control IMF vs. 7 day denervated IMF
Two-tailed P value = 0.2 (NS)
t = 1.55
df = 7

Table 8 *cont*

mtHsp70 protein expression in isolated mitochondrial subfractions (A.U)						
n	**14 day SS control**	**14 day IMF denervated**	**14 day SS den/con**	**14 day IMF control**	**14 day IMF denervated**	**14 day IMF den/con**
1	1.52	0.05	0.04	1.53	0.51	0.33
2	1.46	1.01	0.69	1.89	1.09	0.58
3	1.25	0.05	0.04	1.28	1.10	0.86
4	0.47	0.87	1.85	0.96	0.59	0.62
5	1.64	0.04	0.03	0.74	0.02	0.03
6	1.63	0.02	0.01	0.67	0.02	0.03
7	1.50	0.03	0.02	0.42	0.02	0.05
8	1.11	0.03	0.03	0.68	0.03	0.04
X ± SE	**1.32 ± 0.14**	**0.26 ± 0.15**	**0.34 ± 0.23**	**1.02 ± 0.18**	**0.42 ± 0.17**	**0.32 ± 0.12**

Paired t test
Control SS vs. 14 day denervated SS
Two-tailed P value = 0.004
t = 4.27
df = 7

Paired t test
Control IMF vs. 14 day denervated IMF
Two-tailed P value = 0.0004
t = 6.31
df = 7

mtHsp70 protein expression in isolated mitochondrial subfractions (denervated/control)						
	SS mitochondria			**IMF mitochondria**		
n	**3 day**	**7 day**	**14 day**	**3 day**	**7 day**	**14 day**
1	0.41	0.66	0.04	0.91	1.21	0.33
2	0.63	1.33	0.69	1.37	0.87	0.58
3	0.48	0.84	0.04	0.74	1.08	0.86
4	0.16	0.91	1.85	0.49	0.85	0.62
5	0.42	0.73	0.03	0.61	0.69	0.03
6	0.71	0.12	0.01	0.18	0.91	0.03
7	0.62	0.18	0.02	0.48	0.15	0.05
8	0.66	0.05	0.03	0.25	0.04	0.04
X ± SE	**0.51 ± 0.06**	**0.60 ± 0.15**	**0.34 ± 0.23**	**0.63 ± 0.14**	**0.73 ± 0.14**	**0.32 ± 0.12**

Two-way ANOVA		
mtHsp70 (denervated/control)	**Sig?**	**F (df)**
Interaction	No	0.24 (2,21)
Main effect of days of denervation	No	1.90 (2,21)
Main effect of mitochondrial subfraction	No	0.57 (1,21)

Table 9

Mitochondrial OCT import in the presence of H_2O_2 (% mature OCT/ total OCT)						
	SS mitochondria			IMF mitochondria		
n	**0μM**	**5μM**	**10μM**	**0μM**	**5μM**	**10μM**
1	25.2	19.95	18.06	62.44	43.91	43.82
2	39.19	17.79	21.2	60.05	27.43	10.7
3	31.83	24.96	15.8	41.82	38.51	27.3
4	38.85	20.01	14.57	47.15	31.16	31.25
5	25.52			50.64		29.12
6				54.38		
7				50.14		
X ± SE	**32.12 ± 3.06**	**20.68 ± 1.52**	**17.41 ± 1.46**	**52.37 ± 2.72**	**35.25 ± 3.69**	**28.44 ± 5.30**

Two-way ANOVA	Sig?	F (df)
Interaction	No	1.01 (5,23)
Main effect of [H_2O_2]	Yes	18.81
Main effect of mitochondrial subfraction	Yes	29.34

Bonferroni posttests	t	P
0μM SS vs. 5μM SS	11.44	$P < 0.05$
0μM SS vs. 10μM SS	14.71	$P < 0.01$
5μM SS vs. 10μM SS	3.27 (ns)	$P > 0.05$
0μM IMF vs. 5μM IMF	17.12	$P < 0.05$
0μM IMF vs. 10μM IMF	23.94	$P < 0.01$
5μM IMF vs. 10μM IMF	6.81 (ns)	$P > 0.05$

APPENDIX B

Additional data

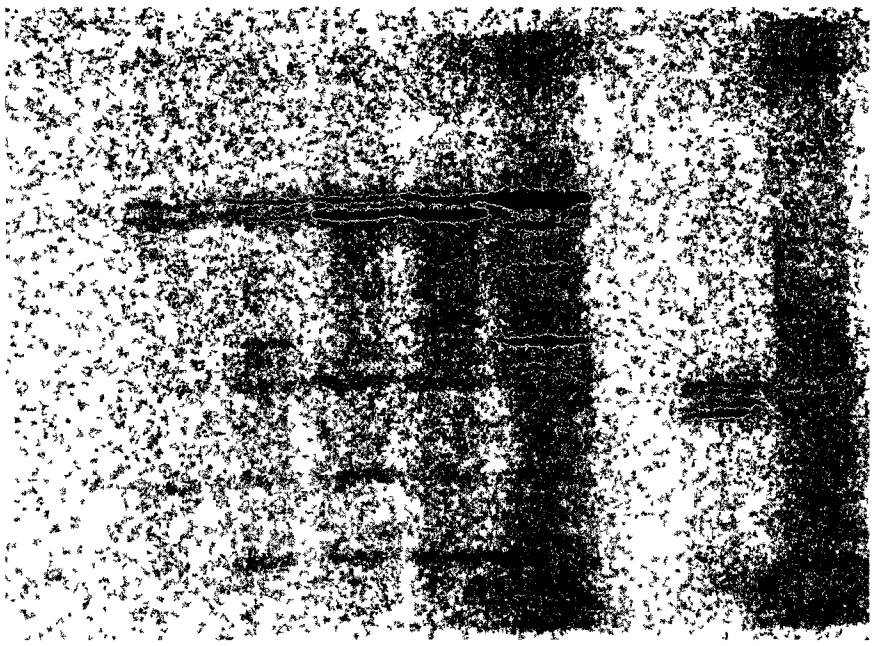

Fig. 1. mtHsp70 import in IMF mitochondria. Autoradiograph showing import of varying concentrations of mtHsp70 lysate and IMF mitochondria. *Lane 1*, 12 µl lysate: 25 µg mitochondria. *Lane 2*, 25 µl lysate: 25 µg mitochondria. *Lane 3*, 25 µl lysate: 50 µg mitochondria. *Lane 4*, 50 µl lysate: 50 µg mitochondria. *Lane 5 (positive control)*, 12 µl OCT lysate: 25 µg mitochondria.

APPENDIX C

Experimental protocols

Surgery for denervation of skeletal muscle

1. Sterilize surgical instruments in autoclave machine for 20 minutes.
2. Anaesthetize rat with 0.2 mls/100g body weight of Ketamine/Xylazine.
3. Shave animal's right hindlimb close to the skin.
4. Wipe the shaved area with 1% topical iodine antiseptic solution.
5. Make a 2 cm incision in the skin approximately 1 cm posterior and 1 cm inferior to the knee.
6. Carefully blunt dissect through the exposed superficial muscle until the common peroneal nerve is visualized. This nerve innervates the tibialis anterior (TA) and extensor digitorum longus (EDL) muscles.
7. Cut out a small 5mm section of the nerve. This ensures that the nerve endings will not regenerate during the experiment and thus effectively denervates the TA and EDL muscles.
8. Inject a small volume (~0.1mls) of sterile ampicillin in the local incision site.
9. Using the 5.0 surgical silk, suture close the superficial muscle tear. Seal the overlying skin on the hindlimb using surgical staples.
10. Monitor the animal over the next 24 hours to ensure recovery. The animal is free to move about the cage and feed/drink *ad libitum*.
11. Recovering animals are given amoxicillin in their drinking water (0.025% w/v) for 1 week after surgery.

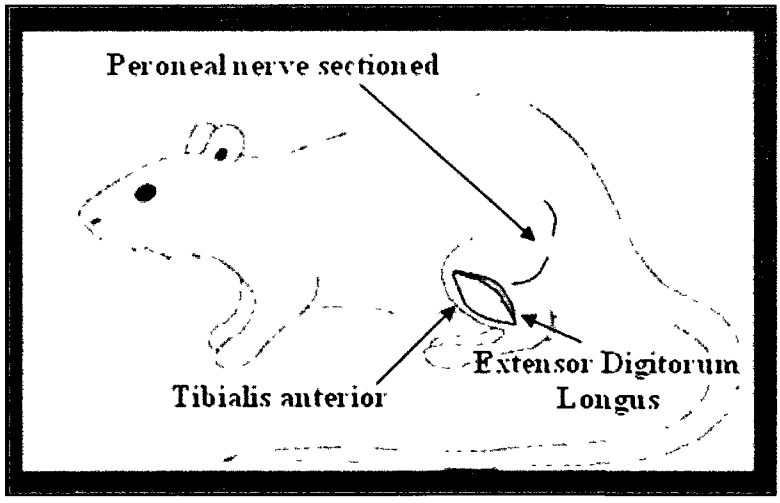

Alkaline lysis plasmid DNA preparation

The purpose of this method is to isolate plasmid DNA from bacteria. It results in DNA which can be used both for *in vitro* and *in vivo* transfections. The DNA may or may not be good enough for *in vitro* transcription. The entire procedure takes 3 or 4 days depending on the length of the ethanol precipitations. Usually 4 plasmids samples are done together.

Solutions

1. LB medium:
   10 g tryptone
   5 g yeast extract
   10 g NaCl
   Make up to 1000 ml with H_2O (it is not necessary to pH).
   Autoclave

2. Ampicillin stock: 50 mg/ml in sterile H_2O. Store at -20 °C. Use 1 □l/ml LB + agar to make AMP plates.

3. M9 medium (10X) :
   30 g Na_2HPO_4
   15 g KH_2PO_4
   5 g NH_4Cl
   2.5 g NaCl
   480 ml H_2O

   Autoclave, cool and use 48 ml along with the volumes of supplements below for a total volume of 500 ml.

   The addition of the following supplements gives you supplemented M9 medium which is used on Day 2, step 1. First autoclave 437 ml H_2O in a 2 litre Erlenmeyer (1 erlenmeyer/plasmid), then add the following sterile M9 supplements to each flask:

	Stock solutions
48 ml 10X M9 medium	
10 ml 20% (w/v) casamino acids	100 g/500 ml, autoclave
2.5 ml 40 % (w/v) glucose	20 g/100 ml, filter sterile
2.5 ml 1 mg/ml thiamine	filter sterile, store at 4°C
0.5 ml 1 M $MgSO_4$	12.04 g/100 ml, autoclave
1.0 ml 50mM $CaCl_2$	5.55 g/1000 ml, autoclave

4. Solution I:

	Stock solutions
20 ml 0.25 M EDTA (pH 8.0)	9.31 g /100 ml, pH to 8, autoclave
12.5 ml of 1M Tris-HCl (pH 8.0)	12.11 g/100 ml, pH to 8, autoclave
456 ml H_2O	
Autoclave, then add: 11.25 ml 40% glucose	40 g/100 ml, filter sterile

5. Lysozyme: make fresh the day of the experiment.
   28 mg/ml (Sigma L-6876) in solution I. Use 6 mls (168 mg) for 4 plasmids.

6. Solution II: make fresh the day of the experiment. No sterilizing.
   70 ml H_2O
   1.6 ml 10 M NaOH
   8.0 ml 10% SDS

7. Solution III: no sterilizing.

	Stock solution
180 ml 5M potassium acetate	122.7 g/250 ml
34.5 ml glacial acetic acid	
85.5 ml H_2O	

8. Solution IV: no sterilizing.

	Stock solutions
16.7 ml 3 M sodium acetate (pH 6.0)	12.3 g/50 ml
25 ml 1 M Tris-HCl (pH 8.0)	12.11 g/100 ml, pH to 8, autoclave
458 ml H_2O	

   Check that final the pH = 8.0 (if around 7.9, then add 1.5 ml 1 M NaOH).

9. Lithium chloride: 84.8 g/250 ml, autoclave.

10. RNAse A: 10 mg /ml pancreatic RNAse (Sigma R-5503, 100 mg) in 50 mM sodium acetate (pH 4.8). Dissolve heat in boiling H_2O for 10 min and cool at room temperature. Aliquot and store at -20 °C.

11. TEN:

	Stock solutions
5 ml 1 M Tris-HCl (pH 8.0)	12.11 g/100 ml, pH to 8, autoclave
2 ml 0.25 M EDTA (pH 8.0)	9.31 g/100 ml, pH to 8, autoclave
1 ml 5 M NaCl	29.22 g/100 ml, heat and adjust the volume as close as possible to 100 ml to dissolve

   Add around 450 ml H_2O, pH to 7.5, and then make up to 500 ml. Autoclave.

12. Ethanol: Keep a stock of 500 ml of 100% ethanol (unmatured) from stores at -20 °C.

Protocol

Day 1

1. Inoculate 10 ml of LB medium containing the selective antibiotic (e.g. 10 □l of 50 mg/ml AMP). Shake overnight at 37°C in a 250 ml Erlenmeyer flask.

Day 2

1. Pour the 10 ml growth culture evenly into 500 ml of supplemented M9 medium in a 2 litre flask.
2. Grow with vigorous shaking (200 rpm) at 37°C until the OD_{600} = 0.4 (2-3 hours). Check the OD by removing 1 ml aliquots with a sterile 1 ml pipette.
3. Add 0.5 ml of either: a) 135 mg/ml streptomycin (dissolved in H_2O)
   Or b) 170 mg/ml chloramphenicol (dissolved in ethanol)
   This step is done to stop chromosome replication and protein synthesis, and amplify the plasmid replication to thousands of copies/cell.
4. Incubate overnight at 37°C with shaking (200 rpm).

Day 3

1. Distribute each plasmid culture into 2 X 50 ml sterile centrifuge bottles.
2. Spin 5 min at 11,000 g (11,500 rpm in JLA 10.50 rotor). Discard supernate and drain the pellets on a paper towel.
3. Resuspend the 2 pellets in a total of 6 ml of solution I (i.e. add 6 ml to one bottle, resuspend by pipetting up and down, transfer to the second bottle. Resuspend the pellet, and transfer to the third bottle. Resuspend the third pellet.).
4 Transfer to a 50 ml sterile Nalgene tube.
5. Add 1.5 ml of lysozyme solution to each tube (1 tube/plasmid). Vortex and incubate on ice 30 min.
6. Add 18 ml of solution II to each tube. Close tube, and invert the tubes gently to mix several times (3-4). Avoid excessive agitation as this will shear chromosomal DNA. Yellowish and clear layers will form. Incubate on ice 5 min.
7. Add 14 ml of solution III to each tube. Cover again and invert sharply several times (7-8). A white clot of genomic DNA will form. Incubate on ice 20 min.
8. Spin at 27,000 g (19,500 rpm in JA 25.50 rotor) for 20 min to pellet cell debris (the failure to form a compact pellet is usually a consequence of inadequate mixing of the bacterial lysate with solution III). Pour the supernate into a fresh labelled tube. Cover and invert several times. Sometimes suspended materials and precipitates form upon mixing.
9. Split the supernate into two 50 ml tubes (2 tubes/plasmid). Balance and add 25 ml cold 95% ethanol to each tube. Cover with parafilm and mix well.
10. Incubate overnight at -20°C.

Day 4

1. Spin at 23,000 g (18,500 rpm in JA 25.50 rotor) for 15 min.
2. Discard the supernate and drain the pellet on a paper towel.
3. Add 4.5 ml of solution IV to one tube. Resuspend and transfer to second tube. Resuspend by pipetting.
4. Add 3 ml 8M LiCl to each tube (1 tube/plasmid, now 4 tubes total).
5. Incubate on ice 20 min.
6. Spin at 23,000 g (15,000 rpm in JA 25.50 rotor) for 15 min.
7. Transfer the supernates to new 50 ml tubes (1 tube/plasmid) and add 25 ml cold 95% ethanol. Cover with parafilm and mix well. Store at -20 °C overnight.

Day 5

1. Spin at 23,000 g (18,000 rpm in JA 25.50 rotor) for 15 min.
2. Discard the supernate and drain the pellet on a paper towel. Resuspend each pellet in 3 ml TEN. Transfer each to a 15 ml Corex tube (1 tube/plasmid).
3. Add 12.5 □l pancreatic RNAse A per tube and incubate at 37 °C for 20 min.
□ Add 1 volume of phenol (3 ml), vortex and spin for 5 min at 5,000 g (7,000 rpm in 870 rotor).
5. Transfer the upper aqueous phase to a new tube and add 1 volume of P:C:I (25:24:1, v/v/v). Vortex and spin as above.
6. Repeat PCI step again (Total of 2 PCI reactions)
7. Transfer the upper aqueous phase to a new tube and add 1 volume of C:I (24:1, v/v). Vortex and spin as above.
8. Transfer the upper aqueous phase to a new tube and add 1 volume ether. Vortex and spin as above.
9. Discard the upper ether phase and add 1 volume of ether. Repeat 2 times more (3 ether extractions in total).
10. Add 150 □l 5M NaCl + 5 ml cold 95% ethanol. Cover with parafilm and mix well.
11. Store at -20 °C overnight.

Day 6

1. Spin at 16,000 g (13,000 rpm in 870 rotor) for 15 min.
2. Discard the supernate and vacuum dry the pellet (it takes approximately 10-15 min to dry the pellet).
3. Resuspend in 0.4-1 ml of TE buffer (pH 8.0). For example, use 0.2 ml for resuspension, transfer to an eppendorf tube, and wash the tube with 0.2 ml and spin to recover the volume. Combine the volumes.
4. Measure the DNA concentration.
5. Check the plasmid on a gel.

Cytochrome *c* oxidase activity assay

Reagents

- 100 mM KPO_4 buffer
  - 0.1 M KH_2PO_4
  - 0.1 M $K_2HPO_4 \cdot 3H_2O$
  - Mix equal portions of above, pH to 7.0

- 10 mM KPO_4 buffer
  - Dilute the 100 mM KPO_4 buffer 1:10 with ddH_2O.

- Sodium dithionite (Fisher, S-310)
  - 10 mg/ml in 10 mM KPO_4 buffer

- Test solution (prepare in tinted jar)
  - 20 mg horse heart cytochrome c (Sigma, C-2506)
  - 1 ml 10 mM KPO_4 buffer
  - 40 µl sodium dithionite
  - 8 ml ddH_2O
  - 1 ml 100 mM KPO_4 buffer

- Muscle extraction buffer
  - 100 mM Na/K PO_4
  - 2 mM EDTA
  - pH to 7.2

Procedure

1. Add ~5-10 µg of frozen, powdered muscle tissue to 10-200 µl (to obtain a 80-fold dilution) of extraction buffer in an Eppendorf tube.
2. Add a micro stir bar to the tube and stir the tissue extract for 15 min on ice. Make the Test solution during this time and wrap the tinted jar in foil.
3. Sonicate each sample 3 X 3 s.
4. Pipette 250 µl of the Test solution into a 96 well plate and incubate them at 30 °C for 10 min.
5. In a second 96 well plate, pipette 30 µl of sample into 4-8 empty plates. Using the multipipette, quickly draw up the test solution and pipette into the wells with the sample extracts.
6. Place well plate into microplate reader and start recording the change in absorbance at 550 nm for 1 min.
7. Calculate cytochrome c oxidase enzyme activity (µmol/min/g or U/g) using the following formula:

$$\frac{\Delta \text{ Abs/min} \times \text{total volume (ml)} \times 80 \text{ (dilution)}}{18.5 \text{ Abs/µmol} \times \text{sample volume (ml)}}$$

Mitochondrial isolation

Reagents

All buffers are set to pH 7.4 and stored at 4 °C

Buffer 1
- 100 mM KCl
- 5 mM $MgSO_4$
- 5 mM EDTA
- 50 mM Tris base

Buffer 1 + ATP
- Add 1 mM ATP to Buffer 1

Buffer 2
- 100 mM KCl
- 5 mM $MgSO_4$
- 5 mM EGTA
- 50 mM Tris base
- 1 mM ATP

Resuspension medium
- 100 mM KCl
- 10 mM MOPS
- 0.2% BSA

Nagarse protease (Sigma, P-4789)
- 10 mg/ml in Buffer 2
- Make fresh for each isolation, keep on ice

Procedure

1. Remove the tibialis anterior (TA) muscle from the rat, and put it in a beaker containing 5 ml Buffer 1, on ice immediately.
2. Place TA on a watch glass that is also on ice and trim away fat and connective tissue. Proceed to thoroughly mince the muscle sample with forceps and scissors, until no large pieces are remaining.
3. Place the minced tissue in a plastic centrifuge tube and record the exact weight of tissue.
4. Add a 10-fold dilution of Buffer 1 + ATP to the tube.
5. Homogenize the samples using the Ultra-Turrax polytron with 40% power output and 10 s exposure time. Rinse the shaft with 0.5 ml of Buffer 1 + ATP to help minimize sample loss.
6. Using a Beckman JA 25.50 rotor, spin the homogenate at a centrifuge setting of 800 g for 10 min. This step divides the IMF and SS mitochondrial subfractions. The supernate will contain the SS mitochondria and the pellet will contain the IMF mitochondria.

SS mitochondrial isolation:

7. Filter the supernate through a single layer of cheesecloth into a second set of 50 ml plastic centrifuge tubes.
8. Spin tubes at 9000 g for 10 min. Upon completion of the spin discard the supernate and gently resuspend the pellet in 3.5 ml of Buffer 1 + ATP. Since the mitochondria are easily damaged, it is important that the resuspension of the pellet is done carefully.
9. Repeat the centifugation of the previous step (9000 g for 10 min) and discard the supernate.
10. Resuspend the pellet in 200 µl of Resuspension medium, being gentle so as to prevent damage to the SS mitochondria. Some extra time is needed during this final resuspension to ensure the SS pellet is completely resuspended.
11. Keep the SS samples on ice while proceeding to islolate the IMF subfraction.

IMF mitochondrial isolation:

7. Gently resuspend the pellet (from step 6) in a 10-fold dilution of Buffer 1 + ATP using a teflon pestle.
8. Using the Ultra-Turrax polytron set at 40% power output, polytron the resuspended pellet for 10 s. Rinse the shaft with 0.5 ml of Buffer 1 + ATP.
9. Spin at 800 g for 10 min and discard the resulting supernate.
10. Resuspend the pellet in a 10-fold dilution of Buffer 2 using a teflon pestle.
11. Add the appropriate amount of nagarse. The calculation for the appropriate volume is 0.025 ml/g of tissue. Mix gently and let stand exactly 5 min.
12. Dilute the nagarse by adding 20 ml of Buffer 2.
13. Spin the diluted samples at 5000 g for 5 min and discard the resulting supernate.
14. Resuspend the pellet in a 10-fold dilution of Buffer 2. Gentle resuspension is with a teflon pestle.
15. Spin the samples at 800 g for 10 min. Upon the completion of the spin, the supernate is poured into another set of 50 ml plastic tubes (on ice), and the pellet is discarded.
16. Spin the supernate at 9000 g for 10 min. The supernate is discarded and the pellet is resuspended in 3.5 ml of Buffer 2.
17. Spin samples at 9000 g for 10 min and discard the supernate.
18. Gently resuspend the pellet in 300 µl of Resuspension medium.

Bradford protein assay

Reagents

- Extraction buffer
  - 100 mM Na/K PO_4
  - 2 mM EDTA
  - pH to 7.2

- 5 X Bradford dye
  - 250 ml 85% Phosphoric acid
  - 250 ml 100% Ethanol
  - 500 ml ddH_2O
  - 0.235 g Coomassie Brilliant Blue G250

- Bovine Serum Albumin (BSA)
  - 2 mg/ml in ddH_2O

Procedure

1. Prepare the test tubes allowing for duplicates of each sample.
2. Add 95 µl of extraction buffer to each tube.
3. Add 5 µl of sample to each tube containing the extraction buffer.
4. To generate the standard curve, add the following volumes (in µl) of extraction buffer: BSA, each in separate tubes – 100:0, 95:5, 90:10, 85:15, 80:20, 75:25.
5. Pipette 5 ml of 1 X Bradford reagent into each tube and mix by gentle vortexing.
6. In duplicate, add 0.2 ml of each test tube to 96 well plate wells.
7. Measure absorbance of wells at 595 nm with a microplate reader.
8. Calculate the protein concentration of each sample using the standard curve.

SDS polyacrylamide gel electrophoresis (SDS-PAGE)

Reagents

- Polyacrylamide solution
  30% (w/v) Acrylamide
  0.8% (w/v) Bisacrylamide
  Filter and store at 4 °C

- Ammonium Persulfate (APS)
  10% (w/v) in ddH_2O
  Store at 4 °C

- Over Tris buffer
  1 M Tris•HCl
  Spatula tip of Bromophenol Blue
  pH to 6.8, store at 4 °C

- 15% Acrylamide separating gel
  5 ml 30% acrylamide
  1.8 ml ddH_2O
  3 ml Under Tris
  0.1 ml SDS
  0.1 ml APS
  0.01 ml TEMED

- 3% Acrylamide stacking gel
  0.5 ml 30% Acrylamide
  3.75 ml ddH_2O
  0.625 ml Over Tris
  0.05 ml SDS
  0.05 ml APS
  7.5 µl TEMED

- Under Tris buffer
  1 M Tris•HCl
  pH to 8.8, store at 4 °C

- Sodium Dodecyl Sulfate (SDS)
  10% (w/v) in ddH_2O

- TEMED (Sigma, T-9281)
  Store at 4 °C

- Electrophoresis buffer
  25 mM Tris
  192 mM Glycine
  0.1% (w/v) SDS
  pH to 8.3

- Lysis buffer
  10% (w/v) glycerol
  2.3% (w/v) SDS
  62.5 mM Tris•HCl
  pH to 6.8
  add 5% β-mercaptoethanol

- Sample dye
  40% (w/v) sucrose in electrophoresis buffer
  spatula tip of Bromophenol Blue
  store at -20 °C

Procedure

1. Prepare the separating gel solution and pour it between the glass plates of a gel apparatus assembly.
2. Add 100 µl of Tert-amyl alcohol overlay and allow 30 min for gel polymerization.
3. Prepare the stacking gel.
4. Once the separating gel has polymerized, pour off the Tert-amyl alcohol, insert the lane comb, and pipette the stacking gel around the comb. Allow 30 min for the stacking gel to polymerize.
5. Turn on the block heater to 95 °C.
6. Mix each sample with a 1:1 volume of lysis buffer.
7. Add 10 µl of sample dye to each sample and mix by tapping.
8. Denature the samples at 95 °C for 5 min, followed by a quick cool on ice and a brief spin.
9. Remove the comb and place the gel in the electrophoresis chamber. Fill the chamber with electrophoresis buffer.
10. Add 10 µl of protein molecular weight marker to the first lane.
11. Load the samples into the remaining lanes by slowly ejecting the entire sample volume at the bottom of the lane.
12. Run the gel for 2 hr at 120 V.

Once the Bromophenol Blue band has reached the bottom of the gel, turn off the power supply and remove the gel. The gel slab is ready for electroblotting (see Western Blot)

Western Blot

Reagents

- Transfer buffer
  - 0.025 M Tris•HCl
  - 0.15 M Glycine
  - 20% Methanol
  - pH to 8.3

- Wash buffer
  - 10 mM Tris•HCl
  - 100 mM NaCl
  - 0.1% TWEEN
  - pH to 7.5

- Ponceau stain (Sigma)
  - Dilute with 150 ml ddH_2O

- Blocking buffer
  - % skim milk powder in wash buffer

- Enhanced chemiluminescence (ECL) fluid (Santa Cruz)
  - Store at 4 °C

Procedure

1. Remove the gel from the electrophoresis chamber, and separate the glass plates from the gel slab, keeping the gel moist at all times with transfer buffer.
2. Place three sheets of Whatman paper soaked in transfer buffer onto the plastic sandwich, with a scrubbie. These sheets must be cut to the exact dimensions of the gel slab.
3. Carefully place the gel on top of the Whatman paper.
4. Cut a piece of nitrocellulose membrane to the exact specifications of the gel, soak it in ddH_2O, and place it on top of the gel slab.
5. Stack three more sheets of transfer buffer-soaked Whatman paper (same dimensions as gel) on top of membrane. Roll out any air bubbles with a glass rod.
6. Secure the top of the sandwich with a scrubbie soaked in transfer buffer.
7. Transfer the proteins from the gel to the membrane for 1.5 hours at 120V.
8. Once the transfer is complete, place the membrane in Ponceau stain and gently agitate. Pour off the stain and rinse with ddH_2O until the protein bands on the blot are revealed.
9. Wrap the membrane in plastic wrap and scan.
10. Remove the membrane from the wrap and rinse off the stain with wash buffer.
11. Pour off the wash buffer and block the membrane in blocking solution on a shaker for 1 hour at room temperature.
12. Incubate the membrane with primary antibody diluted in blocking buffer overnight at 4°C. This is done by placing the membrane face-down on a pool of the antibody solution.
13. The following morning, wash the membrane with rotation 3 X 5 min in wash buffer.

14. Incubate the membrane with the appropriate secondary antibody for 1 hr at room temperature. This is done by laying the membrane face-up and pipetting the secondary antibody solution on top of it.
15. Wash the membrane with rotation 3 X 5 min in wash buffer.
16. In the dark room, apply ECL fluids (1:1) to the membrane for 2 min.
17. Remove the membrane from the ECL fluid, wrap the membrane in plastic wrap, turn off the lights, and expose the blot to film.
18. Develop until bands are visualized and place the film into fixer fluid for 2 min.

Mitochondrial respiration

Reagents

- VO_2 buffer
  - 250 mM sucrose
  - 50 mM KCl
  - 25 mM Tris base
  - 10 mM K_2HPO_4
  - pH to 7.4, store at 4 °C

- 10 mM Glutamate (Sigma, G-1501)

- 0.44 mM ADP (Sigma, A-2754)

- 30 mM NADH (Sigma, N-9534)

Procedure

1. Set water circulation temperature through respiration chambers to 30 °C. Place a stir bar in a chamber.
2. Add 250 µl of respiration buffer to the chamber, and begin stirring. Allow the buffer to equilibrate to the chamber temperature for 5-10 min.
3. Cease spinning and pipette 50 µl of the mitochondrial suspension into the chamber.
4. Carefully close the chamber, ensuring no air bubbles remain. Resume spinning.
5. Set the Strathkelvin 782 oxygen consumption software to begin recording data.
6. Once a steady state VO_2 is reached, add glutamate through the electrode port to initiate state 4 respiration.
7. After a satisfactory gradient has been achieved (~3 min later), add ADP to begin state 3 respiration.
8. To assess the integrity of the inner membrane, add NADH during state 3 respiration.
9. Calculate state 4 and state 3 respiration rate (natoms O_2/min/mg) as follows:

$$\text{Respiration rate (\%/mg/min)} = \frac{\text{respiration rate (\%/min)}}{\text{([protein] (µg/µl) x sample vol. (µl)) / 1000}}$$

followed by:

$$\text{Respiration rate (natoms}O_2\text{/min/mg)} = \frac{\text{respiration rate (\%/mg/min) x 112.5 (natoms } O_2\text{)}}{100\%}$$

Mitochondrial ROS production

Background: Mitochondria are the primary source of reactive oxygen species (ROS) to the cell. It is estimated that about 2% of total cellular oxygen is converted ROS by the inappropriate reduction of molecular oxygen by intermediate members of the electron transport chain (ETC). ROS are damaging molecules that are capable of compromising the integrity of macromolecules within the mitochondria and may lead to overall organelle dysfunction. In particular, mtDNA may be prone to attack by ROS because 1) mtDNA is located in close proximity to the ETC, 2) mtDNA lacks the protective sheath of histones compared to nuclear DNA and, 3) mitochondria have an insufficient repair system for mtDNA mutations. ROS can exist in a variety of molecular permutations such as superoxide (O_2^-), hydroxyl radical (OH^-) and hydrogen peroxide (H_2O_2).

DCF (2, 7,-dichloro-fluorescein; Fig.1) is a reagent that is non-fluorescent until the acetate groups are removed by intracellular esterases and oxidation occurs within the mitochondria (Fig.1). DCF is oxidized by all of the different forms of ROS and this can be detected by monitoring the increase in fluorescence with a fluorometric plate reader. The appropriate plate reader filter settings for fluorescein are the following:

Excitation 485/20 and Emission 528/20 (See fig.2).

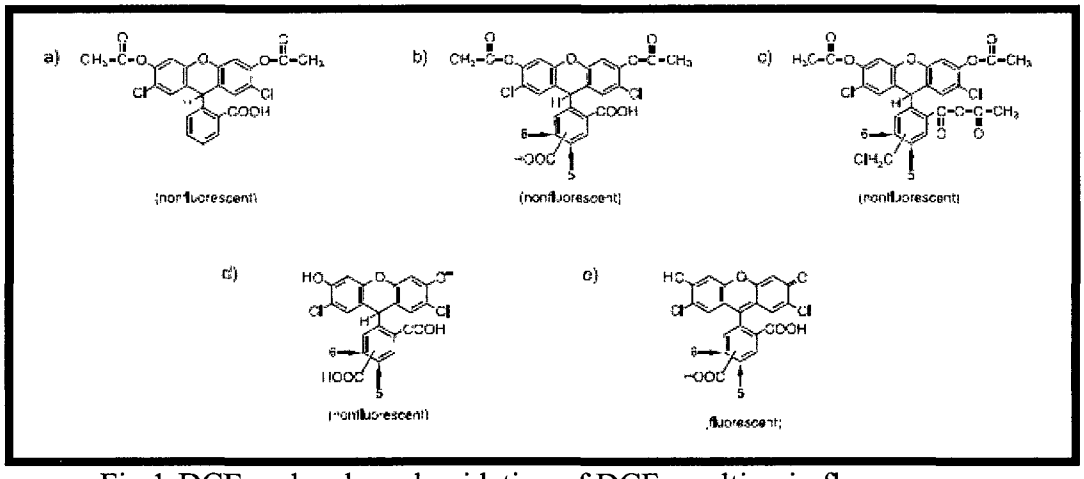

Fig.1-DCF molecule and oxidation of DCF resulting in fluorescence

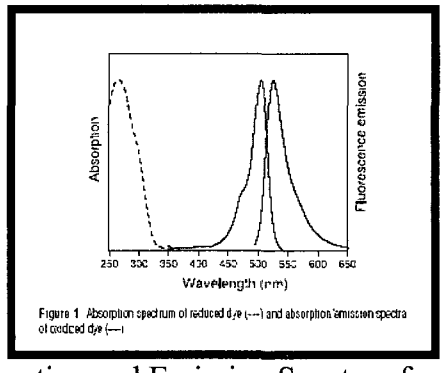

Fig.2-Absorption and Emission Spectra of oxidized dye

KC4 Software Settings: The Settings icon in the upper left corner allows the alteration of various parameters. Once clicked, another window appears, click on the Wizard Icon. In this window there will be a variety of components that can be altered. The following are the parameters that need to be changed in order to utilize the DCF and measure time-dependent ROS production from isolated mitochondria:

1) Top Middle Panel- Absorbance, Fluorescence, Luminescence- choose **Fluorescence**
2) Top Left Panel- End Point, Kinetic, Spectrum- choose **Kinetic**
3) Top Middle Panel- Click on larger box labeled Kinetic to set parameters- **Run Time 0:30:00, Interval 0:30 (takes a measure every 30 seconds),** click on box labeled **Allow Well Zoom during Read,** and also click on box labeled **Individual Well Auto Scaling**- The Well Zoom and Auto scaling allows for monitoring each individual well during the experiment and scales it appropriately.
4) Middle Panel-***Filter Set***- Choose #1, then set the **excitation to 485/20**, and **emission to 528/20** as described above. The optics position should be set to the **TOP** (i.e. readings are taken from the top of the well) and the sensitivity is set at **50** (depending upon the amount and/or nature of the sample).
5) Plate-Type-choose **96-well plate**, choose which wells are to be read i.e. **A1-C12.**
6) Shaking-**Intensity** set at **1, Duration** set at **15s** and then click the box that is labeled **before every reading** (it shakes the samples for 15 s before every reading).
7) Temperature Control- Click on the box indicating **YES ,** also click on box labeled pre-heating, and put 37°C into the temperature box.

DCF Reagent and VO_2 Buffer
DCF (2,7,-dichlorodihydrofluorescein diacetate) reagent (Molecular Probes D-399)

1°STOCK- Make up **50mM** Stock Solution in EtOH- 24 mg/ml- only make about 500ul i.e. 14 mg per 500ul EtOH. Wrap stock solution in aluminum foil and limit exposure to light since DCF is light-sensitive.
Working Stock Solution-2° STOCK- Dilute 50mM by 100-fold by taking 10ul and adding 990ul of EtOH to attain a **500uM DCF Stock Solution**. This will be the DCF concentration used to add to the reaction mixture.

VO_2 Buffer- refer to mitochondrial respiration protocol
10 mM Glutamate (Sigma, G-1501)
0.44 mM ADP (Sigma, A-2754)

Procedure
1. SS and IMF mitochondria are isolated as described in the mitochondrial isolation protocol.
2. Determine the volume necessary for 75ug of mitochondria. Typical volumes should range between 5-40ul depending upon concentration of mitochondrial extracts.

3. Final concentration of DCF is 50uM. The total volume of the reaction mixture is 250ul. Thus, 25ul of DCF is used in the reaction mixture since this represents a 10-fold dilution. Set up table (***as shown below***) and determine the amount of VO_2 buffer necessary to make each of the reaction mixtures equal to 250 ul. (Remember to include a ***control*** with only VO2 buffer and DCF reagent as in Well #1 shown below)

	SS/IMF mitochondria				
		Control	Denervated	Control	Denervated
	Blank	State 4	State 4	State 3	State 4
	Well #1	Well #2	Well #3	Well #4	Well #5
ug mito	0	75	75	75	75
ul mito	0	11.77	9.8	11.77	9.8
glutamate (10mM)	0	10	10	10	10
ADP (0.44 mM)	0	0	0	10	10
VO_2 Buffer	225	203.23	205.2	193.23	195.2
DCF (50uM)	25	25	25	25	25
Total Volume	250	250	250	250	250

4. Once table is complete and volumes for all samples have been determined, place the frozen (already thawed) or fresh mitochondria, VO_2 buffer and DCF (500uM) into a 37°C circulating water bath for 5-10 min.
5. Pipette the volume of VO_2 buffer required for each of the samples followed by the mitochondrial samples into the appropriate wells of a 96-well plate. In addition, include a well (usually in the corner well) with only 250 ul of VO_2 buffer to monitor temperature (see below). Place the 96-well plate with the VO_2 buffer and mitochondria into a 37°C incubator. Using the YSI temperature probe, place the recording electrode into the well with buffer only and monitor the temperature until 37°C is reached. During this time, be sure that the KC4 software is set up and that the microplate reader is pre-heating to 37°C.
6. Once mitochondria and buffer have reached temperature (37°C), take the substrates and DCF out of the circulating water bath (37°C) and quickly add the reagents accoding to the pipette planto each of the reaction mixtures. Following addition of DCF, promptly place the plate into the Biotek plate reader for fluorescence measurement and start the KC4 program by pressing **READ** plate on the upper left portion of the computer screen. Kinetic program will operate for 30 min.

Mitochondrial protein import

Reference: Takahashi and Hood, J. Biol. Chem. (1996) 271, 27285-27291

The majority of nuclear-encoded mitochondrial proteins require a mechanism of import. Proteins destined for this organelle also require a presequence. This will provide a "passport" containing instructions for the final destination for that protein. Once the protein has reached its final destination, the presequence is cleaved, leaving a "mature" protein. By taking advantage of this change in protein size, we are able to establish a means by which imported proteins can be discerned. This can be accomplished by radiolabelling the precursor proteins in vitro then allowing them to be imported. The samples can be electrophoresed on a polyacrylamide gel and will appear as two bands (precursor and mature) when the gel is exposed to film.

A. In Vitro Transcription And Translation

1. Linearize DNA

Combine the following in an eppendorf:

40 µl DNA at 5 µg/µl (200 µg)
5 µl 10x Enzyme buffer
5 µl Restriction enzyme

Incubate for 1 hour at 37°C.

2. Phenol extraction / ethanol precipitation

a) Add appropriate volume of sterile dH_2O so that the final volume equals 400 µl.
b) Add 400 µl phenol.
c) Mix by inversion and spin in microfuge for 30 sec.
d) Withdraw and save upper phase.
e) Add 400 µl Phenol:Chloroform:Isoamylalcohol (25:24:1, v:v:v).
f) Mix by inversion and spin in microfuge for 30 sec.
g) Withdraw and save the upper phase.
h) Add 400 µl Chloroform:Isoamylalcohol (24:1, v:v).
i) Mix by inversion and spin.
j) Withdraw and save the upper phase
k) Add 40 µl 3 M Na Ac (1/10 vols) and 1 ml of -20 °C 100% ethanol (2.5 vols).
l) Mix by inversion and precipitate at -70 °C overnight.
m) Spin 10 min. at 4 °C and discard the supernate.
n) Gently wash pellet with 400 µl 70% ethanol.
o) Spin 3 min. at 4°C, discard the supernate.
p) Dessicate pellet.
q) Resuspend the pellet in 30-50 µl TE, pH 8.0.

3. **Measure [DNA]**

Read the O.D. at A_{260} to determine the concentration of DNA.
Dilute the DNA to 0.8 µg/µl in TE (pH 8.0).

4. **Transcription**

Combine the following in the order indicated:

60.8 µl plasmid (0.8 µg/µl in TE)
8.4 µl dH_2O
5.2 µl NTP (10 mM)
10.0 µl ATP (10 mM)
11.6 µl 7-MGG (1 mM)
15.6 µl Mix 1
5.2 µl RNA guard
4.8 µl of appropriate RNA polymerase
121.6 µl total volume

Incubate for 90 min. at the optimum temperature for the polymerase (37°C for T7, 40 °C for SP6).

5. **Phenol extraction / ethanol precipitation**

Bring volume up to 400 µl with sterile dH_2O (using 280 µl)
Proceed exactly as described in step 3, above.
Resuspend the pellet in 25-40 µl sterile dH_2O

6. **Measure [mRNA]**

Read the O.D. at A260 to determine the concentration of mRNA Dilute mRNA to 2.8 µg/µl in sterile dH_2O. Store at -20 °C in 50 µl aliquots.

B. In vitro translation

Reference: Promega Technical Manual: "Rabbit Reticulocyte Lysate System"

1. Combine the following:

Promega lysate		(For 1 reaction -- in µl)	For 10µl of TL
Lysate	64.1%	11.8	6.38
AA(-met)	2.2%	0.4	0.22
st. dH_2O	21.6%	3.97	2.15
^{35}S-met	7.2%	1.33	0.72
mRNA	5.4%	1.0	0.54
		18.5 µl	

Notes: i) The Promega manual suggests that lysate should be thawed slowly on ice. It also suggests that the number of freeze/thaw cycles be limited to two.
ii) The volume of mRNA can be adjusted to optimize translational efficiency by altering the dH_2O volume accordingly.

2. Incubate for 30 min. at 30 °C (note: time may vary with mRNA)
3. Record ^{35}S use (10 µCi/µl).

C. Protein Import

1. Preincubate both the mitochondria and lysate for 10 minutes @ 30^0C, and then combine lysate and mitochondria to initiate import reaction.
2. Incubate at 30^0C for the times indicated.
3. To stop reaction, place eppendorfs on ice
4. To recover the mitochondria following import, spin the entire volume through a 20% sucrose gradient (600µl) for 15 minutes at 4°C.
5. Remove the supernate with a 1ml pipette and discard in liquid radioactive waste
6. Resuspend mitochondrial pellet in 20µl of breaking buffer
7. Add 20µl of 1X lysis buffer and 10µl of sample dye
8. Denature samples for 5 minutes at 95°C, then quickly cool on ice
9. Apply samples to a 12% SDS-polyacrylamide gel and run until blue marker reaches the bottom of the gel.

D. Fluorography

1. Remove gel from chamber and cut out the appropriate section of the gel. Identify the orientation of the gel.
2. Boil the gel in approximately 200 ml of 5% TCA for 5 min. in metal container, over the Bunsen burner in the fume hood.
3. Using a spatula, transfer the gel to a radioactive tupperware container and rinse the gel briefly in dH_2O (approximately 30 seconds).
4. Wash in 10 mM Tris-base for 5 min. on shaker (approximately 100 ml).
5. Wash in 1 M salicylic acid for 30 min. on shaker (approximately 100 ml).
6. Dry the gel for 1 hr. at 80°C.

Solutions for Transcription and Translation

Note: because mRNA is involved in both transcription and translation, sterile conditions should be adhered to at all times. Use sterile glassware, eppendorfs, dH_2O, etc. Autoclave or sterile filter solutions where indicated.

10 X Proteinase K buffer	For 10 ml
500 mM NaCl	0.2922g or 5 ml of 5 M NaCl
50 mM EDTA	0.1861g or 0.5 ml of 0.5 M EDTA, pH 8
100 mM Tris-HCl	0.1576g or 1 ml of 1 M Tris, pH 8
pH to 8.0	3.5 ml sterile dH_2O

20 mM HEPES Use 0.4766g/100 ml, pH to 7.0, autoclave.
1 M HEPES Use 23.83 g/100ml, pH to 7.9, autoclave. Store at RT.

NTPs	MW(g/mol)	For 50 mM (stocks)
CTP	483.2	24.16 mg/ml
GTP	523.2	26.16 mg/ml
UTP	484.1	24.21 mg/ml
ATP	551.1	27.56 mg/ml

Note: These NTPs should be made up in 20 mM HEPES. Make up 1 ml of each as stock and filter sterile (using sterile acrodisk).

10 mM NTPs	For 500 µl
10 mM GTP	100 µl of 50 mM GTP stock
10 mM CTP	100 µl of 50 mM CTP stock
10 mM UTP	100 µl of 50 mM UTP stock
20 mM HEPES (pH 7.0)	200 µl of 20 mM HEPES (pH 7.0)

- Store in 50 µl aliquots at -20 °C

10 mM ATP	For 500 µl
10 mM ATP	100 µl of 50 mM ATP
20 mM HEPES (pH 7.0)	400 µl of 20 mM HEPES
Store in 50 µl aliquots at -20 °C	(pH 7.0)
(pH 7.0)	

- Store in 50 µl aliquots at -20 °C

7-MGG (Pharmacia 27-4635-02)
1 mM stock is made from Pharmacia pellet. 25U is ordered; added to this is 1208 µl of 20 mM HEPES (pH 7.0), yielding a 1 mM stock. Aliquot into 300 µl, store at -20 °C.

Mix 1	For 1200 µl
0.167 M HEPES (pH 7.9)	200 µl of 1 M HEPES (pH 7.9)
0.083 M $MgAc_2$	100 µl of 1 M $MgAc_2$
1.667 M KAc	500 µl of 4 M KAc
1.667 mM spermidine	100 µl of 20 mM spermidine
0.042 M DTT	100 µl of 0.5 M DTT
(Store in 100 µl aliquots at -20 °C)	200 µl of dH_2O

RNA guard -- Pharmacia #27-0815-01 **Lysate** -- Fisher (Promega) L4960
^{35}**S-met** -- Amersham SJ-1515 **T7 RNA Polymerase** -- Boehringer 881767 (20 U/ µl)
SP6 RNA Polymerase -- Boehringer 1487671 (20 U/ µl)

Solutions for Import

PMSF
Prepare stock of 130mM in DMSO (i.e. 22.65 mg PMSF / ml DMSO). Store at -20 °C.

Breaking Buffer (can leave up to 1 month)	for 100ml
0.6 M Sorbitol	25 ml of 2.4 M Sorbitol -store at 4 °C
20 mM HEPES	2 ml of 1 M Hepes (pH 7.4)
	72 ml dH_20

2.4 M Sorbitol Use 43.73 g / 100 ml. Store at 4 °C.
2.5 M KCl Use 18.64 g / 100 ml. Store at 4 °C.
1 M $MgCl_2$ Use 2.033 g / 10 ml. Store at 4 °C.
1 M HEPES (pH 7.4) Use 238.3 mg/ml, pH to 7.4. Store at 4 °C.

Sucrose cushion (make fresh per experiment)	for 25 ml
0.6 M Sucrose	5 g
0.1 M KCl	1 ml of 2.5 M KCl
2 mM $MgCl_2$	50 µl of 1 M $MgCl_2$
20 mM HEPES	0.5 ml of 1 M HEPES (pH 7.4)